Identification of a Gap Junction Communication Pathway Critical in Innate Immunity

By

Suraj Jagdish Patel

S.B. Mechanical and Aerospace Engineering
Cornell University, 2003

Submitted to the Harvard-MIT Division of Health Sciences and Technology
in partial fulfillment of the requirements for the degree of

DOCTOR OF PHILOSOPHY

at the

MASSACHUSETTS INSTITUTE OF TECHNOLOGY

September 2010

Signature of the Author .....
Division of Health Sciences and Technology
June 24, 2010

Certified by .....
Martin L. Yarmush, M.D., PhD
Helen Andrus Benedict Professor of Surgery and Bioengineering
Thesis supervisor

Accepted by .....
Ram Sasisekharan, PhD
Edward Hood Taplin Professor of Health Sciences and Technology and Biological Engineering
Director, Harvard-MIT Division of Health Sciences and Technology

This thesis has been examined by a committee approved by the Harvard-MIT Division of Health Sciences and Technology as follows:

Signature: ....
(Kenneth L. Rock, M.D. – Thesis Reader)

Kenneth L. Rock, M.D.
Professor, University of Massachusetts Medical School
Chair of Pathology

Signature: ... .
(Sangeeta N. Bhatia, M.D., Ph.D. – Thesis Reader)

Sangeeta N. Bhatia, M.D., Ph.D.
Professor of Heath Sciences and Technology, Harvard-MIT
Professor of Electrical Engineering and Computer Science, MIT
Director, Laboratory for Multiscale Regenerative Technologies

Signature: ....
(Richard N. Mitchell, M.D., Ph.D. – Committee Chairman)

Richard N. Mitchell, M.D., Ph.D.
Associated Professor of Pathology and Heath Sciences and Technology, Harvard Medical School
Brigham and Women's Hospital

Signature: ... .
(Martin L. Yarmush, M.D., Ph.D. – Thesis Supervisor)

Martin L. Yarmush, M.D., Ph.D.
Helen Andrus Benedict Professor of Surgery and Bioengineering, Harvard Medical School
Harvard-MIT Division of Heath Sciences and Technology
Director, Center for Engineering in Medicine

Identification of a Gap Junction Communication Pathway Critical in Innate Immunity

By
Suraj Jagdish Patel

Submitted to the Harvard-MIT Division of Health Sciences and Technology on June 24, 2010 in partial fulfillment of the requirements for the degree of Doctor of Philosophy

Abstract

The innate immune system is the first line of host defense, and its ability to propagate antimicrobial and inflammatory signals from the cellular microenvironment to the tissue at-large is critical for survival. In a remarkably complex microenvironment, cells are constantly processing external cues, initiating convoluted intracellular signaling cascades, and interacting with neighboring cells to generate a global, unified response. At the onset of infection or sterile injury, individual cells sense danger or damage signals and elicit innate immune responses that spread from the challenged cells to surrounding cells, thereby establishing an overall inflammatory state. However, little is known about how these dynamic spatiotemporal responses unfold. Through the use GFP reporters, *in vitro* transplant coculture systems, and *in vivo* models of infection and sterile injury, this thesis describes identification of a gap junction intercellular communication pathway for amplifying immune and inflammatory responses, and demonstrates its importance in host innate immunity.

The first section describes **development** of stable GFP reporters to study the spatiotemporal activation patterns of two key transcription factors in inflammation and innate immunity: Nuclear factor-KappaB (NFκB) and Interferon regulatory factor 3 (IRF3). Stimulation of NFκB-GFP reporters resulted in a spatially homogeneous pattern of activation, found to be largely mediated by paracrine action of the proinflammatory cytokine TNFα. In contrast, the activation of IRF3 was spatially heterogeneous, resulting in the formation of multicellular colonies of activated cells in an otherwise latent background. This pattern of activation was demonstrated to be dependent on cell-cell contact mediated communication between neighboring cells, and not on paracrine signaling.

The second section describes the **discovery** of a gap junction intercellular communication pathway responsible for the formation of IRF3 active colonies in response to immune activation. Cell sorting and gene expression profiling revealed that the activated reporter colonies, collectively, serve as the major source of critical antimicrobial and inflammatory cytokines. Using *in vitro* transplant coculture systems, colony formation was found to be dependent on gap junction communication. Blocking gap junctions with genetic specificity severely compromised the innate immune system's ability to mount antiviral and inflammatory responses.

The third section illustrates an **application** of the gap junction-induced amplification of innate immunity phenomenon in an animal model of sterile injury. Drug-induced liver injury was shown to be dependent on gap junction communication for amplifying sterile inflammatory signals. Mice deficient in hepatic gap junction protein connexin 32 (Cx32) were protected against liver damage, inflammation, and death in response to hepatotoxic drugs. Coadministration of a selective pharmacologic Cx32 inhibitor with hepatotoxic drugs significantly limited hepatocyte damage and sterile inflammation, and completely abrogated mortality. These finds suggests that coformulation of gap junction inhibitors with hepatotoxic drugs may prevent liver failure in humans, and potentially limit other forms of sterile injury.

In summary, this thesis demonstrates the development of novel tools for investigating the spatiotemporal dynamics of cellular responses, describes how these tools were utilized to

discover a basic gap junction communication pathway critical in innate immunity, and provides evidence for the clinical relevance of this pathway in sterile inflammatory injury.

Thesis supervisor: Martin L. Yarmush
Title: Helen Andrus Benedict Professor of Surgery and Bioengineering

Acknowledgements

My graduate years have truly been a process of self-discovery, not just academically but also personally, and for that I am greatly indebted to many for their individual contributions, without which this process would have ended prematurely.

I would first like to acknowledge Maish for not only been a wonderful mentor, but also a role model and close advocate. Maish gave me the most valuable gift of all in academic research, freedom with unwavering support. From the day I stepped into the lab, I was given the opportunity to work in an open and wonderfully stimulating environment, where I was afforded the research freedom many graduate students desire. With extremely patient mentoring and continuous guidance, Maish allowed me to develop a research vision and gave me the flexibility to work on multiple ideas simultaneously. He compelled me to constantly focus on the bigger picture and challenged me to perform well beyond the level I ever thought I was capable of. He offered a perfect balance of helpful support when needed, and willingness to let me make my own mistakes.

I am also grateful to my thesis committee members for their invaluable additions to this thesis and my graduate experience. Rick chaired my thesis committee, and introduced me to the world of medicine and fortified my interest in immunology. His teachings served as my archetype for what clinically relevant biomedical research should be, and his valuable experience helped refine and focus the scope of this work. Ken introduced me to the process of sterile inflammation, and his extensive work in the field served a foundation for this thesis. Sangeeta provided important scrutiny of experiments and offered valuable discussions related to applications of this work.

I would like to thank the HST community, and in particular Collin Stultz for his commitment to my career development. Collin gave me the opportunity to teach in his class, and through this experience I learned human physiology from a practical perspective. He provided an unlimited source of inspiration on my academic journey, and introduced me to clinical medicine. His passion for medicine and basic research inspired me to pursue a career as a physician-scientist. I thoroughly enjoyed my time working with you on the cardiology wards last summer, and I thank you for teaching, by example, how to be a clinician. Collin has been an incredible friend, teacher, advisor, mentor, and role mole. I am greatly indebted to you for your belief in me, and for your persistent commitment to my career.

I benefited greatly from my associations with past and present members at the CEM, in particular Kevin King. I had a great time working with Kevin to study the innate immune response to dsDNA. His intellectual support and incredible scientific intuition lead to the genesis of this work, and his continued help and encouragement have been pivotal in my graduate career. Kevin has been an outstanding colleague, mentor, and role model. Though our relationship began as a simple lab collaboration, it has evolved into a great friendship. I wish him luck as he continues his career, and hope that we get a chance to re-experience the research synergy we create when working together.

My collaborations with Rohit Jindal, and Jack Milwid have been instrumental for this thesis and my graduate experience. Rohit provided the necessary depth for this work, while Jack provided the critical breadth. They have been great friends through the years, and have been a constant source of entertainment in lab. I would also like to thank Kaushal Rege, Monica Casali, Arno Tilles, and Biju Parekkadan for their valuable support. It was a pleasure working with all of them.

Lastly, I would like to thank my friends and family for their unconditional love and unwavering support. Without them, this work would have never been possible. My friends, Rupal Patel and Priyesh Shah, provided daily encouragement for the past 5 years, and walked with me through the trails and tribulations of graduate school. They celebrated the highs and endured the lows with me, and for that I'm sure they are wondering when they get their honorary PhD. Thank you for your support and patience, I don't say this enough, but I sincerely appreciate it.

I am the most indebted to family: my mom and dad, my sister Seema, my brother (in-law) Sanjay, and my grandmothers. Their unconditional love and persistent belief in me has made this work possible. Though they never completely understood what I was doing, and at many times, why I was doing it, they never stopped believing in me and trusted me to pave my own path. Mom, I thank you for your selfless love and unconditional support. Dad, I thank you for leading me by example to set high standards and work hard in life. Seema, I thank you for tireless encouragement and unrivalled patience. Sanjay, I thank you for constant enthusiasm and for keeping me well grounded through the years. I thank my grandmothers for their inspiration. I dedicate this work to my family.

TABLE OF CONTENTS

Chapter 1
Introduction

1.1 Introduction

This thesis describes the identification of novel gap junction communication pathway for amplifying immune and inflammatory responses triggered by activation of the innate immune system. Through the use of green fluorescent protein (GFP) reporters, *in vitro* transplant coculture systems, and *in vivo* models of infection and sterile injury, we attempted to bridge the gap between basic discovery, at the cellular level, and application at the level of animal models. The first section describes the development of stable GFP reporters to study the spatiotemporal activation patterns of two key transcription factors in inflammation and innate immunity: Nuclear factor-KappaB (NFκB) and Interferon regulatory factor 3 (IRF3). Stimulation of NFkB-GFP reporters resulted in a spatially homogeneous pattern of activation, found to be largely mediated by the paracrine action of proinflammatory cytokine tumor necrosis factor (TNFα). In contrast, the activation of IRF3 was spatially heterogeneous, leading to the formation of multicellular colonies in an otherwise dark background of non-activated cells. The second section describes the discovery of a gap junction intercellular communication pathway necessary for the formation of these IRF3 active colonies of cells that collectively expressed more than 95% of critical secreted cytokines, including interferon β (IFNβ) and TNFα. Blocking gap junctions, with genetic specificity, limited the secretion of IFNβ and TNFα and the corresponding antiviral and inflammatory state. The third section demonstrates an application of the gap junction communication phenomenon in an animal model of sterile injury. Drug-induced liver injury was shown to be dependent on gap junction communication for amplifying sterile inflammatory signals. Mice deficient in hepatic gap junction protein connexin 32 (Cx32) were protected against liver damage, inflammation, and death in response to hepatotoxic drug-induced injury. Coadministration of a selective pharmacologic Cx32 inhibitor with the hepatotoxic drugs significantly limited hepatocyte damage and sterile inflammation, and completely abrogated mortality, confirming the importance of hepatic gap junction communication in amplifying sterile injury and providing a potential novel therapeutic strategy for preventing drug hepatotoxicity.

This chapter begins with motivation for the thesis, followed by a review of relevant background literature, and finally concludes with an organizational overview of the thesis.

1.2 Motivation

The cellular microenvironment within a tissue is remarkably complex, and is characterized by an intricate geometry, with unique structural and physicochemical properties, and by cellular heterogeneity, with various parenchymal and stromal cells forming homotypic and heterotypic interactions [1, 2]. Within their local surroundings, cells are constantly processing external cues, and initiating complex intracellular signal transduction cascades to modulate their gene expression profile and ultimately their phenotype. In an effort to ensure a desired outcome, activated cells communicate with neighboring cells by propagating signals and recruiting them to generate an amplified overall tissue wide response [3]. These intercellular communication pathways are dynamic, both in space and time, and involve multiple modes of signaling including the paracrine action of soluble secreted factors and cell-contact mediated communication.

In the case of infection or injury, the ability of the innate immune system to propagate antimicrobial and inflammatory signals from the local cellular microenvironment to the tissue at-large becomes critical for survival [4]. At the onset of an infection or injury, individual cells sense danger or damage signals and elicit innate immune responses that spread from the challenged cells to surrounding naïve cells, thereby establishing an overall inflammatory state [5]. However little is known about how these complex spatiotemporal responses unfold. It is well documented that the secretion of antimicrobial cytokines, such as type I interferons, from infected cells is pivotal for establishing immunity [6, 7, 8]. Similarly, it has also been shown that the secretion of proinflammatory cytokines, such as TNFα, interleukin 1 beta (IL1β), and interleukin 6 (IL6), is essential for creating an inflammatory state to infection or sterile injury [9, 10, 11, 12, 13]. Cytokines secreted from initially challenged cells activate surrounding cells, priming them to resist further infection or injury. They also function to recruit innate immune cells, such as neutrophils and monocytes, to combat invading pathogens or to begin the process of tissue repair. While the overall importance of paracrine-mediated intercellular communication cannot be denied for amplifying immune and inflammatory responses, the spatiotemporal details remain speculative, and the possibility of cell contact-mediated communication in innate immunity unexplored.

Compared to amplification by secreted cytokines, contact-dependent signaling is faster and spatially localized, and therefore better suited for anticipating and preventing the rapid spread of infection or sterile injury [14]. Cell-cell contact mediated communication has been shown to greatly influence cellular responses during inflammatory and infectious conditions [15, 16, 17, 18, 19, 20]. In the liver, direct contact between parenchymal hepatocytes and stromal kupffer

cells amplifies the robust production of proinflammatory cytokines during endotoxin shock, and plays a pivotal role in the development of fulminate hepatic failure [15]. Similarly, cell-contact mediated signaling in both airway epithelial cells and alveolar endothelial cells has been shown to amplify innate immune and inflammatory responses to infection prior to the involvement of secreted cytokines [18, 20, 21]. Given the significance of contact-mediated intercellular communication in intensifying immune responses to infection or injury, an urgent need exists for investigating the underlying molecular mechanisms. These investigations may implicate new signaling pathways to target for limiting injury at the cellular level, before it gets propagated to the tissue at-large and causes organ dysfunction and systemic disease. In the case of infection, these pathways can be upregulated to further increase immune amplification for ensuring pathogen eradication and immunity. However, in the case of sterile injury these pathways can be inhibited to prevent host damage and disease progression.

1.3 Background

1.3.1 The Innate Immune System

The integrated human immune system is divided into of two branches: innate and adaptive (or acquired) immunity [22]. The innate immune system includes all aspects of host immune defense mechanisms that are encoded by germline genes [23]. These include physical barriers, such as epithelial cell and mucosal layers, soluble proteins that are either constitutively present (such as the complement proteins, defensins, and ficolins) or that are released from activated cells (including cytokines that regulate the function of other cells, chemokines that attract inflammatory leukocytes, lipid mediators of inflammation, and reactive free radicals that also contribute to tissue inflammation) [24, 25, 26, 27]. Additionally, the innate immune system relies on a limited repertoire of receptors, including membrane-bound receptors and cytoplasmic proteins that detect invading microbes by binding pathogen-associated molecular patterns (PAMPs), and host injury by binding endogenous damage-associated molecular patterns (DAMPs) [28, 29, 30, 31].

The innate immune system is the first line of host defense against pathogens and is mediated by nonhematopoietic cells as well as specialized hematopoietic cells including macrophages and dendritic cells [23, 24]. In contrast to the adaptive immune system, which depends on T and B lymphocytes, innate immune protection is a task performed by cells of both hematopoietic and nonhematopoietic origin [23]. Hematopoietic cells involved in innate immune responses include macrophages, dendritic cells, mast cells, neutrophils, eosinophils, natural

killer (NK) cells, and NK T cells [23]. In addition to these hematopoietic cells, innate immune responsiveness is a property of epithelial and endothelial cells alike.

Speed is a defining characteristic of the innate immune system. Within minutes of pathogen exposure or sterile injury, the innate immune system is activated and begins generating an antiviral and inflammatory response [32, 33]. Moreover, innate immunity plays a central role in activating the subsequent adaptive immune response **(Fig. 1)** [32, 33]. The adaptive immune system is involved in eliminating pathogens during the late phase of infection, as well as generating immunological memory [34]. In contrast to the limited number of pathogen receptors used by the innate immune system, the adaptive immune system boasts an extremely diverse, randomly generated repertoire of receptors by clonal selection of lymphocytes developed due to gene rearrangements [34].

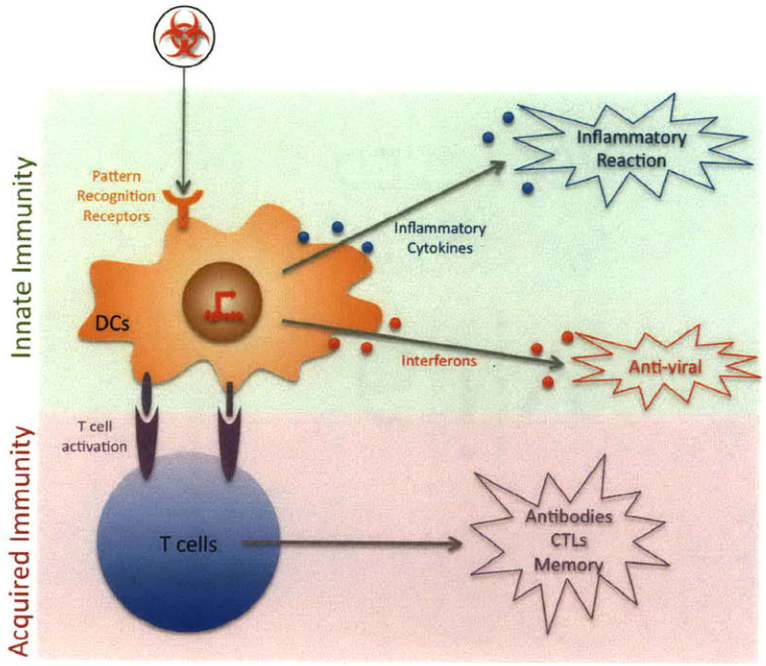

Figure 1. Functions of the Innate Immune System. Innate immune cells sense invading pathogens and trigger proinflammatory and antiviral reactions. The activated dendritic cells also upregulate co-stimulatory molecules and MHC molecules for secondary activation of the acquired immune system.

1.3.2 The Intracellular Signaling Pathways of Innate Immunity

The innate immune system utilizes an array of germline-encoded receptors for recognizing microbial PAMPs during infection and host DAMPs during sterile injury [28, 29, 30, 31]. Upon detection, these receptors engage adaptor molecules and initiate complex intracellular signaling cascades which ultimately results in the activation of NFκb, IRF3, and other transcription

factors, for driving the production of proinflammatory cytokines and other immunologic responses **(Fig. 2)** [35, 36, 37, 38]. These signaling cascades involve multiple Toll like receptor (TLR) pathways for detecting extracellular stimuli, and nucleotide oligomerization domain (NOD)–like receptor (NLR) pathways for sensing cystolic stimuli. During infection, the innate immune system uses pattern recognition receptors (PRRs) to detect "microbial nonself" ligands, such as LPS, double stranded RNA, CpG DNA, and viral DNA [28]. In sterile injury conditions, the innate immune system uses these PRRs to detect immunologic danger in the form of DAMPs. DAMPs represent common intracellular host molecules that are normally immunologically inert, but become active when released during cell damage and tissue injury. Well-characterized DAMPs include high mobility group box 1 (HMGB1), uric acid, and host DNA [30, 31].

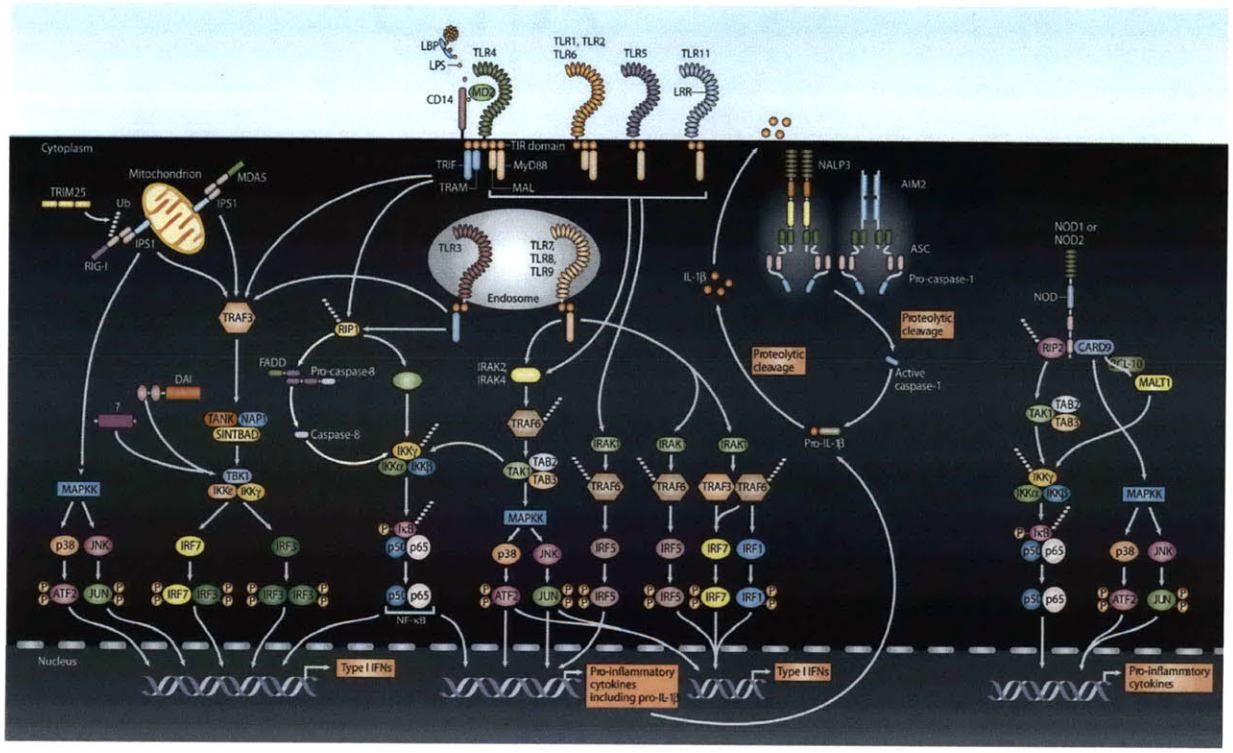

Figure 2. Sensing and Signaling in the Innate Immune System. Cells sense infection or injury-associated stimuli through the use of germline encoded receptors, and initiate signaling pathways for the activation of proinflammatory and innate immune transcription factors (http://www.umassmed.edu/igp/-faculty/fitzgerald.cfm).

1.3.3 Innate Immune Sensing of DNA

The innate immune system senses nucleic acids during infection or tissue damage[39, 40, 41, 42]. Pathogen-derived nucleic acids generate potent immune responses, as they are not

typically found in a host cell or in particular intracellular locations [43, 44]. DNA in pathogens or host cells in normally hidden from the immune system as it is tightly sequestered within the nuclear or mitochondrial membrane in eukaryotes, the cell wall in bacteria, or the envelope in viruses. However, following infection or sterile tissue injury, DNA is released into sub-cellular compartments where it becomes an active immunostimulatory molecule [33, 39]. Double stranded DNA (dsDNA) derived from host, viral, bacterial, or synthetic sources, elicits a potent innate immune response [43]. CpG-rich DNA from bacteria stimulates immune responses by activating the endosomal DNA-sensing TLR9 [45]. Following CpG DNA detection by TLR9, the adaptor molecule MyD88 (myeloid differentiation primary response gene 88) associates with the intracellular domain of TLR9, signaling for the activation of transcription factor IRF5 (interferon regulatory factor 5), IRF7 (interferon regulatory factor 7), NFκB, and the MAP (mitogen-activated protein) kinase pathway, resulting in the production of proinflammatory cytokines and type I interferons (**Fig. 3**) [45].

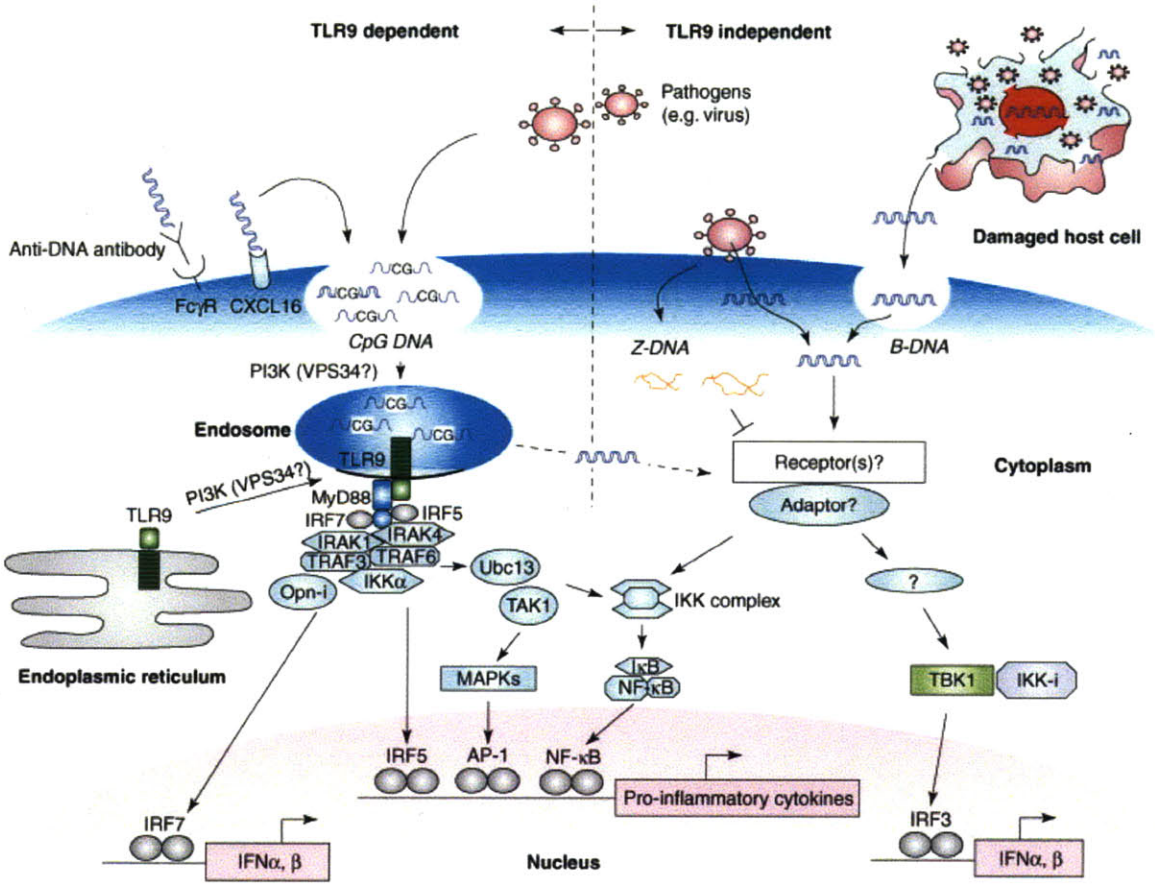

Figure 3. Innate Immune Recognition of DNA. In infection and/or sterile tissue damage, DNA is exposed to DNA-sensing PRRs. DNA is sensed by the innate immune system in a TLR9-dependent or

independent manner. The TLR9 pathway senses CpG-rich DNA, commonly found in bacterial genomic DNA, in the endosomal compartment of host cells, activating the production of interferons and proinflammatory cytokines. The TLR-independent pathway senses dsDNA in the cytosol of host cells, through a yet unidentified sensor, and activates transcription factors IRF3 and NFκB for the production of IFNβ and proinflammatory cytokines (figure adapted from *Ishii et al* [43]).

Other sources of non-CpG dsDNA, including host, viral, and synthetic, promote an immune response by activating an unidentified TLR-independent cytosolic DNA sensor in a sequence-independent manner [17, 46, 47, 48]. This cytosolic dsDNA sensor is activated when dsDNA is introduced into the cytoplasm of cells, possibly released from intracellular pathogens such as DNA viruses and certain bacteria, or from damaged host cells. The TLR-independent pathway for dsDNA sensing activates TBK1 and IKKε for the phosphorylation of transcription factor IRF3, which binds to interferon-sensitive response element (ISRE) sequences, triggering the robust production of type I interferons such as IFNβ [46, 49, 50]. The pathway also activates IKKα and IKKβ for the phosphorylation of NFκB **(Fig. 3)** [9, 47].

1.3.4 The Local Microenvironment of Infection and Injury

The cellular microenvironment within a tissue is remarkably complex, and is characterized by an intricate geometry (structural and physicochemical), by cellular heterogeneity (within parenchymal and stromal cells), and by soluble components [1, 2]. Within their local surroundings, cells are constantly processing external cues, and initiating complex intracellular signal transduction cascades to modulate their gene expression profile and ultimately their phenotype. As a result, cells are modifying their membrane receptor profiles, secreting cytokines, liberating growth factors, and producing secondary messengers for communicating signals to their neighboring cells, all in an effort to create a synchronized response to the initial external cue. These intercellular communication pathways at the cellular level are dynamic, both in time and space, and exist between multiple cell types, with each cell type playing a unique and critical role in amplifying a response to the tissue level [3]. In the case of infection or injury, the ability of the innate immune system to propagate antimicrobial and inflammatory signals from the local cellular microenvironment to the tissue at-large becomes critical for survival [4].

At the onset of infection or injury, individual cells sense danger or damage signals and elicit innate immune responses that spread from challenged cells to surrounding unstimulated cells, thereby establishing an overall inflammatory state [5]. Secreted cytokines such as IFNβ, TNFα, IL1β, and IL6 are key mediators of this response [9, 10, 11, 12, 13]. Cytokines are produced during the activation of innate immunity, and are considered to be the principal means for

intercellular communication of an infection or sterile injury [3]. They serve to propagate the inflammatory response and define its magnitude, and play a critical role in protecting naïve, neighboring cells from infection or injury. In the case of infection, this response is largely protective and limits the infectious front. However, in the case of sterile injury (i.e. trauma, drug induced, ischemia-reperfusion, autoimmune), this response may be pathologic and contribute to organ dysfunction and disease [51, 52]. While the communication of these responses is commonly attributed to secreted cytokines, the spatiotemporal details remain speculative, and the possibility of contact-mediated communication unexplored.

1.3.5 Cell-cell Contact Mediated Communication in Immunology

Cell-cell contact mediated communication has been shown to greatly influence immunological function during inflammatory and infectious conditions [15, 16, 17, 18, 19, 20]. In the liver, direct contact between parenchymal hepatocytes and stromal kupffer cells amplifies the robust production of TNFα in endotoxin shock, and plays a key role in the development of a fulminating hepatic inflammatory response [15]. This type of heterotypic cell contact mediated interaction between parenchymal cells and surrounding nonparenchymal neighbors has also been shown to be critical for maintaining hepatocyte phenotype and preserving organ function [1]. Additionally, regulator T cells (Tregs) have been shown to suppress and control the immune regulatory network of effector T cells through a cell-cell contact interaction involving gap junction mediated transfer of cAMP [16]. Furthermore, Tregs not only modulate ongoing CD4+T cell–mediated immune reactions at tissue sites but also abrogate the *de novo* induction of CD8+T cell–driven immune reactions by interfering with T-cell stimulatory activity of dendritic cells (DCs) through contact mediated gap junction intercellular communication [16]. Contact-dependent gap junction communication has also been demonstrated to be key in antigen cross presentation on DCs and macrophages [19].

1.3.6 Gap Junction Intercellular Communication

Contact-independent signaling is ideal for long-range communication, while contact-dependent signaling is best suited for spatially localized rapid communication [14]. Gap junction intercellular communication represents an important class of contact-dependent signaling. Gap junctions are assemblies of intercellular channels composed of connexin proteins (Cx) organized into two subsets, alpha connexins (i.e. Cx43) and beta connexins (i.e. Cx32, Cx26). Connexins from each subset oligomerize to form a hemichannel **(Fig. 4)** [53]. A functional channel is formed when a hemichannel from one subset assembles with a hemichannel of the same subset from an adjacent cell [53]. The resulting gap junctions directly connect the cytosol

of the coupled cells, allowing the exchange of ions, nutrients, and secondary messengers for the maintenance of tissue homeostasis [54, 55]. In the context of innate immunity, gap junction communication has been shown to be regulated by pathogen-associated stimuli such as LPS and peptidoglycans, and secreted proinflammatory cytokines such as TNFα, IL1β, and IFNγ [56, 57]. However, the relative contributions of contact-dependent and contact–independent communication in the establishment of host defenses have not been explored. Compared to secreted cytokine amplification, gap junction-mediated signaling is typically faster and therefore better suited for anticipating and preventing the rapid spread of an invading pathogen [53].

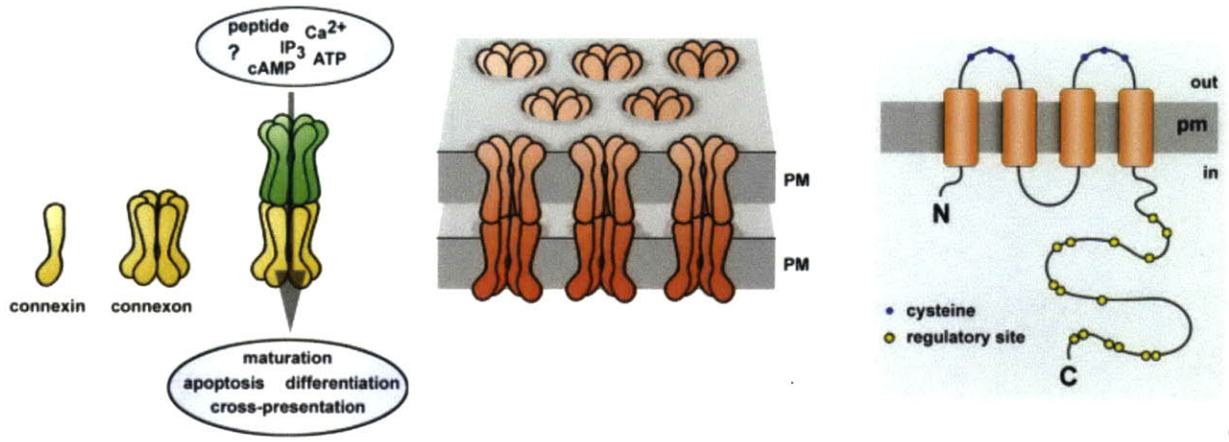

Figure 4. Structural organization of gap junctions. A gap junction is an assembly of six connexin molecules, comprising a hemi-channel called connexon that forms a functional channel when it is connected to a hemi-channel present in the membrane of a neighboring cell. These channels facilitate passive diffusion of small molecules and peptides involved in a number of processes like cell maturation and differentiation, apoptotic cell death and cross-presentation. Connexin molecules span the plasma membrane (pm), which exposes two extracellular loops to the extracellular space. In both extracellular loops three conserved cysteine residues (blue dots) are present, which are critical for the docking of a hemi-channel to a hemi-channel in the membrane of an adjacent cell. The large C-terminal cytoplasmic tail harbors several regulatory sites for phosphorylation (yellow dots) that control the gating of the channel [58].

1.4 Organizational Overview of Thesis

This thesis is organized into five chapters. Chapter 1 provides motivation and context for the work. Chapters 2, 3, and 4 are stand alone bodies of work, each linked to the prior through connections in innate immunity and gap junction communication. Chapter 2 demonstrates that double stranded DNA, a potent ligand of the innate immune system, induces NFκB and TNFα-mediated immune responses for endothelial activation and acute inflammation. This work suggests that endothelial-mediated inflammatory responses play a key role in host defense to

DNA from infection or sterile injury. Chapter 3 illustrates that activation of the innate immune system by dsDNA triggers intercellular communication through a gap junction-dependent signaling pathway, recruiting colonies of cells to collectively secrete antiviral and inflammatory cytokines for the propagation of danger signals across the tissue at-large. This work suggests that gap junction mediated propagation of immune signals lies upstream of the paracrine action of secreted cytokines, and therefore their modulation may represent a novel therapeutic strategy for tailoring the innate immune response to infection or injury. Chapter 4 describes an application of the aforementioned gap junction communication phenomenon in an animal model of sterile injury. Drug-induced liver injury was shown to be dependent on gap junction communication for amplifying sterile inflammatory signals. Mice deficient in hepatic gap junction protein Cx32 were protected against liver damage, inflammation, and death in response to hepatotoxic drug-induced injury. This work suggests inhibition of hepatic gap junctions as a viable clinical strategy for preventing drug hepatotoxicity and potentially other forms of sterile injury. Chapter 5 provides concluding remarks for the thesis.

1.5 References

1. Bhatia, S.N., et al., *Effect of cell-cell interactions in preservation of cellular phenotype: cocultivation of hepatocytes and nonparenchymal cells.* FASEB J, 1999. 13(14): p. 1883-900.
2. Koller, M.R., I. Manchel, and B.O. Palsson, *Importance of parenchymal:stromal cell ratio for the ex vivo reconstitution of human hematopoiesis.* Stem Cells, 1997. 15(4): p. 305-13.
3. Oberholzer, A., C. Oberholzer, and L.L. Moldawer, *Cytokine signaling--regulation of the immune response in normal and critically ill states.* Crit Care Med, 2000. 28(4 Suppl): p. N3-12.
4. Carter, W.A. and E. De Clercq, *Viral infection and host defense.* Science, 1974. 186(4170): p. 1172-8.
5. Kawai, T. and S. Akira, *Innate immune recognition of viral infection.* Nat Immunol, 2006. 7(2): p. 131-7.
6. Honda, K., A. Takaoka, and T. Taniguchi, *Type I interferon [corrected] gene induction by the interferon regulatory factor family of transcription factors.* Immunity, 2006. 25(3): p. 349-60.
7. Taniguchi, T. and A. Takaoka, *The interferon-alpha/beta system in antiviral responses: a multimodal machinery of gene regulation by the IRF family of transcription factors.* Curr Opin Immunol, 2002. 14(1): p. 111-6.
8. Uematsu, S. and S. Akira, *Toll-like receptors and Type I interferons.* J Biol Chem, 2007. 282(21): p. 15319-23.
9. Hiscott, J., *Convergence of the NF-kappaB and IRF pathways in the regulation of the innate antiviral response.* Cytokine Growth Factor Rev, 2007. 18(5-6): p. 483-90.
10. Chen, C.J., et al., *Identification of a key pathway required for the sterile inflammatory response triggered by dying cells.* Nat Med, 2007. 13(7): p. 851-6.
11. Akira, S. and T. Kishimoto, *IL-6 and NF-IL6 in acute-phase response and viral infection.* Immunol Rev, 1992. 127: p. 25-50.
12. Netea, M.G., et al., *IL-1beta processing in host defense: beyond the inflammasomes.* PLoS Pathog. 6(2): p. e1000661.
13. Duewell, P., et al., *NLRP3 inflammasomes are required for atherogenesis and activated by cholesterol crystals.* Nature. 464(7293): p. 1357-61.
14. Downward, J., *The ins and outs of signalling.* Nature, 2001. 411(6839): p. 759-62.

15. Hoebe, K.H., et al., *Direct cell-to-cell contact between Kupffer cells and hepatocytes augments endotoxin-induced hepatic injury.* Am J Physiol Gastrointest Liver Physiol, 2001. 280(4): p. G720-8.
16. Bopp, T., et al., *Cyclic adenosine monophosphate is a key component of regulatory T cell-mediated suppression.* J Exp Med, 2007. 204(6): p. 1303-10.
17. Stetson, D.B. and R. Medzhitov, *Recognition of cytosolic DNA activates an IRF3-dependent innate immune response.* Immunity, 2006. 24(1): p. 93-103.
18. Parthasarathi, K., et al., *Connexin 43 mediates spread of Ca2+-dependent proinflammatory responses in lung capillaries.* J Clin Invest, 2006. 116(8): p. 2193-200.
19. Neijssen, J., et al., *Cross-presentation by intercellular peptide transfer through gap junctions.* Nature, 2005. 434(7029): p. 83-8.
20. Veliz, L.P., et al., *Functional role of gap junctions in cytokine-induced leukocyte adhesion to endothelium in vivo.* Am J Physiol Heart Circ Physiol, 2008. 295(3): p. H1056-H1066.
21. Martin, F.J. and A.S. Prince, *TLR2 regulates gap junction intercellular communication in airway cells.* J Immunol, 2008. 180(7): p. 4986-93.
22. Chaplin, D.D., *Overview of the immune response.* J Allergy Clin Immunol. 125(2 Suppl 2): p. S3-23.
23. Turvey, S.E. and D.H. Broide, *Innate immunity.* J Allergy Clin Immunol. 125(2 Suppl 2): p. S24-32.
24. Janeway, C.A., Jr. and R. Medzhitov, *Innate immune recognition.* Annu Rev Immunol, 2002. 20: p. 197-216.
25. Hiemstra, P.S., *The role of epithelial beta-defensins and cathelicidins in host defense of the lung.* Exp Lung Res, 2007. 33(10): p. 537-42.
26. Holmskov, U., S. Thiel, and J.C. Jensenius, *Collections and ficolins: humoral lectins of the innate immune defense.* Annu Rev Immunol, 2003. 21: p. 547-78.
27. Sjoberg, A.P., L.A. Trouw, and A.M. Blom, *Complement activation and inhibition: a delicate balance.* Trends Immunol, 2009. 30(2): p. 83-90.
28. Akira, S. and S. Sato, *Toll-like receptors and their signaling mechanisms.* Scand J Infect Dis, 2003. 35(9): p. 555-62.
29. Kaisho, T. and S. Akira, *Toll-like receptor function and signaling.* J Allergy Clin Immunol, 2006. 117(5): p. 979-87; quiz 988.

30. Rubartelli, A. and M.T. Lotze, *Inside, outside, upside down: damage-associated molecular-pattern molecules (DAMPs) and redox.* Trends Immunol, 2007. 28(10): p. 429-36.

31. Kono, H. and K.L. Rock, *How dying cells alert the immune system to danger.* Nat Rev Immunol, 2008. 8(4): p. 279-89.

32. Medzhitov, R., *Recognition of microorganisms and activation of the immune response.* Nature, 2007. 449(7164): p. 819-26.

33. Akira, S., S. Uematsu, and O. Takeuchi, *Pathogen recognition and innate immunity.* Cell, 2006. 124(4): p. 783-801.

34. Pancer, Z. and M.D. Cooper, *The evolution of adaptive immunity.* Annu Rev Immunol, 2006. 24: p. 497-518.

35. Kumar, H., T. Kawai, and S. Akira, *Toll-like receptors and innate immunity.* Biochem Biophys Res Commun, 2009. 388(4): p. 621-5.

36. Kawai, T. and S. Akira, *Signaling to NF-kappaB by Toll-like receptors.* Trends Mol Med, 2007. 13(11): p. 460-9.

37. Honda, K. and T. Taniguchi, *IRFs: master regulators of signalling by Toll-like receptors and cytosolic pattern-recognition receptors.* Nat Rev Immunol, 2006. 6(9): p. 644-58.

38. Bryant, C. and K.A. Fitzgerald, *Molecular mechanisms involved in inflammasome activation.* Trends Cell Biol, 2009. 19(9): p. 455-64.

39. Yanai, H., et al., *Regulation of the cytosolic DNA-sensing system in innate immunity: a current view.* Curr Opin Immunol, 2009. 21(1): p. 17-22.

40. Gilliet, M., W. Cao, and Y.J. Liu, *Plasmacytoid dendritic cells: sensing nucleic acids in viral infection and autoimmune diseases.* Nat Rev Immunol, 2008. 8(8): p. 594-606.

41. Hornung, V. and E. Latz, *Intracellular DNA recognition.* Nat Rev Immunol. 10(2): p. 123-30.

42. Imaeda, A.B., et al., *Acetaminophen-induced hepatotoxicity in mice is dependent on Tlr9 and the Nalp3 inflammasome.* J Clin Invest, 2009. 119(2): p. 305-14.

43. Ishii, K.J. and S. Akira, *Innate immune recognition of, and regulation by, DNA.* Trends Immunol, 2006. 27(11): p. 525-32.

44. Kato, H., et al., *Differential roles of MDA5 and RIG-I helicases in the recognition of RNA viruses.* Nature, 2006. 441(7089): p. 101-5.

45. Hemmi, H., et al., *A Toll-like receptor recognizes bacterial DNA.* Nature, 2000. 408(6813): p. 740-5.

46. Ishii, K.J., et al., *A Toll-like receptor-independent antiviral response induced by double-stranded B-form DNA.* Nat Immunol, 2006. 7(1): p. 40-8.

47. Takaoka, A., et al., *DAI (DLM-1/ZBP1) is a cytosolic DNA sensor and an activator of innate immune response.* Nature, 2007. 448(7152): p. 501-5.

48. Hornung, V., et al., *AIM2 recognizes cytosolic dsDNA and forms a caspase-1-activating inflammasome with ASC.* Nature, 2009. 458(7237): p. 514-8.

49. Au, W.C., et al., *Identification of a member of the interferon regulatory factor family that binds to the interferon-stimulated response element and activates expression of interferon-induced genes.* Proc Natl Acad Sci U S A, 1995. 92(25): p. 11657-61.

50. Suzuki, K., et al., *Activation of target-tissue immune-recognition molecules by double-stranded polynucleotides.* Proc Natl Acad Sci U S A, 1999. 96(5): p. 2285-90.

51. Rock, K.L., et al., *The sterile inflammatory response.* Annu Rev Immunol. 28: p. 321-42.

52. Kono, H., et al., *Identification of the cellular sensor that stimulates the inflammatory response to sterile cell death.* J Immunol. 184(8): p. 4470-8.

53. Segretain, D. and M.M. Falk, *Regulation of connexin biosynthesis, assembly, gap junction formation, and removal.* Biochim Biophys Acta, 2004. 1662(1-2): p. 3-21.

54. Goldberg, G.S., V. Valiunas, and P.R. Brink, *Selective permeability of gap junction channels.* Biochim Biophys Acta, 2004. 1662(1-2): p. 96-101.

55. Elfgang, C., et al., *Specific permeability and selective formation of gap junction channels in connexin-transfected HeLa cells.* J Cell Biol, 1995. 129(3): p. 805-17.

56. Chanson, M., et al., *Regulation of gap junctional communication by a pro-inflammatory cytokine in cystic fibrosis transmembrane conductance regulator-expressing but not cystic fibrosis airway cells.* Am J Pathol, 2001. 158(5): p. 1775-84.

57. Jara, P.I., M.P. Boric, and J.C. Saez, *Leukocytes express connexin 43 after activation with lipopolysaccharide and appear to form gap junctions with endothelial cells after ischemia-reperfusion.* Proc Natl Acad Sci U S A, 1995. 92(15): p. 7011-5.

58. Neijssen, J., B. Pang, and J. Neefjes, Gap junction-mediated intercellular communication in the immune system. Prog Biophys Mol Biol, 2007. 94(1-2): p. 207-18.

Chapter 2

DNA Induces NFκB and TNFα-mediated Innate Immune Responses for Endothelial Activation and Acute Inflammation

2.1 Summary

The endothelium plays an important role in many pathological conditions. As a barrier between the vascular space and parenchymal tissue, it can be activated by host DNA released from damaged cells due to sterile injury or by pathogen DNA exposed to cells during viral infection. However, little is known about the role endothelial cells play in the inflammatory response to DNA. Here, we investigated how innate inflammatory responses triggered by DNA sensing result in endothelial activation and acute inflammation. Direct exposure to DNA induced activation of NFκB and MAPK pathways in endothelial cells, leading to expression of adhesion molecules, and leukocyte adhesion to the endothelium. NFκB, JNK, and p38 MAPK were critical for endothelial activation, as pharmacological inhibition resulted in decreased expression of adhesion molecules. We further demonstrated that DNA sensing triggers robust secretion of IRF3 and NFκB-mediated TNFα for sustained secondary activation of the endothelium. Mice deficient in the TNF receptor were unable to mount an acute inflammatory response to dsDNA. Our findings identified NFκB and TNFα axis as critical for initiating and amplifying a proinflammatory response to DNA. Furthermore, this work suggests that endothelial cell-mediated inflammatory responses play a key role in host defense to DNA from infection or sterile injury. Blocking these responses in pathological conditions may prevent endothelial activation and injury, and augmenting during protective situations may reduce infection and related tissue damage.

2.2 Introduction

The endothelium functions as a key barrier between the intravascular compartment and the extravascular parenchymal tissues, and is therefore involved in numerous physiological and pathological processes, such as inflammation [1, 2]. Endothelial cells play a critical role in the inflammatory process, as they can directly detect various molecular patterns associated with infection or sterile injury, and trigger an inflammatory response that results in localized leukocyte recruitment and infiltration at the site of activation [3-5]. Recent investigations have suggested that double stranded DNA from pathogens or from damaged host cells elicits a potent innate immune response in endothelial cells that can be protective, leading to immunity, or pathologic, resulting in amplified sterile injury [6, 7]. This response is comprised of a proinflammatory

component controlled by key alarm cytokines, such as TNFα and IL1β, and an antiviral element regulated by type I interferons [8]. While the molecular pathways of the interferon response to DNA have been intensively investigated, little is known about the mechanism of the inflammatory response triggered by DNA stimulation of the vascular endothelium.

Endothelial cells can detect and respond to DNA directly, or indirectly through the actions of proinflammatory cytokines. DNA stimulation triggers the robust secretion of proinflammatory cytokine IL1β by activating the inflammasome through the cytosolic DNA sensor absent in melanoma 2 (AIM2) and the endosomal DNA sensor TLR9 [9, 10]. Both sensors bind DNA, and associate with inflammasome adaptor molecules for caspase-1 mediated secretion of IL1β for indirectly stimulating the endothelium [6, 9]. Free DNA released from apoptotic cells has also been shown to directly stimulate endothelial cells to secrete IL1β and IL18 [6]. However, whether this direct detection of DNA is sufficient for inducing endothelial adhesion molecules and leukocyte recruitment remains unclear, and the role of secondary indirect endothelial activation by inflammatory cytokines unexplored. Additionally, involvement of endothelial cells in mediating NFκB and TNFα driven inflammatory signals in response to DNA sensing remains speculative.

Given the incomplete understanding of the role of endothelial cells in the inflammatory response to DNA, we investigated the DNA-initiated molecular signaling pathways that lead to activation of the endothelium. We demonstrated that direct exposure to DNA induced activation of NFκB and MAPK pathways in endothelial cells. This lead to increased expression of endothelial adhesion molecules, and resulted in functional leukocyte adhesion to the endothelium. NFκB, JNK, and p38 MAPK were critical for leukocyte adhesion, since pharmacological inhibition resulted in decreased expression of adhesion molecules. We further showed that detection of DNA triggers robust secretion of TNFα for sustained secondary activation of the endothelium. Both IRF3 and NFκB were required for the production of the TNFα, and mice deficient in the TNF receptor were unable to mount an acute inflammatory response to dsDNA. Our findings identify NFκB and TNFα as an alternative innate immune mechanism to the inflammasome and IL1β, capable of initiating and amplifying a proinflammatory response to DNA. This work suggests the involvement of DNA-induced endothelial cell immune responses in host defense to infection or sterile injury.

2.3 Results

2.3.1 Endothelial activation and leukocyte adhesion is triggered by DNA stimulation

Endothelial activation is an early event through which pathogen-associated molecular patterns induce inflammation during infection and tissue injury. Recent studies have established the role of DNA as a potent activator of the innate immune system [11]. For evaluating endothelial activation in response to DNA stimulation, we treated endothelial cells with synthetic B-form Poly(dA-dT):Poly(dA-dT) (hereafter referred to as DNA) [12]. DNA treatment results in increased expression of endothelial adhesion molecules ICAM1, VCAM1, and E-selectin (Fig. 1a). The greatest increase in gene expression was observed for VCAM1 (Fig. 1a). Adhesion molecules play central role in leukocyte recruitment by regulating their attachment to the endothelium. To determine if DNA stimulation results in increased leukocyte adhesion, confluent monolayers of endothelial cells were treated with DNA, and then co-cultured with dye-labeled peripheral blood leukocytes. TNFα stimulated endothelial cells were used as a positive control for measuring leukocyte adhesion under inflammatory conditions. DNA stimulation of endothelial cells lead to significantly enhanced binding of leukocytes (3.5 fold), in comparison to the control (Fig. 1b). Our results indicated that DNA acts as a potent activator of the endothelium by increasing the expression of adhesion molecules, and directly enhancing leukocyte adhesion to the endothelium.

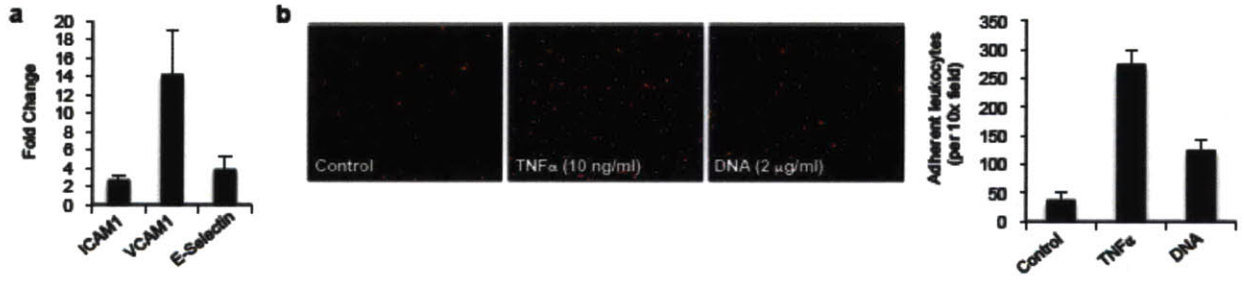

Figure 1. DNA induced activation of the endothelium. (a) Q-PCR for expression of ICAM1, VCAM1, and E-Selectin in RHMECs after stimulation with DNA (2 ug/ml) for 4 hours. (b) Leukocytes adhesion to the RHMECs stimulated with DNA (2 ug/ml) or TNFα (10ng/ml) for 12 hours.

2.3.2 DNA induced activation of NFκB and MAPK pathways

NFκB and MAPK pathways are known to play an important role in regulating the expression of endothelial adhesion molecules [5]. Given that DNA stimulation lead to increased expression of adhesion molecules, we examined the activation of NFκB and MAPK pathways in response to DNA. For evaluating NFκB activation, a reporter clone of endothelial cells that synthesizes

GFP in response to NFκB activation was utilized. DNA stimulated NFκB endothelial cell reporters exhibited elevated levels of GFP in comparison to untreated cells, thereby suggesting NFκB activation by DNA (Fig. 2a-c). These results were verified by fluorescence microscopy and flow cytometry (Fig. 2a-c). A nuclear ELISA for NFκB activation further confirmed that DNA induced dose-dependent activation of NFκB in endothelial cells after 6 hours of stimulation (Fig. 2d). For evaluating activation of MAPKs, phosphorylated protein levels of JNK, p38, and ERK1/2 were measured in endothelial cells stimulated with DNA for 6 hours. Endothelial cells treated with DNA showed elevated levels of phosphorylated JNK and p38 in comparison to the control (Fig. 2e). However, levels of phosphorylated ERK1/2 were similar in both DNA stimulated and control endothelial cells (Fig. 2e). These results indicated that DNA-mediated activation of endothelial inflammatory responses include NFκB, JNK and p38 pathways, but not ERK1/2.

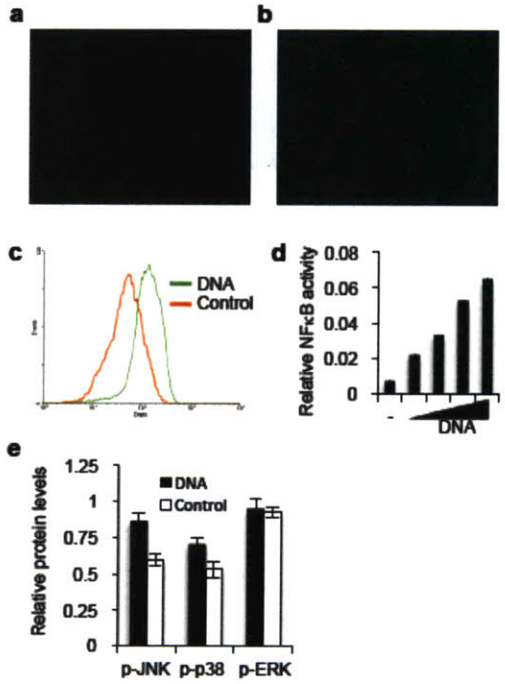

Figure 2. DNA activates NFκB and MAPK pathways in endothelium. (a) and (b) Fluorescence micrographs of NFκB reporter clone of RHMECs treated with control or DNA (2ug/ml) for 16 hours, respectively. (c) Fluorescence histogram of reporter clone treated with DNA. (d) ELISA for NFκB activity in RHMECs stimulated with a dose of DNA (0 to 4 ug/ml) for 6 hours. (e) Phosphorylated protein levels in RHMECs stimulated with DNA (2 ug/ml) for 6 hours.

2.3.3 Regulation of adhesion molecule expression by modulation of NFκB and MAPK pathways

We next sought to determine whether DNA-mediated activation of NFκB, JNK, and p38 was required for endothelial activation. Endothelial cells were treated with DNA for 4 hours in the presence or absence of PDTC, SP600125, or SB202190, known inhibitors of NFκB [13], JNK [14], and p38 MAPK [15] pathways, respectively. Inhibition of NFκB, JNK, and p38 resulted in reduced expression of ICAM1, VCAM1, and E-selectin, implying that all three signaling pathways are involved in DNA stimulated endothelial activation (Fig. 3). Inhibition of NFκB was most potent at reducing expression of adhesion molecules (Fig. 3). Given that JNK and p38 MAPK are known activators of the AP1 family of transcription factors [16, 17, 18, 19], our results suggested that transcription factors AP1 and NFκB are required for DNA driven endothelial activation.

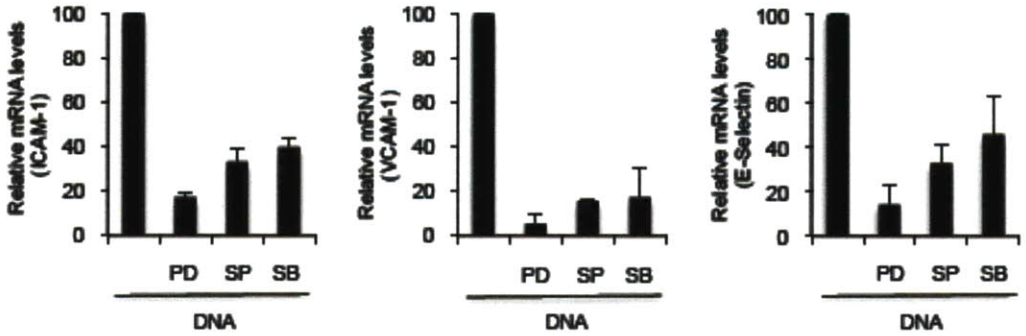

Figure 3. Inhibitors of NFκB and MAPK pathways modulate adhesion molecule expression in endothelial cells. Q-PCR for expression of ICAM1, VCAM1, and E-Selectin in RHMECs after stimulation with DNA (2 ug/ml) for 4 hours in the presence of PDTC(PD), SP600125(SP), or SB202190(SB), which are inhibitors of NFκB, JNK, and p38 MAPK pathways, respectively.

2.3.4 NFκB and IRF3 mediated TNFα production is critical for sustained secondary activation of the endothelium

TNFα is an important mediator of innate inflammation, as it acts on vascular endothelial cells to promote expression of adhesion molecules [20]. Having demonstrated mechanistically how direct stimulation of endothelial cells with DNA results in the expression of adhesion molecules, we next sought to investigate whether DNA induced TNFα production. We showed that DNA stimulation of endothelial cells results in upregulation of TNFα expression and robust secretion of TNFα into the culture supernatant, as assayed by ELISA (Figure 4a,b). To determine the transcription factors necessary for TNFα production in response to dsDNA, we used transgenic knockout mouse embryonic fibroblasts (MEFs). Wildtype MEFs (WT) stimulated with dsDNA induced significant TNFα secretion after 24 hours (Figure 4c). Conversely, MEFs deficient in TBK1 and IKKe (TBK1/IKKe DKO), kinases necessary for IRF3 activation, failed to

produce TNFα in response to dsDNA stimulation (Figure 4c). Similarly, dsDNA-stimulated MEFs deficient in IKKa and IKKb (IKKa/IKKb DKO), kinases essential for NFκB activation, also failed to produce TNFα (Figure 4c). Together, these data suggest that dsDNA-induced TNFα secretion is dependent on both IRF3 and NFκB activation.

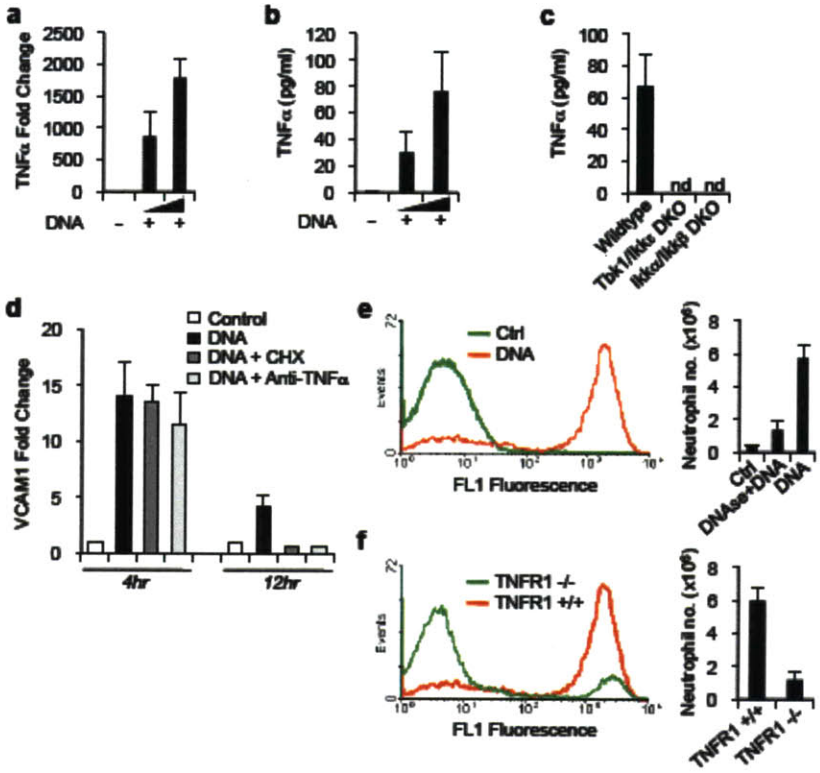

Figure 4. DNA mediated TNFα secretion for sustained secondary activation of the endothelium. (a) Q-PCR for expression of TNFα in RHMECs after stimulation with DNA (1 ug/ml) for 12 hours. (b) ELISA for TNFα in culture supernatant of RHMECs stimulated with a dose of DNA (.5 to 4 ug/ml) for 24 hours. (c) ELISA for TNFα in supernatants of wildtype MEFs (WT), TBK1/IKKe DKO MEFs (TBK1/IKKe DKO), and IKKa/IKKb DKO MEFs (IKKa/IKKb DKO) stimulated with 4 mg/mL of dsDNA for 24 hours. (d) Q-PCR for expression of VCAM1 in RHMECs stimulated with DNA (1 ug/ml) for 3 or 12 hours, in the presence or absence of TNFα neutralizing antibody (+ Anti-TNFα) or cycloheximide (+ CHX). (e,f) Representative fluorescence histograms of Ly-6G expression on peritoneal exudate cells (PEC) in mice injected 16h earlier with PBS, 2 mg/g of undigested DNA, or 2 mg/g of DNAse digested DNA. The Ly-6G+ gate represents neutrophils. Neutrophil numbers in PEC of TNFR1+/+ and TNFR1-/- mice 16h after i.p. challenge with PBS or 2 mg/g of undigested DNA. Neutrophil numbers in PEC were determined by multiplying the total cell numbers by the percentage of Ly-6G+ cells.

We then sought to determine if DNA-induced TNFα influences overall endothelial activation, since the expression of many adhesion molecules, such as VCAM1, is indirectly promoted by

proinflammatory cytokines. Using cycloheximide, a classic inhibitor of protein translation, we first clarified what portion of DNA-induced VCAM1 expression is from direct sensing of DNA and what part is from secondary indirect activation, requiring de novo protein synthesis. After 3 hours of DNA stimulation, VCAM1 expression, in the presence or absence of cycloheximide, was approximately equal (Figure 4d). However, after 12 hours of DNA stimulation, VCAM1 expression in the presence of cycloheximide was reduced to the level in unstimulated cells, whereas expression in the absence of cycloheximide remained high (Figure 4d). These data suggested that at an early time point, most of the measured VCAM1 expression was from direct sensing of DNA by endothelial cells, and that at later time points, VCAM1 expression was sustained by a secondary mechanism which required protein synthesis. Given the secretion of TNFα in response to DNA stimulation, we utilized a TNFα neutralizing antibody to investigate whether this secondary mechanism for sustained VCAM1 expression was due to the paracrine actions of TNFα. After 3 hours of DNA stimulation, VCAM1 expression, in the presence or absence of TNFα neutralizing antibody, was nearly similar (Figure 4d). In contrast, at 12 hours, VCAM1 expression in the presence of TNFα neutralizing antibody was curtailed to the level in unstimulated cells, suggesting that DNA-induced TNFα is required for sustained secondary activation of the endothelium.

2.3.5 DNA-induced acute inflammation is dependent on TNFα

To evaluate the in vivo role of TNFα in acute inflammation triggered by DNA, we developed an in vivo model of DNA-induced inflammation. We injected complexed-DNA, as well as complexed-DNAse1 digested DNA, intraperitoneally (i.p.) into mice. After 16 hours, mice injected with undigested DNA had abundant neutrophils in their abdominal cavities (Figure 4e), indicated by the staining of peritoneal lavage cells with the neutrophil marker Ly-6G. However, mice injected with DNAse1 digested DNA had minimal neutrophil infiltration (Figure 4e), in agreement with prior reports suggesting that DNAse digestion renders DNA inert to innate immune system. Mice deficient in the TNFα receptor (TNFR1-/-) also had significantly reduced neutrophil accumulation when injected with undigested DNA, compared to abundant neutrophils in TNFR1+/+ mice treated with undigested DNA (Figure 4f). Taken together, these results demonstrate that detection of DNA triggers acute inflammation dependent on TNFα signaling.

2.4 Discussion

The endothelium is exposed to DNA during infection and tissue injury. In this chapter, we identify the signaling cascade induced by DNA for activating endothelial cells to express adhesion molecules and facilitate leukocyte recruitment. Our results indicate that DNA activates

NFκB, JNK, and p38 MAPK pathways, for expression of endothelial adhesion molecules. Furthermore, our study determined that DNA sensing leads to the robust secretion of TNFα, which acts as a paracrine mediator for the sustained secondary activation of the endothelium. We also demonstrated the requirement for TNFα signaling in establishing an acute inflammatory response to DNA *in vivo*.

DNA stimulation resulted in the activation of NFκB, JNK, and p38 MAPK in endothelial cells. Although DNA induced NFκB activation has been previously reported in literature [12, 21], it is unclear whether DNA directly activates NFκB or indirectly through a secondary mediator [22]. We observed that early in infection, DNA directly activated NFκB, and this activation is limited by pharmacologic inhibition of NFκB but not by cycloheximide, suggesting that *de novo* protein synthesis is not required. Similarly, our results suggest that DNA directly activates JNK and p38 MAPK as well. The activation of MAPK pathways by DNA is relatively unexplored. While some reports show no activation of MAPK or NFκB in response to DNA [23], others demonstrate the contrary [22, 24]. Recent investigations have suggested this discrepancy in NFκB activation can be attributed to the use of different DNA ligands, stimulating different receptors [22, 24]. We demonstrated that the DNA ligand poly(dA:dT) directly activates JNK and p38 pathways by potentially the same receptor that activates NFκB.

TNFα and IL1β are potent proinflammatory cytokines involved in the expression of endothelial adhesion molecules [5]. The molecular pathways involved in DNA-induced IL1β secretion have been recently established [8, 9]. DNA activates the inflammasome pathway, which leads to maturation and secretion of pro-IL1β. In contrast, the mechanism by which DNA induces formation of TNFα and its role in DNA-mediated inflammation is relatively unexplored. In this report, we established that DNA sensing by endothelial cells leads to potent expression and secretion of TNFα. This agrees with other reports in which undigested mammalian DNA induced TNFα in DNase II deficient macrophages [25], and enhanced expression of TNFα in DNA stimulated hepatocytes [26]. We also identified that DNA-mediated TNFα formation was abrogated in MEFs deficient in kinases necessary for NFκB and IRF3 activation. LPS-induced TNFα secretion has also been shown to require both NFκB and IRF3 [27, 28]. We further demonstrated that DNA-induced TNFα lead to the sustained activation of the endothelium, and TNFα signaling was required for establishing an acute inflammatory response to DNA sensing *in vivo*. It remains to be identified, the critical cell types required for sensing DNA and secreting TNFα in the *in vivo* model of acute inflammation.

DNA-induced endothelial activation has several physiological implications. DNA viruses such as cytomegalovirus (CMV) are known to infect endothelial cells [4], and their infection has been associated with up regulation of adhesion molecules [29-30]. These viruses are also investigated for their possible role in initiating atherosclerosis and inflammatory responses resulting in vascular injury [31]. It remains to be determined if DNA-sensing by endothelial cells plays a role in the etiology of cardiovascular diseases. Another area that requires consideration of DNA-induced immune responses is gene therapy. The endothelium is an attractive target for gene therapy because of its easy accessibility, and its importance in pathophysiological conditions. Various strategies are directed towards designing appropriate gene therapy vectors that minimize activation of the endothelium [32]. Perhaps the gene therapy approaches should also take into account DNA-induced immune responses for achieving full therapeutic efficacy.

2.5 Materials and Methods

Materials

Dulbecco's Modified Eagle Medium (DMEM), penicillin-streptomycin, and fetal bovine serum (FBS) were acquired from Invitrogen Life Technologies (Carlsbad, CA). Pyrrolidine dithiocarbamate (PDTC), SP600125, SB202190 were obtained from Tocris bioscience (Ellisville, MO). Synthetic polydeoxynucleotide, poly(dA-dT):poly(dA-dT) dsDNA, was purchased from Amersham Biosciences. MCDB-131-complete medium was obtained from VEC Technologies (Rensselaer, NY). Rat tumor necrosis factor-α (TNFα) was purchased from R&D Systems (Minneapolis, MN).

Transfection of endothelial cells

Primary rat heart microvessel endothelial cells (RHMECs) were acquired from VEC Technologies and maintained in MCDB-131 medium supplemented with 10% FBS, 10 ng/ml EGF, 1 μg/ml hydrocortisone, 200 μg/ml EndoGro, 90 μg/ml heparin, and 1% antimycotic solution. For transfections, RHMECs were switched to DMEM media supplemented with 10% FBS, and 2% penicillin-streptomycin. DNA transfections were performed by using Lipofectamine LTX (Invitrogen) at a ratio of 1.5:1 (volume/weight) with DNA as per manufacturer's protocol. For experiments involving the use of inhibitors, cells were pretreated with PDTC (5 μg/ml), SP600125 (20 μM), or SB202190 (10 μM) in DMEM for 1 h before dsDNA stimulation and during stimulation. For some experiments, RHMECs were pretreated with a TNFα neutralizing antibody (2 mg/ml; R&D Systems), or cycloheximide (20 mg/ml; Sigma Alrich) for 1 hour before DNA stimulation and during stimulation.

Real time polymerase chain reaction

RNA was extracted from cells using nucleospin RNA II kit (Macherey-Nagel Inc., Bethlehem, PA) according to the manufacturer's instructions. Quantitative Reverse Transcription PCR was performed using the Superscript III two-Step qRT-PCR kit purchased from Invitrogen (Carlsbad, CA). 500 ng of cellular RNA was reverse transcribed according to the manufacturer's directions. Real-time quantitative PCR was performed using the Stratagene (La Jolla, CA) MX5000P QPCR system. Each reaction was carried out with 10 ng cDNA and 0.6 μM primers. During amplification, the cycling temperatures were 95^0 C for 15 seconds, 57^0 C for 1 minute and 72^0 C for 30 seconds. The following primers were used for amplifying DNA: E-Selectin forward primer: CAACACATCCTGCAGTGGTC; E-Selectin reverse primer: AGCTGAAGGAGCAGGATGAA; ICAM1 forward primer: CCTCTTGCGAAGACGA GAAC; ICAM1 reverse primer: ACTCGCTCTGGGAACGAATA; VCAM1 forward primer: TGAAGGGGCTACATCCACAC; VCAM1 reverse primer: GACCGTGCAGT TGACAGTGA; TNFα forward primer: GTCTGTGCCTCAGCCTCTTC; TNFα reverse primer: GCTTGGTGGTTTGCTACGAC; β-actin forward primer: GTCGTACCACTGGCATTGTG; and β-actin reverse primer: CTCTCAGCTGTGGTGG TGAA. By using the comparative cycle threshold method, all data were normalized to endogenous reference gene β -actin and then compared with appropriate controls for calculation of fold change.

TNFα ELISA

Supernatants from RHMECs and MEFs were used to determine the amount of rat TNFα and mouse TNFα, respectively, that was secreted as measured by ELISA (R&D Systems) according to the manufacturer's protocol.

Fluorescent Microscopy

Images were acquired using a Zeiss 200 M microscope (Carl Zeiss Inc., Thornwood, NY). The fluorescence images were captured using a CCD camera (Carl Zeiss Inc.) and Zeiss imaging software (Axiovision LE).

Leukocyte adhesion experiments

Peripheral blood leukocytes were purified from heparinized peripheral blood of rat using Histopaque density gradient (Sigma) according to manufacturer's instructions. Leukocytes were labeled with CM-DiI (2.5 μg/ml) at 37^0 C for 10 minutes and then added to RHMECs that were stimulated with DNA (2 ug/ml) or TNFα (10 ng/ml) for 12 hours. Leukocytes were allowed to adhere for 60 minutes at 37^0 C and then washed 3 times with PBS for removing non adhered cells. Fluorescence images were captured and analyzed using Image J software (National Institute of Health, Bethesda, MD) to estimate the degree of leukocyte adhesion to endothelial cells.

Construction of NFκB reporter clone of endothelial cells

NFκB reporter plasmid consisted of multiple response elements upstream of destabilized green fluorescent protein gene that encodes for d2EGFP reporter protein. The details of plasmid construction are described elsewhere [33]. RHMECs (2.5 million) were electroporated with the NFκB reporter plasmid (10 μg) using a BTX Electro Cell Manipulator 600 (Biotechnology and Experimental Research, San Diego, CA) at 280 V and 960 μF. Stably transfected clones were selected by addition of geneticin to a final concentration of 700 μg/ml. The clone that exhibited maximum shift in fluorescence upon stimulation with TNFα was used in experiments.

Measuring NFκB and MAPK activity

RHMECs were stimulated with different dose of DNA ranging from 0 to 4 μg/ml for 6 hours. Nuclear extract was prepared from cells using Panomics Nuclear Extraction Kit (Affymetrix, Inc., Santa Clara, CA) as per manufacturer's protocol. Nuclear extracts were kept frozen in -80^{0}C until further analysis. NFκB activity was determined by estimating the levels of NFκB p65 protein in the nuclear extract using ELISA kit (TransFactor NFκB p65 kit, Clontech, Mountain View, CA) according to manufacturer's instruction. Samples were normalized by total protein concentration of the nuclear extract, determined by Bradford reagent.

RHMECs were stimulated with DNA (2 μg/ml) for 6 hours in 96 well plate. Phosphorylated protein levels of JNK, p38 MAPK, and ERK1/2 were determined using cell based ELISA kit (RayBio Cell-Based ERK1/2 ELISA Sampler Kit, Ray Biotech Inc., Norcross, GA) as per manufacturer's instructions.

Animals

C57BL/6 and TNFR1-/- mice were purchased from Jackson Laboratory. All animal protocols were approved by Massachusetts General Hospital Subcommittee on Research Animal Care.

DNA-induced inflammation

DNA was complexed with LyoVec transfection reagent according to the manufacturer's protocol (Invivogen). DNAse I digested DNA was prepared by treating 100 mg of DNA with 5U of DNAse I (Ambion) at 37C for 30 minutes. DNAse was then heat inactivated, and the digested DNA was complexed with LyoVec. Mice were injected intraperitoneally with DNA (2 mg/kg) in .1 ml PBS, DNAse digested DNA (2 mg/kg) in .1 mL PBS, 5U of heat inactivated DNAse in .1 mL PBS, or PBS alone. At 16 hours after challenge, the numbers of neutrophils (Ly-6G+) in the peritoneum were evaluated as previously described [34].

Acknowledgements

The authors thank S. Akira for the generous gift of Tbk1$^{-/-}$Ikke$^{-/-}$ MEFs and I. Verma for Ikka$^{-/-}$ Ikkb$^{-/-}$ MEFs. S.J.P was supported in part by a Department of Defense CDMRP Prostate Cancer

Predoctoral Training Award. The work was supported by grants from the US National Institutes of Health (DK059766 and P41 EB-002503) and from the Shriners Hospital for Children.

2.6 References

1. Kuvin JT, Karas RH. Clinical utility of endothelial function testing: Ready for prime time? *Circulation*. 2003;107:3243-3247
2. Vane JR, Anggard EE, Botting RM. Regulatory functions of the vascular endothelium. *N Engl J Med*. 1990;323:27-36
3. Andonegui G, Zhou H, Bullard D, Kelly MM, Mullaly SC, McDonald B, Long EM, Robbins SM, Kubes P. Mice that exclusively express tlr4 on endothelial cells can efficiently clear a lethal systemic gram-negative bacterial infection. *J Clin Invest*. 2009;119:1921-1930
4. Grundy JE, Lawson KM, MacCormac LP, Fletcher JM, Yong KL. Cytomegalovirus-infected endothelial cells recruit neutrophils by the secretion of c-x-c chemokines and transmit virus by direct neutrophil-endothelial cell contact and during neutrophil transendothelial migration. *J Infect Dis*. 1998;177:1465-1474
5. Pober JS, Sessa WC. Evolving functions of endothelial cells in inflammation. *Nat Rev Immunol*. 2007;7:803-815
6. Imaeda AB, Watanabe A, Sohail MA, Mahmood S, Mohamadnejad M, Sutterwala FS, Flavell RA, Mehal WZ. Acetaminophen-induced hepatotoxicity in mice is dependent on tlr9 and the nalp3 inflammasome. *J Clin Invest*. 2009;119:305-314
7. Li J, Ma Z, Tang ZL, Stevens T, Pitt B, Li S. Cpg DNA-mediated immune response in pulmonary endothelial cells. *Am J Physiol Lung Cell Mol Physiol*. 2004;287:L552-558
8. Muruve DA, Petrilli V, Zaiss AK, White LR, Clark SA, Ross PJ, Parks RJ, Tschopp J. The inflammasome recognizes cytosolic microbial and host DNA and triggers an innate immune response. *Nature*. 2008;452:103-107
9. Hornung V, Ablasser A, Charrel-Dennis M, Bauernfeind F, Horvath G, Caffrey DR, Latz E, Fitzgerald KA. Aim2 recognizes cytosolic dsdna and forms a caspase-1-activating inflammasome with asc. *Nature*. 2009;458:514-518
10. Hemmi H, Takeuchi O, Kawai T, Kaisho T, Sato S, Sanjo H, Matsumoto M, Hoshino K, Wagner H, Takeda K, Akira S. A toll-like receptor recognizes bacterial DNA. *Nature*. 2000;408:740-745
11. Takeshita F, Ishii KJ. Intracellular DNA sensors in immunity. *Curr Opin Immunol*. 2008;20:383-388
12. Ishii KJ, Coban C, Kato H, Takahashi K, Torii Y, Takeshita F, Ludwig H, Sutter G, Suzuki K, Hemmi H, Sato S, Yamamoto M, Uematsu S, Kawai T, Takeuchi O, Akira S. A toll-like

receptor-independent antiviral response induced by double-stranded b-form DNA. *Nat Immunol*. 2006;7:40-48

13. Schreck R, Meier B, Mannel DN, Droge W, Baeuerle PA. Dithiocarbamates as potent inhibitors of nuclear factor kappa b activation in intact cells. *J Exp Med*. 1992;175:1181-1194
14. Bennett BL, Sasaki DT, Murray BW, O'Leary EC, Sakata ST, Xu W, Leisten JC, Motiwala A, Pierce S, Satoh Y, Bhagwat SS, Manning AM, Anderson DW. Sp600125, an anthrapyrazolone inhibitor of jun n-terminal kinase. *Proc Natl Acad Sci U S A*. 2001;98:13681-13686
15. Lee JC, Laydon JT, McDonnell PC, Gallagher TF, Kumar S, Green D, McNulty D, Blumenthal MJ, Heys JR, Landvatter SW, et al. A protein kinase involved in the regulation of inflammatory cytokine biosynthesis. *Nature*. 1994;372:739-746
16. Dong C, Davis RJ, Flavell RA. Map kinases in the immune response. *Annu Rev Immunol*. 2002;20:55-72
17. Ueno H, Pradhan S, Schlessel D, Hirasawa H, Sumpio BE. Nicotine enhances human vascular endothelial cell expression of icam-1 and vcam-1 via protein kinase c, p38 mitogen-activated protein kinase, nf-kappab, and ap-1. *Cardiovasc Toxicol*. 2006;6:39-50
18. Ahmad M, Theofanidis P, Medford RM. Role of activating protein-1 in the regulation of the vascular cell adhesion molecule-1 gene expression by tumor necrosis factor-alpha. *J Biol Chem*. 1998;273:4616-4621
19. Jersmann HP, Hii CS, Ferrante JV, Ferrante A. Bacterial lipopolysaccharide and tumor necrosis factor alpha synergistically increase expression of human endothelial adhesion molecules through activation of nf-kappab and p38 mitogen-activated protein kinase signaling pathways. *Infect Immun*. 2001;69:1273-1279
20. Pober JS. Endothelial activation: Intracellular signaling pathways. *Arthritis Res*. 2002;4 Suppl 3:S109-116
21. Takaoka A, Wang Z, Choi MK, Yanai H, Negishi H, Ban T, Lu Y, Miyagishi M, Kodama T, Honda K, Ohba Y, Taniguchi T. Dai (dlm-1/zbp1) is a cytosolic DNA sensor and an activator of innate immune response. *Nature*. 2007;448:501-505
22. Takaoka A, Taniguchi T. Cytosolic DNA recognition for triggering innate immune responses. *Adv Drug Deliv Rev*. 2008;60:847-857
23. Stetson DB, Medzhitov R. Recognition of cytosolic DNA activates an irf3-dependent innate immune response. *Immunity*. 2006;24:93-103

24. Hornung V, Latz E. Intracellular DNA recognition. *Nat Rev Immunol*. 2010;10:123-130
25. Okabe Y, Kawane K, Akira S, Taniguchi T, Nagata S. Toll-like receptor-independent gene induction program activated by mammalian DNA escaped from apoptotic DNA degradation. *J Exp Med*. 2005;202:1333-1339
26. Patel SJ, King KR, Casali M, Yarmush ML. DNA-triggered innate immune responses are propagated by gap junction communication. *Proc Natl Acad Sci U S A*. 2009;106:12867-12872
27. Yao J, Mackman N, Edgington TS, Fan ST. Lipopolysaccharide induction of the tumor necrosis factor-alpha promoter in human monocytic cells. Regulation by egr-1, c-jun, and nf-kappab transcription factors. *J Biol Chem*. 1997;272:17795-17801
28. Covert MW, Leung TH, Gaston JE, Baltimore D. Achieving stability of lipopolysaccharide-induced nf-kappab activation. *Science*. 2005;309:1854-1857
29. Burns LJ, Pooley JC, Walsh DJ, Vercellotti GM, Weber ML, Kovacs A. Intercellular adhesion molecule-1 expression in endothelial cells is activated by cytomegalovirus immediate early proteins. *Transplantation*. 1999;67:137-144
30. Shahgasempour S, Woodroffe SB, Garnett HM. Alterations in the expression of elam-1, icam-1 and vcam-1 after in vitro infection of endothelial cells with a clinical isolate of human cytomegalovirus. *Microbiol Immunol*. 1997;41:121-129
31. Cheng J, Ke Q, Jin Z, Wang H, Kocher O, Morgan JP, Zhang J, Crumpacker CS. Cytomegalovirus infection causes an increase of arterial blood pressure. *PLoS Pathog*. 2009;5:e1000427
32. Rafii S, Dias S, Meeus S, Hattori K, Ramachandran R, Feuerback F, Worgall S, Hackett NR, Crystal RG. Infection of endothelium with e1(-)e4(+), but not e1(-)e4(-), adenovirus gene transfer vectors enhances leukocyte adhesion and migration by modulation of icam-1, vcam-1, cd34, and chemokine expression. *Circ Res*. 2001;88:903-910
33. Wieder KJ, King KR, Thompson DM, Zia C, Yarmush ML, Jayaraman A. Optimization of reporter cells for expression profiling in a microfluidic device. *Biomed Microdevices*. 2005;7:213-222
34. Chen CJ, Shi Y, Hearn A, Fitzgerald K, Golenbock D, Reed G, Akira S, Rock KL. Myd88-dependent il-1 receptor signaling is essential for gouty inflammation stimulated by monosodium urate crystals. *J Clin Invest*. 2006;116:2262-2271

Chapter 3

DNA-triggered Innate Immune Responses are Propagated by Gap Junction Communication

3.1 Summary

Cells respond to infection by sensing pathogens and communicating danger signals to non-infected neighbors; however little is known about this complex spatiotemporal process. Here we show that activation of the innate immune system by dsDNA triggers intercellular communication through a gap junction-dependent signaling pathway, recruiting colonies of cells to collectively secrete antiviral and inflammatory cytokines for the propagation of danger signals across the tissue at-large. Using live cell imaging of a stable IRF3-sensitive GFP reporter, we demonstrate that dsDNA sensing leads to multi-cellular colonies of IRF3-activated cells that express the majority of secreted cytokines, including IFNβ and TNFα. Inhibiting gap junctions decreases dsDNA-induced IRF3 activation, cytokine production, and the resulting tissue-wide antiviral state, indicating that this immune response propagation pathway lies upstream of the paracrine action of secreted cytokines and may represent a host-derived mechanism for evading viral anti-interferon strategies.

3.2 Introduction

The ability of the innate immune system to propagate antiviral and inflammatory signals from the local cellular microenvironment to the tissue at-large is critical for survival [1]. At the onset of a viral infection, individual cells sense invading pathogens and elicit innate immune responses that spread from infected to uninfected cells, establishing an overall antiviral state [2]. Secreted cytokines such as interferon β (IFNβ) and tumor necrosis factor (TNFα) are two key mediators of these responses [3]. To evade the host immune system, viruses have evolved strategies for limiting the secretion of these cytokines [4]. Nevertheless, the immune system remains capable of clearing many viral pathogens, suggesting that the host may have subsequently evolved additional mechanisms for propagating antiviral and inflammatory signals, beyond the paracrine action of cytokines [5].

The innate immune system uses pathogen recognition receptors to sense nucleic acids during infection or tissue damage [6]. Pathogen-derived nucleic acids generate potent immune responses, as they are not typically found in a host cell or in particular intracellular locations [7,8]. Several receptors have been identified for recognizing viral RNA, and their mechanistic details have been well studied[8]. In contrast, the sensing of viral DNA and the subsequent

triggering of a host antiviral response remain poorly understood. Double stranded DNA (dsDNA) derived from host, viral, or synthetic sources elicits a potent immune response by activating a TLR-independent cytosolic DNA sensor [9,10], such as the recently identified DAI (DNA-dependent activator of IFN regulatory factors) [11]. The TLR-independent pathway for dsDNA sensing activates TBK1 and IKKε for the phosphorylation of transcription factor IRF3, which binds to interferon-sensitive response element (ISRE) sequences, triggering the robust production of type I interferons such as IFNβ [9,12,13]. In addition to IFNβ, a successful antiviral response requires the establishment of an inflammatory state through cytokines such as TNFα [14]. The secretion of IFNβ and TNFα is thought to play an important role in propagating antiviral innate immune responses from individual infected cells to non-infected neighbors, priming them to resist the spread of infection [14]. However, while this communication is commonly attributed to secreted cytokines, the spatiotemporal details remain speculative, and the possibility of contact-mediated communication unexplored.

Cell-cell communication can be categorized by its dependency on contact. Contact-independent signaling is ideal for long-range communication, while contact-dependent signaling is best suited for spatially localized rapid communication [15]. Gap junction intercellular communication represents an important class of contact-dependent signaling. Gap junctions are assemblies of intercellular channels composed of connexin proteins (Cx) organized into two subsets, alpha connexins (i.e. Cx43) and beta connexins (i.e. Cx32, Cx26). Connexins from each subset oligomerize to form a hemichannel. A functional channel is formed when a hemichannel from one subset assembles with a hemichannel of the same subset from an adjacent cell [16]. The resulting gap junctions directly connect the cytosol of the coupled cells, allowing the exchange of ions, nutrients, and secondary messengers for the maintenance of tissue homeostasis [17]. In the context of innate immunity, gap junction communication has been shown to be regulated by pathogen associated stimuli such as LPS and peptidoglycans, and secreted proinflammatory cytokines such as TNFα, IL1β, and IFNγ [18,19]. However, the relative contributions of contact-dependent and contact–independent communication in the establishment of host defenses have not been explored.

Given the incomplete understanding of host innate immune response propagation, we used a stable ISRE-GFP monoclonal reporter to explore the spatiotemporal patterns of IRF3 activation in response to dsDNA stimulation, and investigated the intercellular signaling pathways between infected and non-infected cells for establishing an antiviral state. We found that dsDNA stimulation induced spatially heterogeneous responses characterized by the formation of multi-cellular colonies of IRF3 activated cells that collectively expressed more than

95% of critical secreted cytokines, including IFNβ and TNFα. Functional gap junctions were necessary for the formation of these IRF3 active colonies and blocking gap junctions with genetic specificity limited the secretion of IFNβ and TNFα and the corresponding antiviral state. Our findings describe a previously unknown intercellular signaling pathway triggered by cytosolic dsDNA sensing and provide evidence that gap junction communication is critical for the amplification of antiviral and inflammatory responses, prior to paracrine-mediated propagation by cytokines.

3.3 Results

3.3.1 GFP reporters sensitive and specific for IRF3-activating stimuli

Double-stranded DNA (dsDNA) is known to stimulate the expression of genes with ISRE consensus sequences in their promoters through activation of the IRF3 transcription factor [9,12]. To investigate the spatiotemporal evolution of dsDNA-induced gene expression, we created a stable monoclonal ISRE-GFP reporter cell line in a hepatocyte-derived H35 cell line and selected clones exhibiting low baseline GFP expression in the absence of stimuli, and high dsDNA-induced GFP expression (**Fig. 1a**). To characterize the reporter, we first assessed its specificity for IRF3-dependent gene expression by exposing confluent reporter monolayers to various immunostimulatory molecules and measuring ISRE reporter fluorescence using flow cytometry (**Fig. 1b**). When reporters were exposed to synthetic B-form Poly(dA-dT):Poly(dA-dT) (hereafter referred to as dsDNA) or dsRed plasmid DNA, total population fluorescence increased in a dose-dependent fashion. Similarly, when cells were stimulated with polyinosinic:polycytidylic acid (poly(I:C)), a synthetic double-stranded RNA known to activate IRF3, dose-dependent increases in total fluorescence were also observed. In contrast, IRF3-independent stimuli such as TLR9-dependent CpG DNA, IFNβ, poly(A) ssDNA, and siRNA did not elicit measurable increases in ISRE reporter fluorescence at any of the doses examined. As anticipated, LPS, which classically signals through TLR4 and IRF3, failed to activate the ISRE reporter, consistent with the fact that nonimmune cells do not express significant levels of TLR4 (confirmed by qPCR – data not shown). To verify that the ISRE reporters retained previously reported dsDNA-induced responses [9], we confirmed the expression of IFNβ and TNFα after 12 hours of dsDNA stimulation (**Fig. 1c**). Taken together, these results demonstrate that the ISRE reporters are sensitive for both dsDNA and Poly(I:C) stimulation, and specific for IRF3-activating stimuli.

When we examined the distribution of ISRE reporter fluorescence after dsDNA stimulation by flow cytometry, we found that increasing doses of dsDNA resulted in increasing numbers of

activated cells rather than increasing levels of activation in all cells, indicating that the cellular response was heterogeneous (**Fig. 1d,e**). Therefore, we used fluorescence microscopy to examine the distribution of dsDNA-induced GFP expression and discovered a striking spatial pattern. dsDNA stimulation of confluent reporter monolayers exhibited well-delineated clusters of GFP positive cells or "colonies" in an otherwise dark background of non-activated cells. Increasing doses of dsDNA led to increasing numbers of colonies with eventual bridging of adjacent colonies (**Fig. 1f,g**). To gain further insight into colony formation, we examined the temporal evolution of ISRE-activated colonies by monitoring GFP reporter induction with time-lapse fluorescence microscopy and quantifying colony area using custom automated image analysis software (**Fig. 1h-j**). Colony activation began 8-12 hours after dsDNA-stimulation and grew to a steady-state size, with clearly demarcated colony borders characterized by highly induced reporter cells inside and uninduced cells outside. These findings confirm that dsDNA stimulation leads to spatially heterogeneous patterns of ISRE-activated colonies in an otherwise uninduced confluent monolayer of cells. Interestingly, Poly(I:C) stimulation also led to ISRE reporter activation, however the response was spatially homogeneous across the reporter monolayer and did not result in colony formation (data not shown).

Since dsDNA requires polyelectrolyte complexing for immunogenicity, and high molecular weight complexes have short diffusion distances, we reasoned that dsDNA complexes land in discrete locations within the cultured monolayer, stimulate individual dsDNA-sensing cells, and ISRE colony-formation arises by a secondary intercellular communication signal. To clarify which cells were directly and indirectly activated by dsDNA, ISRE reporters were stimulated with dsDNA encoding the red fluorescent protein (dsRED). dsRED stimulation of ISRE-GFP reporters resulted in multi-cellular ISRE reporter cell colonies surrounding individual dsRED DNA sensing cells (**Fig. 1k**, see Supplementary Data Figure S1). Using the custom automated image analysis software discussed above, we determined that the average colony was comprised of 23.5 ISRE activated cells, of which 2.3 cells were dsRED DNA sensing cells (see Supplementary Data Figure S1d).

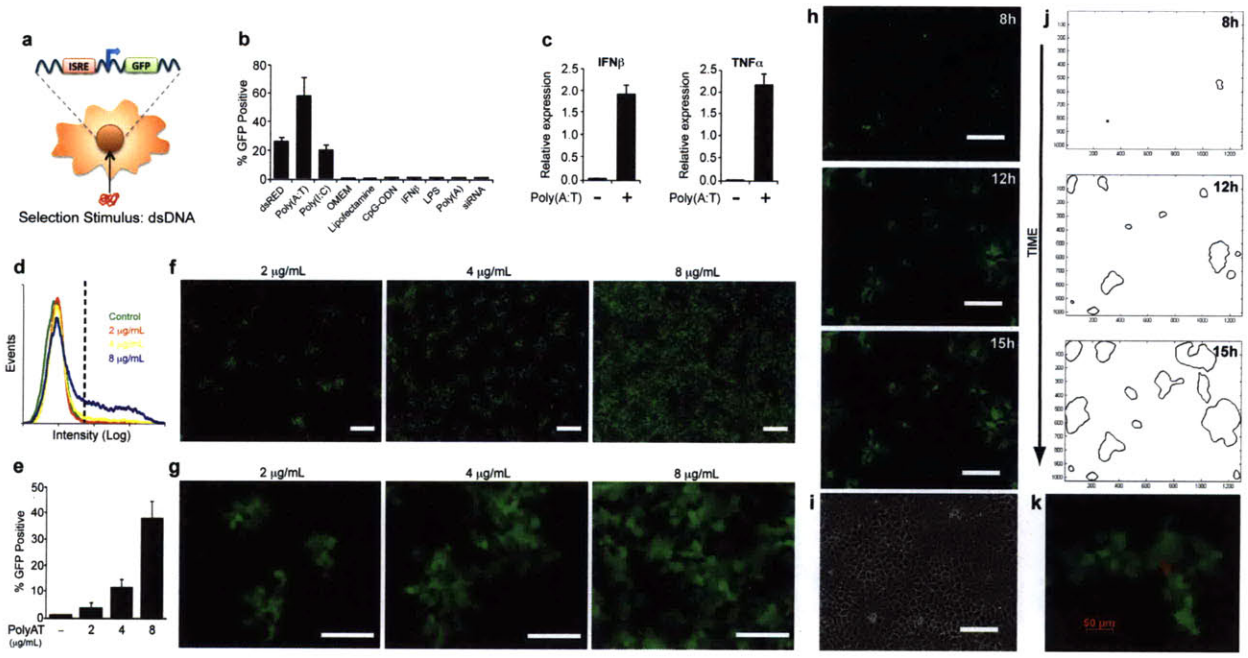

Figure 1 Stable ISRE reporters reveal dsDNA-induced spatiotemporal patterns (a) ISRE-GFP reporter cell line was created to study dsDNA-induced responses in living cells. (b) Percent of GFP+ reporter cells measured by flow cytometry after 24h stimulation with pdsRED, poly(AT) (B DNA), poly(I:C), OptiMEM, Lipofectamine, CpG-ODN, IFNβ, LPS, ssDNA (Poly(A)), and siRNA. (c-d) Reporter expression of IFNβ and TNFα measured by qPCR after 10h stimulation with 4 μg/mL poly(AT). (d) Flow cytometry distribution of ISRE reporter fluorescence 24h after exposure to poly(AT). (e) Percent of GFP+ reporter cells measured by flow cytometry after 24h stimulation with increasing dose of poly(AT). (f) Representative 5X (scale bar ~200 μm) and (g) 16X (scale bar ~120 μm) fluorescence images of reporters stimulated with poly(AT) for 24h. (h) Fluorescence time-lapse microscopy of poly(AT)-stimulated reporters with (i) a corresponding phase image of the confluent monolayer at 15h (scale bars ~200 μm). (j) Contour maps outlining automated colony identification at each time point. (k) Identification of dsDNA-sensing cells within ISRE-GFP colonies. ISRE-GFP reporters were stimulated with 2 μg/mL of complexed dsRED DNA and imaged 24 hours later by fluorescence microscopy. Representative fluorescence image of ISRE-GFP colony, with identification of dsRED DNA-sensing cell.

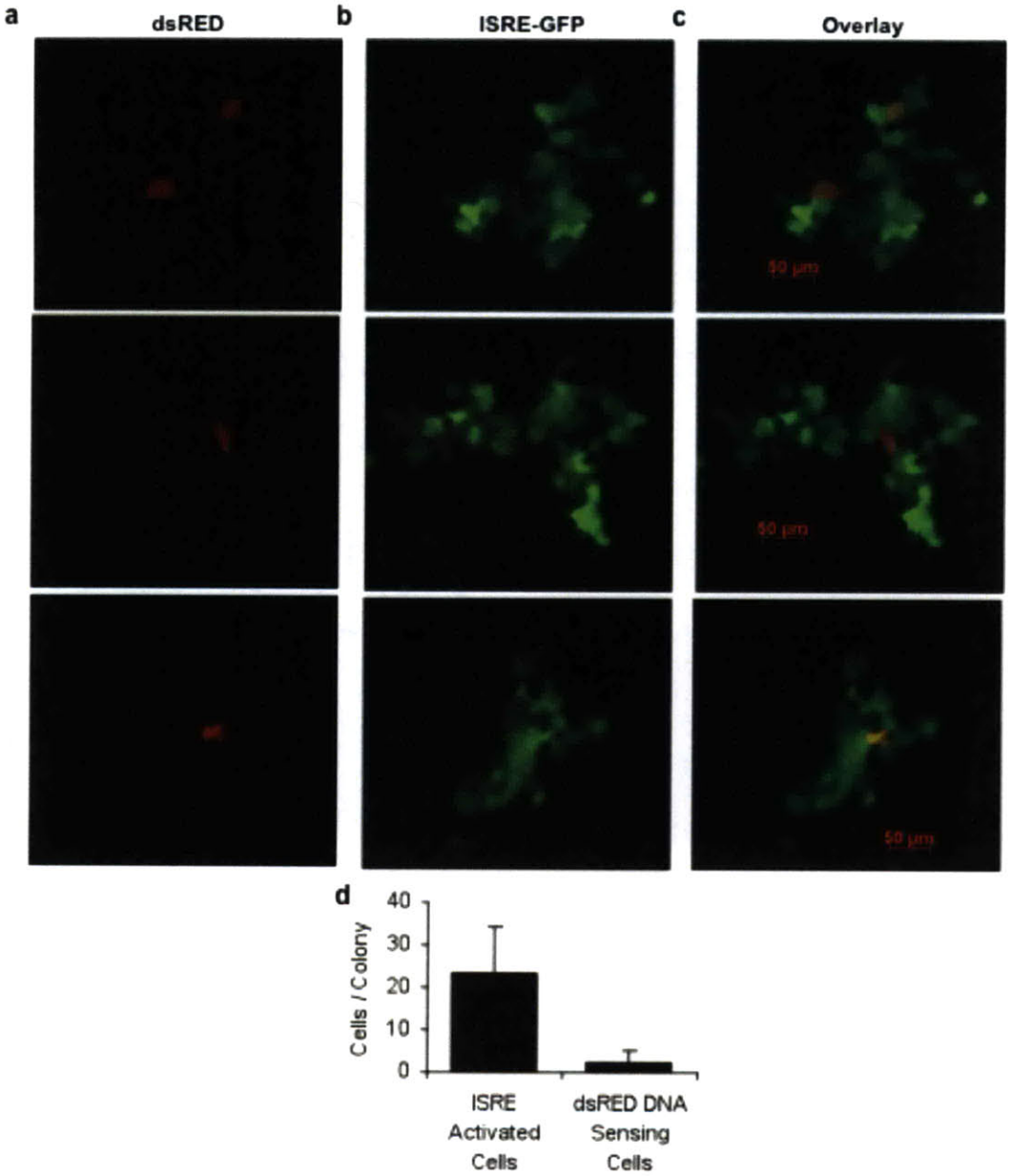

Figure S1. Localization of dsDNA in ISRE-GFP reporter monolayers. ISRE-GFP reporters were stimulated with 2 mg/mL of complexed dsRED DNA. Cells were imaged 24 hours later using fluorescence microscopy. (a-c) Multi-cellular colonies of activated ISRE reporter cells (green) were observed surrounding 1-2 dsDNA sensing cells (red). Three set of representative 10X fluorescence images of (a) dsRED, (b) GFP, and (c) overlay are shown. (d) Custom automated image analysis software was used to generate image corresponding iso-intensity contour maps for colony size identification. Data represent mean and +sd of ten randomly selected 10X images from three independent experiments.

3.3.2 Spatiotemporal IRF3-mediated gene expression

We next sought to determine whether the colonies of GFP+ ISRE reporters had functional significance by examining their gene expression profiles and comparing with their GFP- neighbors. Confluent monolayers of reporters were stimulated with dsDNA for 12 hours, sorted into GFP+ and GFP- populations by FACS, and examined for expression of IRF3-mediated genes by qPCR (**Fig. 2a**). GFP+ cells represented less than 8% of the total population, yet expressed more than 95% of secreted cytokines and chemokines including IFNβ, TNFα, and IP10 (**Fig. 2b**). In contrast, expression of IFNβ-inducible genes, with direct antiviral properties, such as PKR and OAS1, did not differ significantly between the two populations (**Fig. 2c**). Given the commonly held view that antiviral genes are expressed in response to the paracrine action of IFNβ, these results suggest that dsDNA sensing in individual cells leads to IRF3-activation in colonies of cells that collectively secrete cytokines, such as IFNβ and TNFα, to establish an antiviral state across the broader population.

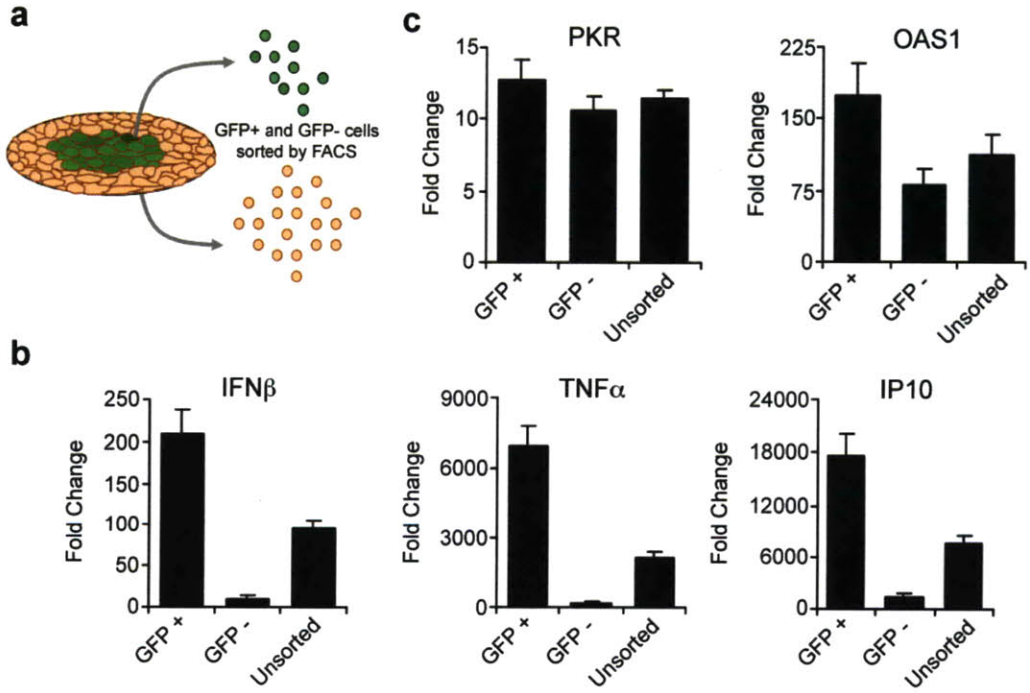

Figure 2 Spatial gene profiling triggered by dsDNA stimulation (a) ISRE-GFP reporter cells were stimulated with 4 μg/mL dsDNA for 12 hours and then sorted by FACS into GFP positive (+) and GFP negative (-) cells. (b) Expression of IFNβ, TNFα, and IP10 in GFP sorted (positive and negative) and unsorted cells, as assessed by qPCR. (c) Expression of IFNβ-mediated antiviral genes, PKR and OAS1. Data were normalized to control mock dsDNA stimulated cells.

3.3.3 IRF3 activation by contact-dependent intercellular communication

We hypothesized that IRF3-activated colony formation required secondary intercellular communication from dsDNA-sensing cells. To test this hypothesis, we developed a transplant co-culture system using dsDNA-stimulated non-reporter cells as donors and unstimulated ISRE reporters as recipients. Donor cells were stimulated with dsDNA for 6 hours, trypsinized, thoroughly washed, and transplanted onto recipient ISRE reporters that had never been exposed to dsDNA (**Fig. 3a**). After 18 hours of co-culture, ISRE reporters were activated in small colonies surrounding donor cells (**Fig. 3b,c**). In contrast, no IRF3 activity was observed in the reporters when mock dsDNA stimulated non-reporter cells were transplanted (**Fig. 3c**). Interestingly, not all dsDNA-stimulated cells were able to activate IRF3 in neighboring reporters. dsDNA-stimulated human cervical cancer cells (HeLa) and mouse neuroblastoma cells (N2A) were unable to activate IRF3 in the reporters (**Fig. 3b,c**), demonstrating that the phenomenon is cell-type specific and not an artifact of nonspecific dsDNA carryover from the donor cells. Donor cells were also stimulated with dsRed DNA, in order to identify them within the co-culture, and to confirm that they make contact and adhere to the reporter cells (see Supplementary Data Figure S4). To investigate whether direct cell contact was necessary for this dsDNA-induced secondary intercellular communication, we cultured dsDNA-stimulated donors and ISRE reporter recipients on opposite surfaces of a microfluidic parallel plate bioreactor (separation gap of ~50 μm, see Supplementary Data Figure S5). Negligible reporter induction was observed, suggesting that dsDNA-induced intercellular communication is contact-dependent. Taken together, these data suggest that dsDNA stimulation induces contact-dependent intercellular communication from dsDNA sensing cells to their unstimulated neighbors, propagating an IRF3-activating signal and amplifying IRF3-dependent gene expression.

To further clarify the pathways connecting donor dsDNA sensing and recipient IRF3 activation, we used genetic knockout mouse embryonic fibroblasts (MEFs) to determine the necessity of critical proteins. Wildtype MEF donors stimulated with dsDNA activated ISRE in reporter recipients (**Fig. 3d,e**). In addition, MEFs deficient in both TBK1 and IKKε (Tbk1-/-Ikbke-/-), kinases necessary for IRF3 activation, also activated ISRE in reporter cells (**Fig. 3d,e**). Similarly, dsDNA-stimulated MEFs deficient in both IKKα and IKKβ (IKKα-/-IKKβ -/-), kinases essential for NFκB activation, also activated ISRE in reporter cells (**Fig. 3d,e**). MEFs deficient in both MyD88 and TRIF (MyD88-/-TRIF-/-) were also able to activate ISRE reporter recipients (data not shown). Together, these data suggest that dsDNA-induced intercellular communication is TLR-independent and occurs upstream of both IRF3 and NFκB activation in dsDNA sensing cells.

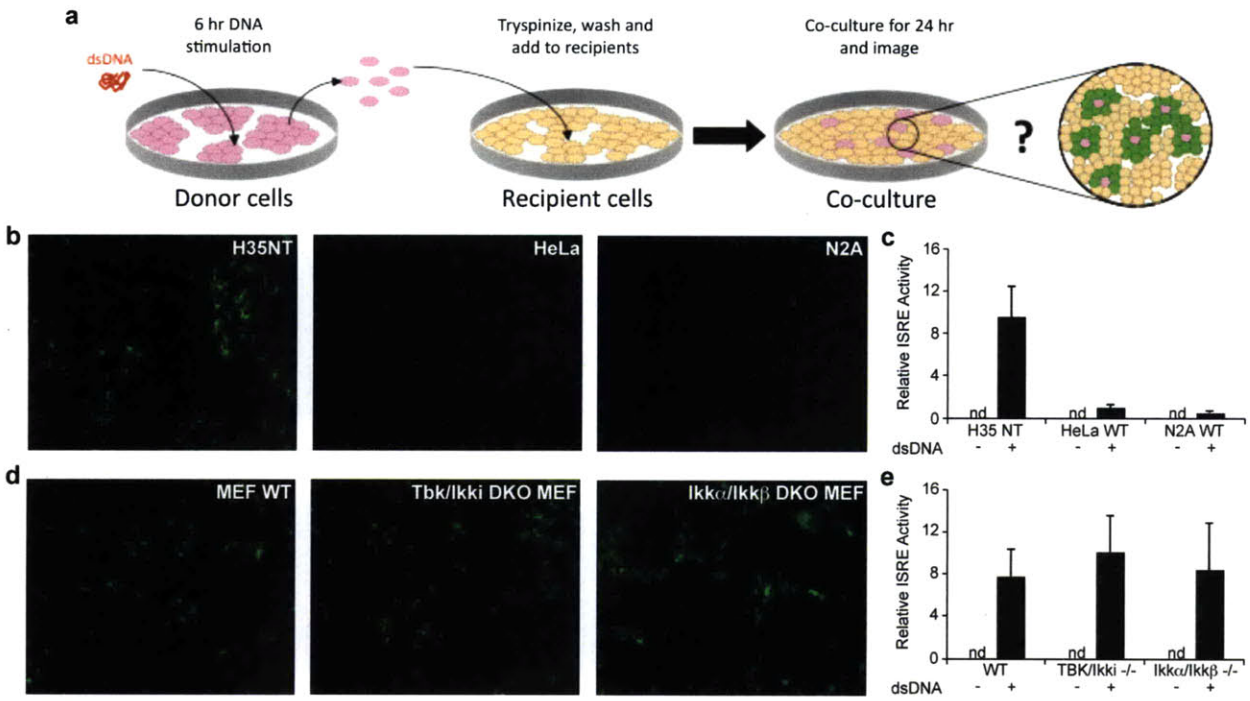

Figure 3 IRF3 activated colonies form by contact dependent cell-cell communication (a) Transplant co-culture system schematic. Non-ISRE reporter donor cells were stimulated with 10 μg/mL dsDNA for 6 hours. The donors were washed and trypsinized, and a subpopulation was co-cultured with ISRE-GFP reporter recipient cells. The co-culture was assayed 18 hours later by fluorescence microscopy and flow cytometry. (b,d) Representative 10X fluorescence images of reporter recipient cells co-cultured with various dsDNA-stimulated donor cells. (c,e) Relative GFP activity quantified by image analysis. Data represent mean and +sd of five representative images from three independent experiments.

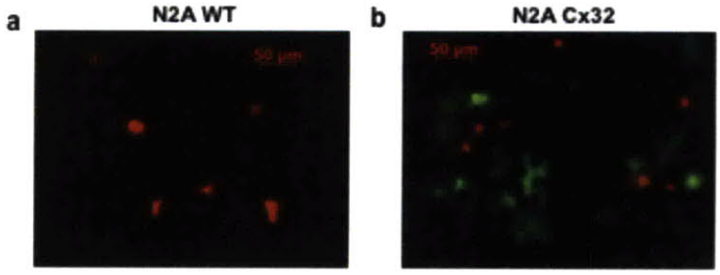

Figure S4. Identification of N2A donor cells in the transplant co-culture system. Wildtype N2A (N2A WT) or Cx32-expressing N2A (N2A Cx32) were stimulated with 10 mg/mL dsRED DNA for 6 hours, washed, trypsinized, and co-cultured with H35 ISRE-GFP reporter cells. The co-culture was assayed 18 hours later by fluorescence microscopy in order to indentify donor cells within the co-culture. Representative 10X fluorescence images of dsRED-stimulated (a) N2A WT or (b) N2A Cx32, co-cultured with H35 ISRE-GFP reporters.

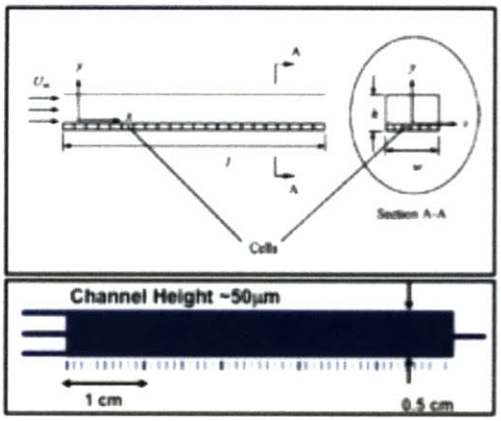

Top Down

Figure S5. Microfluidic parallel plate bioreactor experiment for evaluating cell contact dependency. Schematic of microfluidic device. dsDNA-stimulated non-reporter cells were seeded on the floor of the single channel device through input channel 1. After 2 hours, the device was flipped upside down, and H35 ISRE-reporter cells were seeded on the ceiling of the device through input channel 2. Both input and output channels were clamped off for 18 hours and then imaged for reporter activity.

3.3.4 Gap junctions are necessary for amplified IRF3 activation

Gap junction communication enables the rapid, localized exchange of information between cells linked through connexin protein channels [16]. To determine the necessity of gap junctions in the dsDNA-induced intercellular communication, we pretreated ISRE reporters with 18β-glycyrrhetinic acid (18βGA), a molecular inhibitor of gap junctions [20], prior to dsDNA stimulation. Compared to vehicle controls, pretreatment with 18βGA dramatically reduced colony size, resulting in mostly single cell reporter activation (**Fig. 4a**). Images were quantified by creating iso-intensity contour maps, and calculating the average size per colony for each colony present in the images (**Fig. 4b**). The average size of dsDNA-induced ISRE-activated colonies was reduced by more than 10-fold with 18βGA treatment compared to no 18βGA treatment. More than 75% of all colonies formed in the presence of 18βGA contained fewer than 3 cells, whereas more than 90% of all colonies formed in the absence 18βGA contained more than 3 cells (**Fig. 4c**). In addition, the overall number of ISRE activated-GFP positive cells was decreased from 38% to 5%, as a result of gap junction blockage (**Fig. 4d**). These results were further validated by connexin 32 (Cx32) knockdown analysis, using Cx32-targeted siRNA (see Supplementary Data Figure S3). Compared to control siRNA, Cx32 siRNA knockdown resulted in a significant decrease in both the size of dsDNA-induced ISRE active colonies, and in the overall number of dsDNA-induced GFP positive reporters. More than 70% of all colonies formed in the presence of Cx32 knockdown contained fewer than 3 cells, whereas more than 85% of all

colonies formed in the presence of control knockdown contained more than 3 cells (see Supplementary Data Figure S3).

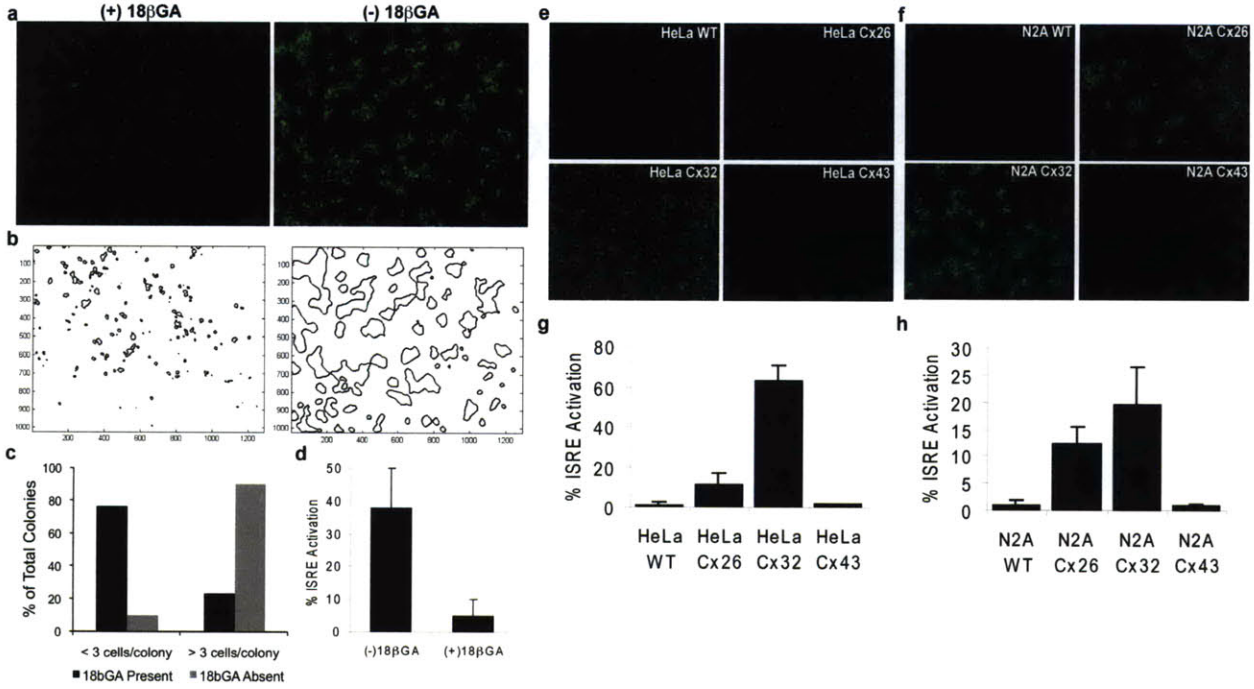

Figure 4 dsDNA-induced IRF3 amplification requires gap junctions (a) ISRE-GFP reporters were stimulated with 4 μg/mL dsDNA and GFP activity was assayed 18 hours later. (a) Representative 5X fluorescence images of dsDNA-stimulated GFP reporters and (b) corresponding contour maps outlining automated colony identification, in the presence (left) or absence (right) of 25 μM 18βGA. (c) Percentage of dsDNA-induced colonies less than 3 cells and more than 3 cells, in the presence (black) or absence (grey) of 18βGA. (d) dsDNA-stimulated ISRE-GFP reporter activity with or without 18-β-GA treatment, as determined by FACS. (e-h) Transplant co-culture experiments with genetically modified cells. Donor HeLa or N2A cells (WT, Cx26 expressing, Cx32 expressing, or Cx43 expressing) were stimulated with 10 μg/mL dsDNA for 6 hours, and then transplanted onto recipient ISRE-GFP reporters for 18 hours. (e) Representative 5X fluorescence images of dsDNA-stimulated HeLa WT, HeLa Cx26, HeLa Cx32, and HeLa Cx43 cells co-cultured with GFP reporters. (g) ISRE-GFP activity in HeLa/reporter co-cultures, as determined by FACS. (f) Representative 5X fluorescence images of dsDNA-stimulated N2A WT, N2A Cx26, N2A Cx32, and N2A Cx43 cells co-cultured with GFP reporters. (h) ISRE-GFP activity in N2A/reporter co-cultures, as determined by FACS.

The utility of chemical gap junction inhibitors such as 18βGA, is limited because of their nonspecific side effects and unknown mechanism of action [21]. Therefore, to definitively demonstrate the necessity of gap junction communication for the propagation of IRF3 activity,

we used the transplant co-culture system with genetically modified cell lines. HeLa and N2A cell lines have been historically shown to be gap junction and connexin deficient [21, 22]. We obtained modified monoclonal HeLa and N2A cells stably transfected with individual connexin transgenes (Cx26, Cx32, or Cx43), thereby reconstituting connexin expression and gap junction communication [21, 22]. PCR analysis was performed to verify appropriate connexin expression in all HeLa and N2A cells (data not shown). PCR analysis showed that ISRE reporters express only connexin 32, of the β-subset, and therefore only form functional gap junction channels with other cells expressing β connexins 26 or 32. When wildtype and Cx43-expressing HeLa and N2A cells were stimulated with dsDNA, minimal ISRE reporter activation was measured (HeLa WT: 0.5%, N2A WT: 1.0%, HeLa Cx43: 2%, N2A Cx43: 1.5%), suggesting a lack of intercellular communication (**Fig. 4e-h**). However, when Cx26 and Cx32 expressing cells were stimulated with dsDNA, significant ISRE reporter activation was measured (**Fig. 4e,f**), with 63% of reporters activated by Cx32-expressing HeLa cells and 23% by Cx32-expressing N2A cells (**Fig. 4g,h**). These data suggest that functional gap junction channels are necessary for dsDNA-induced intercellular communication and for amplifying IRF3 activation. To further generalize the utility of gap junctions for amplifying IRF3 activation in other cell types, we constructed another ISRE-GFP reporter in a stromal hepatic stellate cell line (HSC). When the HSC ISRE-GFP reporters were stimulated with dsDNA, they were able to form multi-cellular colonies of IRF3 activated reporters in a gap junction dependent manner (see Supplementary Data Figure S2).

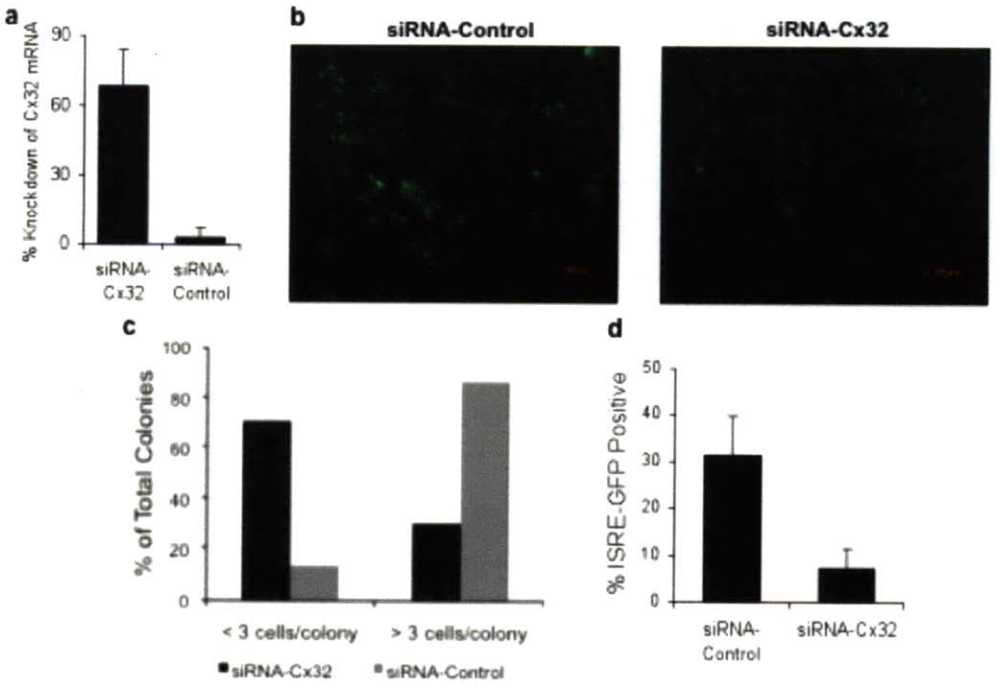

Figure S3. Loss of function analysis by siRNA knockdown of connexin 32 (Cx32). (a) Inhibition of Cx32 mRNA by small interference RNAs (siRNAs). Pooled siRNA targeting against rat Cx32 (siRNA-Cx32) mRNA and control siRNA (siRNA-Control) were transfected into H35 ISRE-GFP reporter cells. Cx32 and b-actin mRNA levels were evaluated by quantitative RT-PCR 36 hours after transient transfection. (b) Effect of Cx32 knockdown on response to dsDNA. ISRE-GFP reporter cells were transfected with siRNA-Cx32 or siRNA-Control for 36 hours, and then stimulated with dsDNA (4 mg/mL) for 16 hours. Representative 10X fluorescence images of ISRE-GFP reporter pretreated with siRNA-Control (left) or siRNA-Cx32 (right), and then stimulated with dsDNA. (c) Custom image analysis software was used to generate contour maps for automated colony identification. Percentage of dsDNA-induced colonies less than 3 cells and more than 3 cells, with siRNA-Control (grey) or siRNA-Cx32 (black) pretreatment. (d) Overall percentage of dsDNA activated ISRE-GFP reporters with siRNA-Control or siRNA-Cx32 treatment, as measured by flow cytometry.

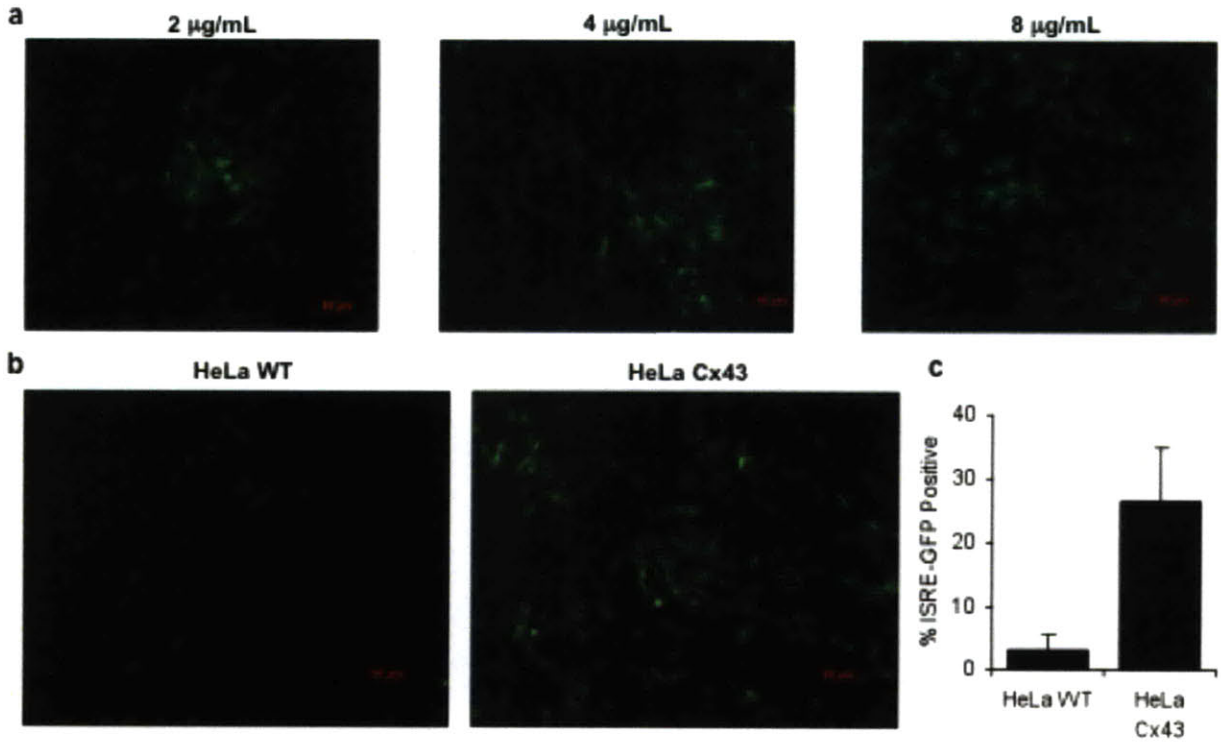

Figure S2. HSC ISRE-GFP reporters generalize dsDNA-induced intercellular communication to stromal cells that utilize Cx43 gap junctions. (a) HSC ISRE reporters were stimulated with increasing doses of dsDNA (2, 4, and 8 mg/mL) and imaged by fluorescence microscopy after 24 hours. Representative 10X fluorescence images HSC ISRE reporters stimulated with dsDNA. (b,c) Transplant co-culture system. Wildtype HeLa or Cx43 expressing HeLa were stimulated with 10 mg/mL dsDNA for 6 hours, washed, trypsinized, and co-cultured with HSC ISRE-GFP reporter cells. The co-culture was assayed 18 hours later by fluorescence microscopy and flow cytometry. (b) Representative 10X fluorescence images of dsDNA-stimulated wildtype HeLa or Cx43 expressing HeLa, co-cultured with HSC

ISRE-GFP reporters. (c) Relative ISRE-GFP activity quantified by flow cytometry. Data represent mean and +sd of five representative images from there independent experiments.

3.3.5 Propagation of antiviral and inflammatory responses by gap junctions

To investigate the physiological significance of gap junction-mediated amplification of IRF3 activity, we disrupted gap junctions and examined the ability of cells to mount innate immune responses. When ISRE reporters were pretreated with 18βGA and stimulated with dsDNA, they expressed significantly lower levels of critical antiviral cytokines in comparison to vehicle pretreatment. After 8 hours of dsDNA stimulation, 18βGA pretreated cells expressed 6-fold less IFNβ than vehicle treated cells (**Fig. 5a**). Expression of the IFNβ-stimulated antiviral protein PKR was also significantly reduced by 2-fold ($p<.05$) in the 18βGA treated cells, compared to vehicle treatment (**Fig. 5a**). Similarly, the expression of the proinflammatory cytokine, TNFα, was reduced by 3.5-fold with gap junction inhibition (**Fig. 5a**).

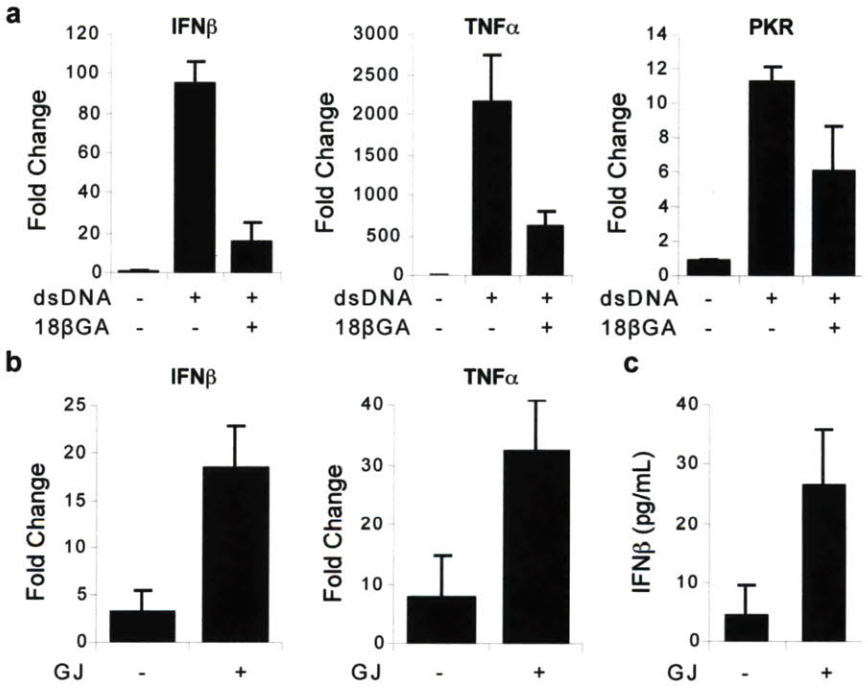

Figure 5 Gap junction communication results in propagation of anti-viral and inflammatory signals in response to dsDNA stimulation (a) ISRE-GFP reporter cells were stimulated with 4 μg/mL dsDNA for 8 hours, in the presence or absence of 18βGA. Expression of IFNβ, TNFα, and PKR was assessed by qRT-PCR. (b,c) Reporter cells (of rat lineage), expressing only connexin 32, were stimulated with 10 μg/mL dsDNA for 6 hours, and then co-cultured with unstimulated gap junction deficient (HeLa WT) or gap junction expressing (HeLa Cx32) human HeLa cells. (b) After 10 hours of co-culture, HeLa cells were analyzed by qRT-PCR for IFNβ and TNFα expression using human-specific PCR primers. (c) ELISA for

human IFNβ, secreted into co-culture supernatants by HeLa cells after 24 hours. dsDNA-stimulated reporter co-culture with HeLa WT is indicated as GJ -, and co-culture with HeLa Cx32 is indicated as GJ+.

We further verified the role of gap junctions in innate immune responses using genetically modified cells and the transplant co-culture system described above. Rat ISRE reporter cells, which express only connexin 32, were stimulated with dsDNA and then co-cultured with unstimulated human HeLa cells that either lacked gap junctions (HeLa WT) or expressed connexin 32 gap junctions (HeLa Cx32). Recipient HeLa cells were then analyzed for cytokine expression and secretion using human-specific PCR primers and ELISAs. When dsDNA-stimulated reporter cells were co-cultured with HeLa Cx32 cells, HeLa IFNβ and TNFα expression was increased by 6 and 4-fold respectively, compared to co-culture with gap junction deficient HeLa WT cells (**Fig 5b**). Additionally, co-culture of dsDNA-stimulated reporters with HeLa Cx32 cells triggered a 5-fold increase in production of human IFNβ compared to co-culture with gap junction deficient HeLa WT cells (**Fig. 5c**). Taken together, these data suggest that gap junctions amplify dsDNA-induced expression and secretion of IFNβ and TNFα, and that without functional gap junctions, cytokine secretion is impaired, consequently reducing the anti-viral state in the overall population.

3.4 Discussion

Investigations of innate immune response propagation have typically focused on the paracrine action of secreted cytokines [23]. Here we provide evidence that gap junctions amplify innate immune responses triggered by cytosolic dsDNA. Using a stable monoclonal GFP reporter cell line that is sensitive and specific for IRF3-mediated gene expression, we visualized the spatiotemporal evolution of IRF3 activity in response to dsDNA stimulation. Sorting these cells by GFP activity, we demonstrated that dsDNA stimulation of confluent cell monolayers leads to the formation of two distinct cell populations, each with a unique gene expression program. The IRF3-active subpopulation was spatially arranged in multi-cellular colonies that collectively served as the dominant source of diffusible cytokines for the establishment of an overall antiviral state. These colonies were formed by gap junction-dependent communication between dsDNA-stimulated cells and their unstimulated neighbors. In the absence of gap junctions, IRF3-activated colonies and total cytokine secretion were significantly diminished, as was the resulting antiviral state. These findings place contact-dependent communication upstream of secreted cytokines, at the earliest stages of dsDNA-induced antiviral and

inflammatory responses, and they offer gap junction communication as a novel mechanism for amplifying dsDNA-mediated innate immunity.

Gap junctions are networks of intercellular communication channels that allow local cell populations to rapidly share and spread signals [16]. This work has indentified a gap junction-dependent 'recruitment' process whereby infected cells engage surrounding non-infected cells to secrete cytokines. The molecular details of this process, its mediator, its regulation, and the pathways that lead to its generation remain unclear and further investigation is necessary. Many common gap junction communication mediators such as Ca^{++}, cAMP, and IP3, have been implicated in the activation of inflammatory transcription factors [24, 25]. For example calcium fluxes have been shown to activate transcription factors such as NFκB and AP1, resulting in the expression of proinflammatory cytokines [24]. While there are links connecting gap junction communication and inflammation, our results represent the first connection to antiviral responses.

Secreted cytokines such as IFNβ and TNFα are known to mediate the spread of antiviral and inflammatory signals for the protection of non-infected cells against subsequent attack [3]. However, at the earliest stages of an infection, when only a limited number of cells have been exposed to the pathogen, recruitment of neighboring non-infected cells and amplification of cytokine production is particularly important. Paracrine feed-forward loops have been proposed to increase the number of cytokine secreting cells beyond those initially infected, however their significance is unclear [23]. For example, dsDNA stimulation of type I interferon receptor deficient macrophages induced similar IFNβ expression compared to wild-type controls, suggesting that the IFNβ paracrine loops are not necessary for amplifying IFNβ secretion [10]. In this work, we show that gap junction communication provides a mechanism for single infected cells to recruit their neighbors and amplify cytokine production prior to paracrine loops. Compared to secreted cytokine amplification, gap junction-mediated signaling is typically faster and therefore better suited for anticipating and preventing the rapid spread of an invading pathogen [16].

While the existence of dsDNA-stimulated intercellular communication is clear, the precise signaling pathway remains unknown. Evidence from transplant co-culture experiments showed the communication does not require MyD88 or TRIF, thereby eliminating the necessity of all known TLR pathways. Additionally, the communication was independent of TBK, IKKε, IKKα and IKKβ in the dsDNA sensing cell, demonstrating that signal generation and transmission occur upstream of dsDNA-induced activation of NFκB- and IRF3-associated kinases. A recently identified dsDNA-sensing molecule, DAI, was shown to bind TBK and IRF3, thereby facilitating

IRF3 phosphorylation and activation [11]. Interestingly, we found that IRF3 can be activated in cells that were never directly exposed to dsDNA. Instead, these cells only required contact with dsDNA-stimulated cells expressing compatible connexins. Since the dsDNA used in these experiments (approximately 400bp) is too large to pass through gap junctions [21], our results point to a novel mechanism for activating TBK- or IKKε–mediated phosphorylation of IRF3.

Viruses have evolved numerous strategies for silencing the defenses of infected cells. Many viruses prevent infected cells from propagating "danger signals" by inhibiting IRF3-mediated production and secretion of antiviral cytokines such as IFNβ [4, 5]. In addition to suppressing antiviral signals, dsDNA viruses such as vaccinia virus, also inhibit host proinflammatory signaling by inhibiting the activation of NFκB and limiting the secretion of TNFα and IL1β [26]. This work demonstrated that gap junctions enable the rapid local spread of dsDNA-induced IRF3-activating signals from infected cells to their non-infected neighbors, potentially allowing the escape of host "danger signals" before the virus has time to disable the antiviral program in the infected cell. This type of immediate response has the advantage of rapidly mobilizing host defenses against infection, resulting in the early secretion of large amounts of cytokines for broadly inducing an antiviral state. Indeed, we found that cells deficient in gap junctions produced significantly less IFNβ and TNFα, resulting in substantial decreases in expression of antiviral genes such as PKR. Furthermore, two dsDNA viruses that represent important causes of human disease, herpesvirus HSV2 and human papilloma virus HPV16, were shown to express viral proteins that close gap junctions of infected cells, suggesting that viruses have identified gap junction communication as a critical mode for host defense signaling, and have begun evolving strategies to inhibit these defenses [27, 28].

Mammalian cells are exposed to intracellular dsDNA during viral and intracellular bacterial infection, during exposure to self-DNA from dying cells, and during DNA-based gene therapy [7, 9-11, 14]. The ability to increase and decrease the innate immune response in these settings would have significant potential as a clinically relevant therapeutic. In this regard, the stable monoclonal ISRE reporter represents an important experimental tool for discovering modulators of the innate immune responses to these stimuli and the intercellular communication mechanisms they utilize for propagation and amplification. However, modulation of gap junction communication continues to be experimentally challenging. Genetic methods are certainly the most definitive; however the degeneracy of connexin proteins required to form functional gap junctions is such that cells deficient in individual connexins may not show significant defects due to compensatory expression of other connexins. Future studies will be needed to evaluate the

full physiologic significance of gap junction communication in augmenting responses to dsDNA-based stimuli.

3.5 Materials and Methods

Cells and reagents

Hepatocyte-derived H35 cells were grown in high glucose DMEM (Gibco) media, supplemented with 10% FBS, 2% penicillin-streptomycin, and 1% MEM sodium pyruvate (100 mM) [29]. Rat hepatic stellate cell line HSC-T6 was a gift (see Acknowledgements). Mouse embryonic fibroblasts from wildtype C57BL/6, Myd88$_{-/-}$Trif$_{-/-}$, Tbk$_{-/-}$Ikke$_{-/-}$, Ikka$_{-/-}$Ikkb$_{-/-}$, and Cx43$_{-/-}$ knockout mice were gifts (see Acknowledgements). Wildtype and connexin 26, 32, and 43 expressing HeLa and N2A cells were also gifts (see Acknowledgements). All cells were maintained in the supplemented DMEM described above. Synthetic polydeoxynucleotides, poly(dA-dT):poly(dA-dT) dsDNA and poly(dA-dT) ssDNA, were purchased from Amersham Biosciences. Synthetic poly(I:C) and CpG ODN were purchased from Invivogen. LPS and 18β-glycyrrhetinic acid were purchased from Sigma Aldrich, and pdsRED was purchased from Clontech. Poly(AT) dsDNA was labeled with CX-Rhodamine (ROX) using a Label-IT nucleic acid localization kit (Mirus Bio), according to the manufacturers' protocol.

ISRE reporter construction and characterization

The construction and characterization of the ISRE-GFP reporter was performed as described previously [29]. Briefly, a reporter plasmid was designed to contain multiple ISRE consensus sequences (GAAACTGAAACT, for monitoring the binding of IRF3 [12]) upstream of a CMV minimal promoter, upstream of an EGFP gene. Plasmid DNA was electroporated into H35 and HSC-T6 cells and antibiotic drug selection was used to isolate stably transfected cells. Using FACS, stably transfected cells were sorted for GFP-positive responses to Poly(AT) dsDNA, and for GFP-negative responses in the absence of dsDNA. As a result, reporter cells with high inducibility and low baseline expression were identified. Limited dilution was performed to obtain single monoclonal ISRE-GFP reporter cell lines.

Quantitative RT-PCR

Total RNA was extracted from target cells using the PureLink RNA Mini kit (Invitrogen), according to the manufacturer's protocol. Total RNA (1 μg) was used as template to generate cDNA by reverse-transcription. Quantitative RT-PCR was performed using the Stratagene Mx3000P QPCR System and the SuperScript Platinum Two-Step qRT-PCR SYBR-Green kit (Invitrogen). cDNA (50 ng) was used as template in real time- quantitative PCR with primers pairs listed in Supplementary Table 1. Using the comparative cycle threshold (C_t) method, all

data was normalized to endogenous reference gene β-actin and then compared to appropriate controls for calculation of fold change.

Rat IFNβ	Forward	TGAATGGAAGGCTCAACCTC
	Reverse	AGTCTCATTCCACCCAGTGC
Rat TNFα	Forward	GTCTGTGCCTCAGCCTCTTC
	Reverse	GCTTGGTGGTTTGCTACGAC
Rat IP10	Forward	TGTCCGCATGTTGAGATCAT
	Reverse	GGTCAGGAGAAACAGGGACA
Rat PKR	Forward	GAGACTGCCCCAGAAAACAG
	Reverse	ATTTGGACTCCCACGTTCAG
Rat OAS1	Forward	GACGGGGAGAGTTCATCAAG
	Reverse	CTTGGGATCAGGATTGCTGT
Rat β-Actin	Forward	GTCGTACCACTGGCATTGTG
	Reverse	CTCTCAGCTGTGGTGGTGAA
Rat-specific primers for transplant co-culture experiments		
IFNβ	Forward	GCTATTACTGGAGGGTACAAAGG
	Reverse	AGAATAATGGAAAAGTTCCTGAAGA
TNFα	Forward	TGACCCCCATTACTCTGACC
	Reverse	CGTGTGTTTCTGAGCATCGT
PKR	Forward	CCCAATTGCCTCACAGATTT
	Reverse	CAGTTTTCGATGGGCTTTTC

Supplementary Table 1: Quantitative real-time PCR primers

Fluorescent microscopy and image analysis

Fluorescence images were captured on a Zeiss 200 Axiovert microscope and quantified using custom image analysis routines written in MATLAB. Briefly, images were median filtered, auto-thresholded, and segregated to identify discreet regions representing colonies. Colony outlines were plotted by displaying iso-intensity lines at the determined threshold level. Colony areas were calculated, sorted and plotted versus colony index. Colony areas are expressed in terms of cell number. Areas were converted to cell number by manually counting large multi-cell colonies and calculating the area-to-cell ratio. In Figures 1 and 4, colonies less than 1 cell were considered an artifact of image analysis and were ignored. In Figure 4, all colonies containing more than 3 cells were binned together and considered multi-cellular colonies, and colonies containing less than 3 cells were binned separately.

ELISA

Human HeLa cells (wildtype and connexin expressing) were grown to 70% confluency in 12-well plates. DNA- stimulated rat H35 cells were co-cultured onto a sub-confluent HeLa monolayer. After 24 hours, co-culture supernatants were used to determine the amount of human IFNβ and TNFα secreted by the HeLa cells, as measured by ELISA (PBL and R&D Systems) according to

manufacturer's instructions. Manufacturers' specifications ensured cross-reactivity between rat and human IFNβ and TNFα was less than 1%.

Transplant co-culture assay

Donor cells were transfected with 10 μg/mL of B-form dsDNA. Six hours after transfection, donor cells were trypsinized, washed 3 times in PBS, and counted. dsDNA-stimulated donor cells ($1x10^5$ cells/mL) were transplanted onto a sub-confluent layer of recipient ISRE reporters, maintaining a 1:10 ratio between donor and recipient cells. After 18 hours of co-culture, recipient reporter cells were analyzed by fluorescent microscopy and FACS for ISRE activity. In some cases, IFNβ and TNFα secretion by recipient cells was measured by ELISA. Gene expression analysis on recipient cells was performed by quantitative real time PCR, using recipient cell species-specific primers, provided in Supplementary Table 1.

RNA Interference

Interference of rat Cx32 mRNA was performed by using Dharmacon designed ON-TARGETplus SMARTpool siRNA duplexes targeting Cx32 (#L-091222-01). Control siRNA (siCONTROL Non-targeting siRNA#1) was also purchased from Dharmacon. H35 ISRE-GFP reporters were transfected with 100 nM siRNA using Lipofectamine 2000 (Invitrogen), according to the manufacturers' protocol. At 36 hours post siRNA transfection, cells were stimulated with dsDNA for further experiments. Knockdown of Cx32 mRNA was verified by quantitative RT-PCR (see Supplementary Data).

Acknowledgements

The authors thank S. Akira for the generous gift of $Myd88^{-/-}Trif^{-/-}$ and $Tbk^{-/-}Ikke^{-/-}$ MEFs, I. Verma for $Ikka^{-/-}Ikkb^{-/-}$ MEFs, S.L. Friedman for HSC-T6 cells, D. Spray for Cx26, Cx32, and Cx43 expressing N2A cells, K. Willecke for Cx26, Cx32, and Cx43 expressing HeLa cells. The authors thank Ken Wieder and Arno Tilles for technical support. S.J.P was supported by a Department of Defense CDMRP Prostate Cancer Predoctoral Training Award. K.R.K was supported by a Shriners Hospital for Children Postdoctoral Fellowship. The work was supported by grants from the US National Institutes of Health (GM065474 and P41 EB-002503) and from the Shriners Hospital for Children.

3.6 References

1. Carter, W.A. & De Clercq, E. Viral infection and host defense. *Science* **186**, 1172-1178 (1974).
2. Kawai, T. & Akira, S. Innate immune recognition of viral infection. *Nat Immunol* **7**, 131-137 (2006).
3. Hiscott, J. Convergence of the NF-kappaB and IRF pathways in the regulation of the innate antiviral response. *Cytokine Growth Factor Rev* **18**, 483-490 (2007).
4. Alcami, A. Viral mimicry of cytokines, chemokines and their receptors. *Nat Rev Immunol* **3**, 36-50 (2003).
5. Marques, J.T. & Carthew, R.W. A call to arms: coevolution of animal viruses and host innate immune responses. *Trends Genet* **23**, 359-364 (2007).
6. Janeway, C.A., Jr. & Medzhitov, R. Innate immune recognition. *Annu Rev Immunol* **20**, 197-216 (2002).
7. Ishii, K.J. & Akira, S. Innate immune recognition of, and regulation by, DNA. *Trends Immunol* **27**, 525-532 (2006).
8. Kato, H. *et al.* Differential roles of MDA5 and RIG-I helicases in the recognition of RNA viruses. *Nature* **441**, 101-105 (2006).
9. Ishii, K.J. *et al.* A Toll-like receptor-independent antiviral response induced by double-stranded B-form DNA. *Nat Immunol* **7**, 40-48 (2006).
10. Stetson, D.B. & Medzhitov, R. Recognition of cytosolic DNA activates an IRF3-dependent innate immune response. *Immunity* **24**, 93-103 (2006).
11. Takaoka, A. *et al.* DAI (DLM-1/ZBP1) is a cytosolic DNA sensor and an activator of innate immune response. *Nature* **448**, 501-505 (2007).
12. Au, W.C., Moore, P.A., Lowther, W., Juang, Y.T. & Pitha, P.M. Identification of a member of the interferon regulatory factor family that binds to the interferon-stimulated response element and activates expression of interferon-induced genes. *Proc Natl Acad Sci U S A* **92**, 11657-11661 (1995).
13. Grandvaux, N. *et al.* Transcriptional profiling of interferon regulatory factor 3 target genes: direct involvement in the regulation of interferon-stimulated genes. *J Virol* **76**, 5532-5539 (2002).
14. Muruve, D.A. *et al.* The inflammasome recognizes cytosolic microbial and host DNA and triggers an innate immune response. *Nature* **452**, 103-107 (2008).
15. Downward, J. The ins and outs of signalling. *Nature* **411**, 759-762 (2001).

16. Segretain, D. & Falk, M.M. Regulation of connexin biosynthesis, assembly, gap junction formation, and removal. *Biochim Biophys Acta* **1662**, 3-21 (2004).
17. Goldberg, G.S., Valiunas, V. & Brink, P.R. Selective permeability of gap junction channels. *Biochim Biophys Acta* **1662**, 96-101 (2004).
18. Chanson, M. *et al.* Regulation of gap junctional communication by a pro-inflammatory cytokine in cystic fibrosis transmembrane conductance regulator-expressing but not cystic fibrosis airway cells. *Am J Pathol* **158**, 1775-1784 (2001).
19. Jara, P.I., Boric, M.P. & Saez, J.C. Leukocytes express connexin 43 after activation with lipopolysaccharide and appear to form gap junctions with endothelial cells after ischemia-reperfusion. *Proc Natl Acad Sci U S A* **92**, 7011-7015 (1995).
20. Martin, F.J. & Prince, A.S. TLR2 regulates gap junction intercellular communication in airway cells. *J Immunol* **180**, 4986-4993 (2008).
21. del Corsso, C. *et al.* Transfection of mammalian cells with connexins and measurement of voltage sensitivity of their gap junctions. *Nat Protoc* **1**, 1799-1809 (2006).
22. Elfgang, C. *et al.* Specific permeability and selective formation of gap junction channels in connexin-transfected HeLa cells. *J Cell Biol* **129**, 805-817 (1995).
23. Honda, K., Takaoka, A. & Taniguchi, T. Type I interferon [corrected] gene induction by the interferon regulatory factor family of transcription factors. *Immunity* **25**, 349-360 (2006).
24. Dolmetsch, R.E., Xu, K. & Lewis, R.S. Calcium oscillations increase the efficiency and specificity of gene expression. *Nature* **392**, 933-936 (1998).
25. Bodor, J. *et al.* Suppression of T-cell responsiveness by inducible cAMP early repressor (ICER). *J Leukoc Biol* **69**, 1053-1059 (2001).
26. Deng, L., Dai, P., Ding, W., Granstein, R.D. & Shuman, S. Vaccinia virus infection attenuates innate immune responses and antigen presentation by epidermal dendritic cells. *J Virol* **80**, 9977-9987 (2006).
27. Fischer, N.O., Mbuy, G.N. & Woodruff, R.I. HSV-2 disrupts gap junctional intercellular communication between mammalian cells in vitro. *J Virol Methods* **91**, 157-166 (2001).
28. Oelze, I., Kartenbeck, J., Crusius, K. & Alonso, A. Human papillomavirus type 16 E5 protein affects cell-cell communication in an epithelial cell line. *J Virol* **69**, 4489-4494 (1995).
29. King, K.R. *et al.* A high-throughput microfluidic real-time gene expression living cell array. *Lab Chip* **7**, 77-85 (2007).

Chapter 4

Identification of a Gap Junction Communication Pathway for Preventing Drug-induced Liver Failure and Sterile Inflammation

4.1 Summary

At the onset of sterile injury, damaged cells stimulate potent inflammatory responses that amplify the overall injury and contribute to organ dysfunction and disease, however little is known about how this process unfolds [1, 2]. An important clinical example of sterile injury is drug-induced liver injury, the most common cause of acute liver failure and a significant public health crisis [3]. Here we show that drug-induced liver injury is dependent on gap junction communication to amplify sterile inflammatory signals generated in response to the initial toxic injury. Mice deficient in hepatic gap junction protein connexin 32 (Cx32) were protected against liver damage, inflammation, and death in response to hepatotoxic drug-induced injury. Administration of these drugs resulted in the production of intracellular free radicals that propagated through gap junctions, damaging naïve surrounding cells and expanding the tissue injury front, thereby establishing the sterile inflammatory response. Coadministration of a selective pharmacologic Cx32 inhibitor, 2-aminoethyoxydiphenyl-borate, with the hepatotoxic drugs significantly limited hepatocyte damage and sterile inflammation, and completely abrogated mortality, confirming the importance of hepatic gap junction communication in sterile injury. These findings suggest inhibition of hepatic gap junctions as a viable novel therapeutic strategy for preventing drug hepatotoxicity and potentially other forms of sterile injury.

4.2 Introduction

Drug-induced sterile liver injury is the most common cause of acute liver failure in the developed world, accounting for up 50% of all clinical cases [3]. It is also the leading cause for termination of drug development and drug withdrawal from the market [4]. At the onset of drug-induced liver failure, toxic drug metabolites lead to hepatocyte death by oxidative stress and necrosis [5]. This results in secondary activation of the innate immune system, as the initially distressed hepatocytes stimulate a potent sterile inflammatory response that spreads from the local cellular microenvironment to the uninjured tissue at-large, triggering parenchymal dysfunction and ultimately liver failure [6, 7, 8, 9]. It is currently unclear which mechanisms are vital for communication of injury from the cellular to the tissue level.

In addition to the paracrine actions of potent proinflammatory cytokines, gap junction intercellular communication (GJIC) pathways have recently been implicated in the propagation

of inflammatory signals [10, 11, 12]. However, the mechanisms underlying these pathways and the relative contribution of gap junctions to sterile injury remain speculative. Gap junctions are composed of connexin proteins (Cx) that directly connect the cytosol of coupled cells to allow free exchange of ions and secondary messengers to locally spread cellular signals [13]. Recent investigations in innate immunity suggest that inflammatory responses are amplified by GJIC, raising the possibility that these communication pathways also play a significant role in establishing drug-induced sterile liver injury [10, 11].

4.3 Results

To examine whether GJIC is involved in drug-induced sterile liver injury, we injected the classic hepatotoxin thioacetamide (TAA) into mice deficient in Cx32 ($Cx32^{-/-}$), the predominant hepatic gap junction protein. After 24 hours, $Cx32^{+/+}$ mice had significantly elevated ALT/AST levels, indicative of hepatocyte damage, while $Cx32^{-/-}$ mice exhibited near normal levels of ALT/AST and significantly reduced histological evidence of damage (Fig. 1a-c). Proinflammatory cytokine expression, representative of the overall sterile inflammatory response of the liver, was also attenuated in $Cx32^{-/-}$ mice, as was the associated recruitment of neutrophils as assayed by myeloperoxidase (MPO) (Fig. 1d,e). This significantly reduced hepatotoxicity resulted in 100% survival of the $Cx32^{-/-}$ mice, compared to 100% mortality in $Cx32^{+/+}$ (Fig. 1f). We further demonstrated that this protection against TAA hepatotoxicity was not a result of defective drug metabolism in the liver by showing that serum concentrations of TAA and its toxic metabolite were the same in $Cx32^{+/+}$ and $Cx32^{-/-}$ mice, as was cytochrome P450 and GST activity (Supplementary Fig. 1,2).

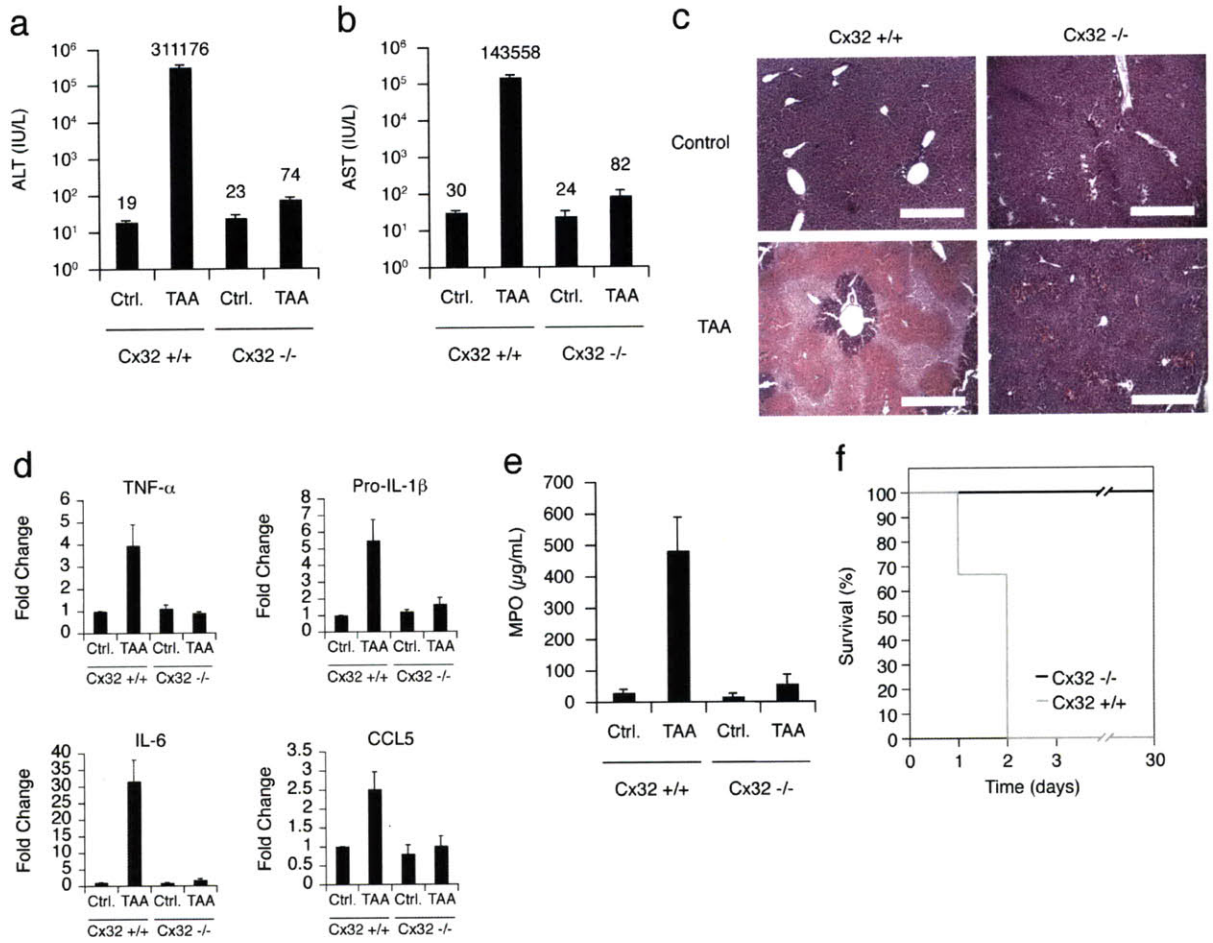

Figure 1. Thioacetamide-mediated liver injury is dependent on connexin 32. (a,b) Significantly lower serum transaminase levels in Cx32-/- compared with Cx32+/+ mice 24 hours after treatment with a single sub-lethal dose of TAA (200 mg/kg). (c) Less liver hemorrhaging, necrosis, and acute inflammation in Cx32-/- mice compared with Cx32+/+ mice 24 hours after TAA treatment (H&E staining; original magnification 10X; scale bar = 400 μm). (d) Increase in total liver TNF-α, pro-IL-1β, IL-6, and CCL5 transcripts, as measured by Q-PCR, in Cx32+/+ mice 12 hours after TAA, compared to Cx32-/- mice. (e) Liver tissue myeloperoxidase activity (MPO) in Cx32+/+ and Cx32-/- mice 24 hours after treatment with TAA. (f) Kaplan-Meier survival curve for Cx32+/+ and Cx32-/- mice over 30 days after a single lethal dose of 500 mg/kg TAA (Cx32+/+ and Cx32-/-: n=12).

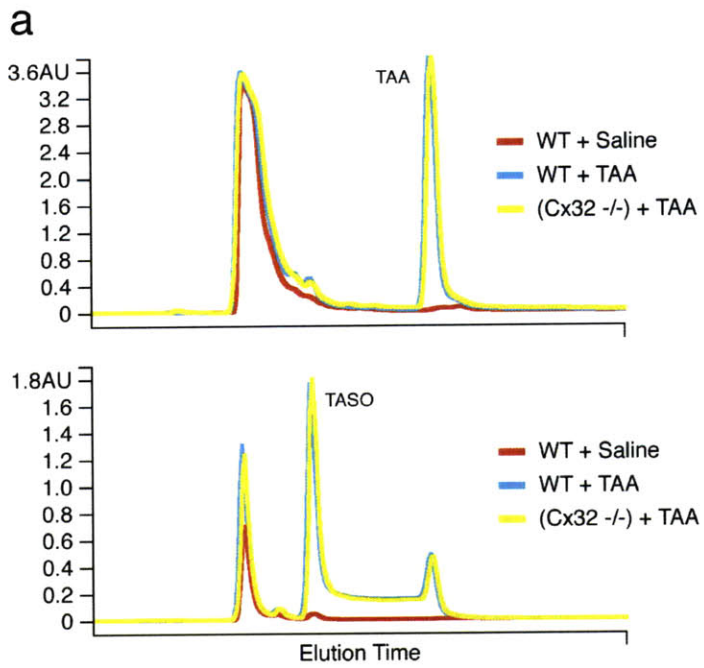

b

	Cx32 +/+ Saline	Cx32 +/+ TAA	Cx32 -/- TAA
TAA (μg/mL)	-	986 ± 31	983 ± 27
TASO (μg/mL)	-	187 ± 13	178 ± 9

Supplementary Figure 1. Deficiency in Cx32 does not affect xenobiotic metabolism. HPLC analysis was performed to demonstrate that the protection against TAA hepatotoxicity in Cx32-/- mice was not a result of defective drug metabolism in the liver. A reverse-phase HPLC assay was used to quantify the serum concentrations of TAA and its toxic metabolite, TASO, in Cx32+/+ and Cx32-/- treated with saline or TAA (1000 mg/kg) for 90 minutes. Standards were prepared by including known amounts of TAA and TASO in plasma from untreated mice. Equal concentrations of TAA and TASO were found in sera of Cx32+/+ and Cx32-/- mice treated with TAA.

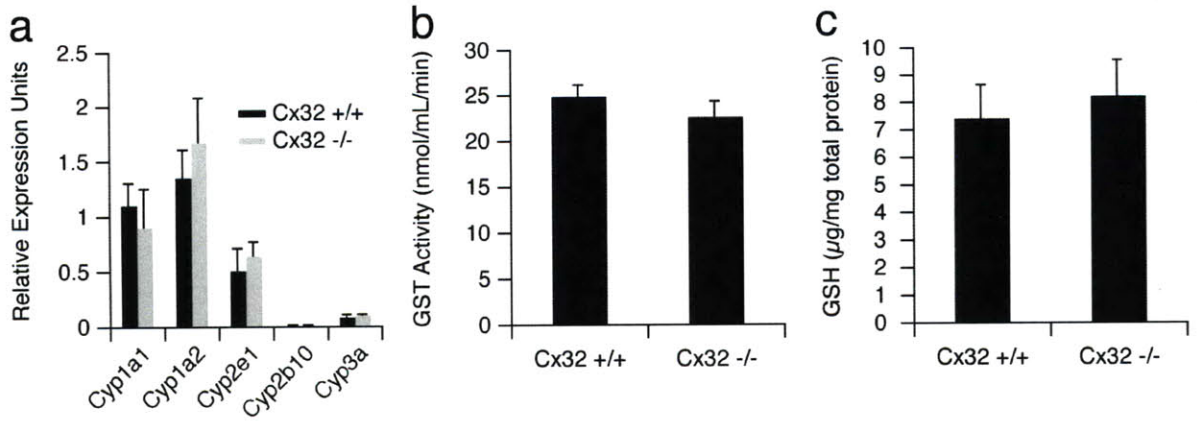

Supplementary Figure 2. Phase I and II drug metabolism efficiency is similar in Cx32+/+ and Cx32-/- mice. Whole livers were excised from untreated Cx32+/+ and Cx32-/- mice and processed for analysis. (a) Q-PCR for cytochrome P450 enzymes Cyp1a1, Cyp1a2, Cyp2e1, Cyp2b10, and Cyp32 reveals approximately equal expression in Cx32+/+ and Cx32-/- livers. (b) Analysis of GST activity shows equal activity in Cx32+/+ and Cx32-/- livers. (c) Total GSH content was found to be similar in Cx32+/+ and Cx32-/- livers.

The dependency of drug-induced liver failure on Cx32 suggested that hepatic GJIC might be involved in propagating sterile tissue injury via permeable mediators. Given the clear role of ROS in drug-induced hepatotoxicity [14, 15], we investigated whether blocking hepatic gap junctions can abrogate the propagation of free radicals during sterile injury. Livers stained *ex vivo* for ROS activity revealed intense focal regions of intracellular ROS in $Cx32^{+/+}$ mice, compared to minimal ROS activity in $Cx32^{-/-}$ mice treated with TAA (Fig. 2a). To determine the dependence of drug-induced sterile injury on ROS, we utilized DMSO as a free radical scavenger [16]. Coadministration of DMSO with TAA significantly reduced serum ALT/AST, and prevented liver injury and inflammation in $Cx32^{+/+}$ mice (Fig. 2b-c). Together, these results suggest that ROS are essential for triggering drug-induced liver injury, and demonstrate that deficiency in Cx32 results in markedly reduced hepatic intracellular free radical levels.

To further clarify how gap junctions regulate ROS levels in liver injury, we determined whether hepatocytes generate ROS when challenged with hepatotoxins *in vitro*. Flow cytometry analysis of hepatocyte-derived H35 cells loaded with an ROS probe and stimulated with TAA, its reactive metabolite (TASO), or hydrogen peroxide (H_2O_2) revealed a significant increase in mean fluorescence intensity of cells treated with H_2O_2 and TASO, compared to those treated with TAA (Fig. 2d). This is consistent with prior investigations showing that cultured hepatocytes often require pharmacological induction to metabolize drugs [17].

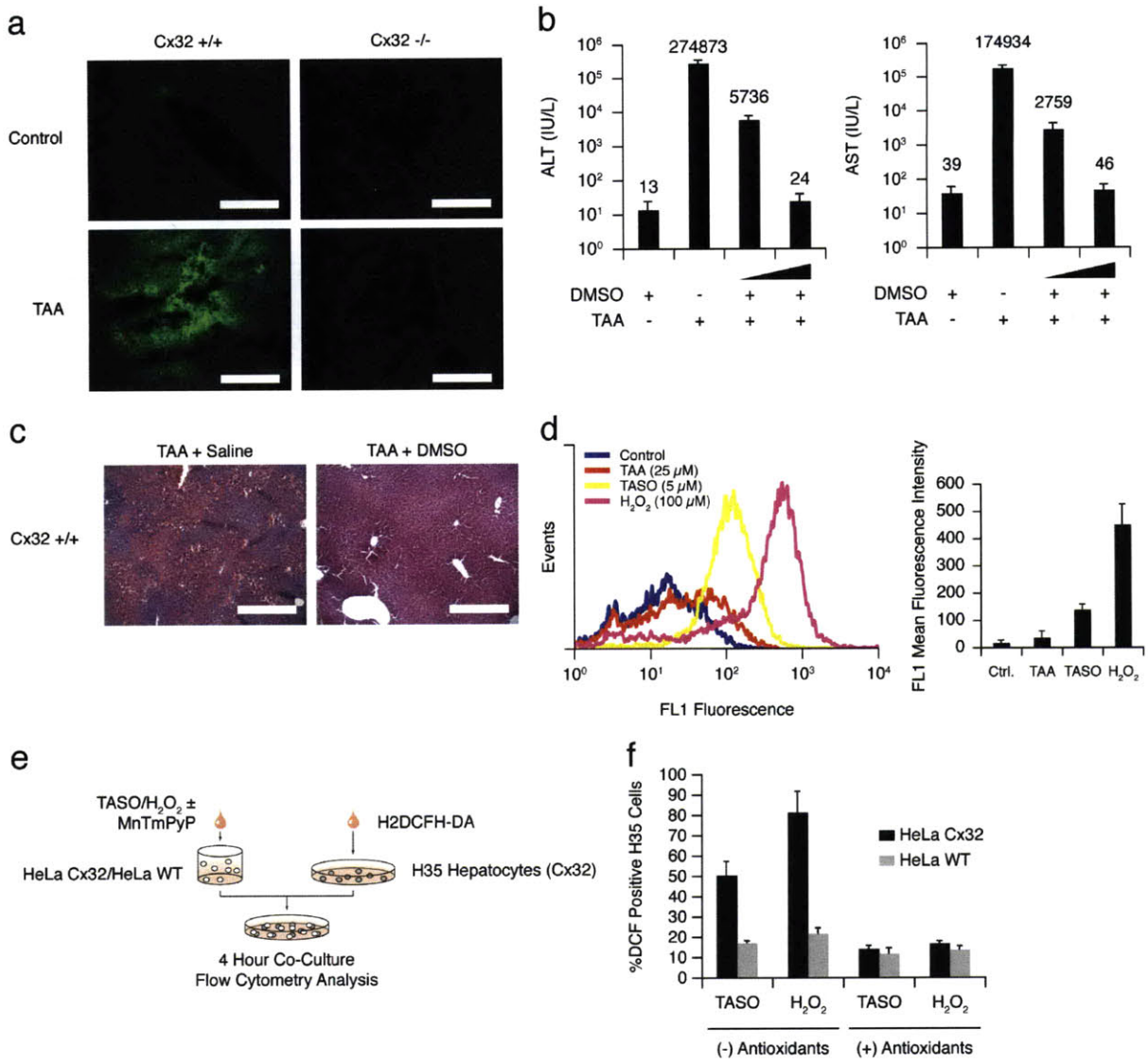

Figure 2. Free radicals are propagated by connexin 32 gap junctions to amplify oxidative stress in response to drug-induced liver injury. (a) Freshly prepared liver cryosections (7 μm) from Cx32+/+ and Cx32-/- mice treated with TAA (200 mg/kg) for 4 hours were stained with H2DCFH-DA, a cell permeable ROS probe that is converted by intracellular ROS to the fluorescent derivative DCF, and analyzed by fluorescence microscopy (original magnification 10X; scale bar = 400 μm; n>5). (b,c) Oxygen free radical scavenger dimethyl sulfoxide (DMSO) was utilized to demonstrate the dependency of drug-induced hepatotoxicity on oxidative stress. (b) Serum transaminase levels in wildtype mice 24 hours after treatment with either saline (1 mL/kg) plus TAA (200 mg/kg) or DMSO (0.1 or 1 mL/kg) plus TAA (200 mg/kg). (c) H&E staining of livers (original magnification 10X; scale bar = 400 μm) from wildtype mice 24 hours after treatment with saline plus TAA or DMSO plus TAA. (d) Hepatocyte-derived H35 cells were treated with 25 μM TAA, 5 μM Thioacetamide S-oxide (TASO, the reactive metabolite of TAA), or 100 μM hydrogen peroxide (H_2O_2; as a positive control) for 2 hours, stained with H2DCFH-DA and analyzed by

cytometry for determining levels of intracellular ROS. Flow cytometry distribution of H2DCFH-DA fluorescence and mean fluorescence intensity. (e) *In vitro* co-culture system schematic. Wildtype HeLa cells (HeLa WT) deficient in connexin proteins and Cx32 expressing HeLa cells (HeLa Cx32) were stimulated with TASO (5 μM) or H_2O_2 (100 μM; as a positive control) for 2 hours, in the presence or absence of cell permeable antioxidant/free radical scavenger MnTMPyP, and plated onto H35 hepatocytes loaded with ROS probe H2DCFH-DA at a cell ratio of 2:1. Four hours later, the co-culture was analyzed by flow cytometry for gap junction mediated transfer of ROS into H35 cells. (f) ROS levels in H35 cells, as determined by flow cytometry.

We next devised an *in vitro* co-culture system to investigate whether intracellular ROS propagate through Cx32 gap junctions. Connexin deficient HeLa cells (HeLa WT) and Cx32 expressing HeLa cells (HeLa Cx32) were stimulated with TASO in the presence or absence of a free radical scavenger [15], and plated onto Cx32 expressing H35 hepatocytes loaded with a ROS probe (Fig. 2e). Flow cytometry analysis of the co-culture revealed that, in the absence of a free radical scavenger, TASO-stimulated HeLa Cx32 cells were able to propagate a ROS inducing signal to H35 cells (Fig. 2f). In contrast, TASO-stimulated HeLa WT cells were unable to transmit this signal to H35 cells (Fig. 2f). To determine the nature of this signal, we incubated the HeLa cells with a free radical scavenger concurrently with TASO to remove generated free radicals. In the presence of the scavenger, TASO-stimulated HeLa Cx32 cells were unable to propagate the ROS inducing signal to H35 cells (Fig. 2f). These findings suggest that connexin 32 amplifies drug-induced liver failure by allowing for the propagation of free radicals from hepatotoxin-injured cells to surrounding naïve cells, thereby augmenting the downstream sterile inflammatory response.

We then sought to explore whether pharmacological inhibition of hepatic gap junctions can prevent drug-induced liver injury. Although many inhibitors of gap junctions lack specificity, 2-aminoethoxydipenyl-borate (2-APB) has been shown to exclusively inhibit Cx32 gap junction channels *in vitro* [18]. We first tested whether 2-APB can exogenously inhibit hepatic gap junctions *in vivo* by developing a tissue version of the classic "scrape and load" gap junction assay. In this assay, 2-APB was administered *in vivo*, and livers were excised for *ex vivo* analysis. Liver slices were damaged locally, loaded with gap junction permeable Lucifer yellow (LY) and impermeable Texas red-dextran (TRD), and analyzed for fluorescent dye spread. $Cx32^{+/+}$ mice treated with saline showed significant gap junction connectivity, as demonstrated by the spread of gap junction permeable LY, compared to gap junction impermeable TRD (Fig. 3a). In contrast, $Cx32^{-/-}$ mice showed minimal gap junction connectivity as did $Cx32^{+/+}$ mice treated with 2-APB (Fig. 3a). Contour maps of the images, where the red and green regions

depict the spread of the TRD and LY, respectively, were used to aid in visualization and quantification (Fig. 3a). We further demonstrated that coadministration of TAA with 2-APB in $Cx32^{+/+}$ mice significantly abrogated ROS levels (Supplementary Fig. 3). These data indicate that small molecule inhibitors of gap junctions, such as 2-APB, can be utilized to specifically block hepatic gap junctions *in vivo*.

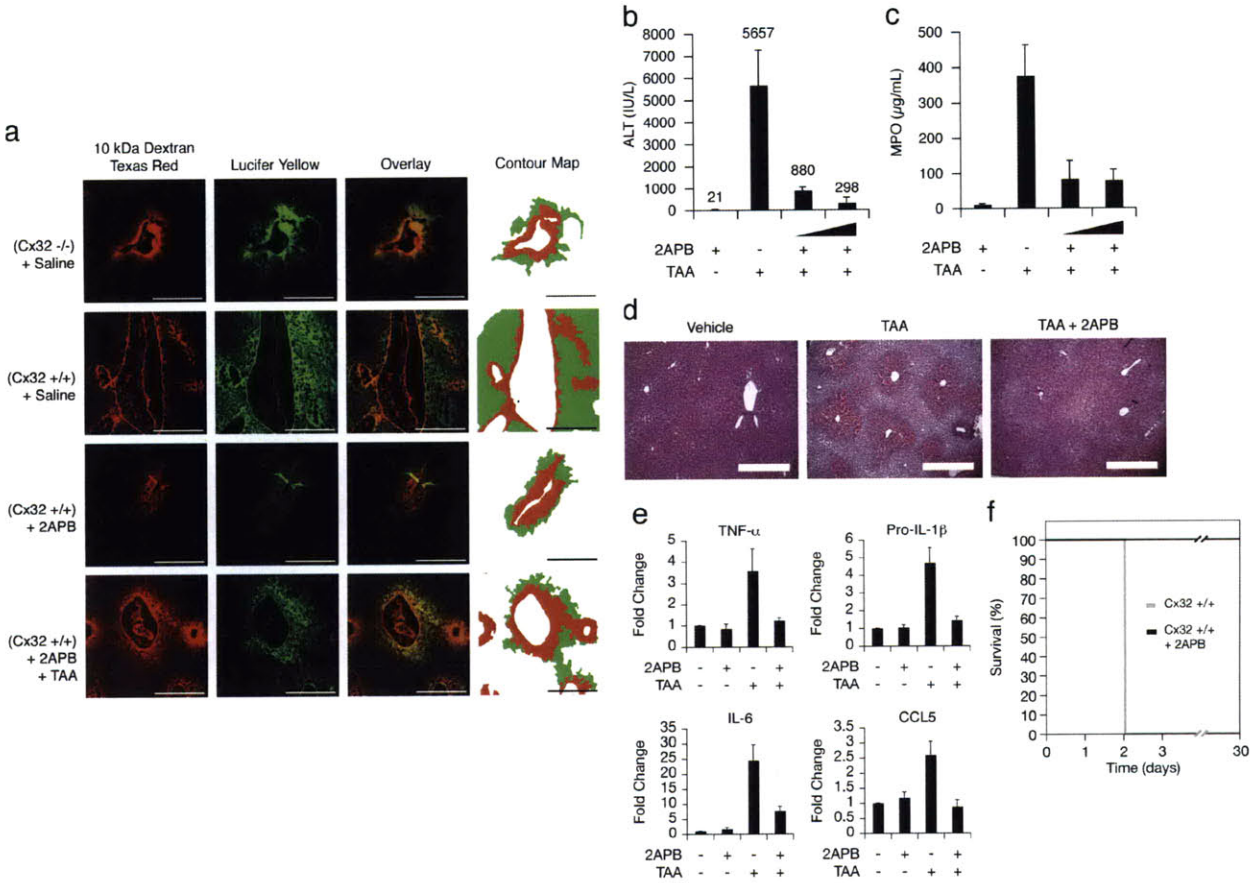

Figure 3. Pharmacologic inhibition of hepatic gap junctions prevents drug-induced liver failure and enhances survival. (a) A tissue version of the scrape and load test was developed to demonstrate functional gap junction intercellular communication in liver tissue. Cx32+/+ and Cx32-/- mice were treated with saline, 2APB (20 mg/kg), or 2APB plus TAA (200 mg/kg) for 3 hours. Livers were excised, cut into 2-3 mm slices, and a small area of each slice was mechanically damaged with the insertion of a 27 gauge needle coated with 0.5% Lucifer yellow (gap junction permeable) and 0.5% Texas red labeled dextran (gap junction impermeable). Slices were washed, fixed, cryosectioned (7 μm), and analyzed by fluorescence microscopy (n>5) and custom automated image analysis software to produce iso-intensity contour maps outlining spread of Lucifer yellow and dextran-Texas red. (b) Serum transaminase levels and (c) liver tissue myeloperoxidase activity (MPO) in wildtype mice 24 hours after treatment with 2APB alone, TAA (200 mg/kg) plus vehicle, or TAA (200 mg/kg) plus 2APB (1 or 20 mg/kg). (d) H&E staining of

livers (original magnification 10X; scale bar = 400 μm) from wildtype mice 24 hours after treatment with vehicle, TAA (200 mg/kg), or TAA (200 mg/kg) plus 2APB (20 mg/kg). (e) Q-PCR for TNF-α, pro-IL-1β, IL-6, and CCL5 from whole livers of mice treated as described above. (f) Kaplan-Meier survival curve for Cx32+/+ mice over 30 days after a single dose of TAA (500 mg/kg) plus vehicle, or TAA (500 mg/kg) plus 2APB (20 mg/kg). (n=10).

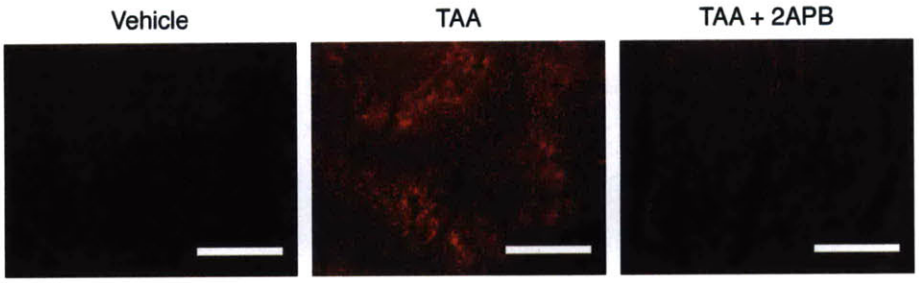

Supplementary Figure 3. Coadministration of TAA with 2-APB abrogated hepatic ROS levels. Liver cryosections from Cx32+/+ mice treated with vehicle, TAA (200 mg/kg) plus vehicle, or TAA (200 mg/kg) plus 2APB (20 mg/kg) for 4 hours were stained with dihydroethidium, a cell permeable free radical probe that binds nucleic DNA and becomes fluorescent when reduced, and analyzed by fluorescence microscopy for ROS activity (n>5).

To determine whether liver injury could be reduced by inhibition of hepatic gap junctions *in vivo*, we co-injected 2-APB with TAA. Coadministration of 2-APB with TAA significantly reduced serum ALT, histological evidence of hepatic damage, and neutrophil infiltration (Fig. 3b-d). Additionally, the sterile inflammatory response was also curtailed (Fig. 3e). We then sought to determine whether a single administration of 2-APB concordantly with TAA could improve survival from drug-induced liver failure. Remarkably, administration of 2-APB with TAA resulted in 100% survival, compared to 100% mortality in mice that received TAA with vehicle (Fig. 3f). Together, these results further confirm the importance of connexin 32 gap junctions in drug-induced sterile liver injury, and also identify a new therapeutic strategy of specifically inhibiting hepatic gap junctions to prevent hepatotoxicity.

In order to test the broader applicability of these findings, we used another classic hepatotoxic drug, acetaminophen (APAP). APAP hepatotoxicity is the most common cause of death due to acute liver failure [19]. A single dose of APAP resulted in liver failure, as indicated by markedly elevated serum ALT and neutrophil recruitment (Fig. 4a,b). In contrast, a single dose of 2-APB coadministered with APAP resulted in significantly reduced serum ALT levels by 270-fold, and diminished neutrophil infiltration (Fig. 4a,b). Histological evidence of hepatic necrosis and inflammation was also substantially minimized in mice treated with 2-APB (Fig.

4c). We further demonstrated the ability of pharmacologic hepatic gap junction inhibition to minimize APAP induced liver failure by utilizing a higher, lethal concentration of APAP (Supplementary Fig. 4).

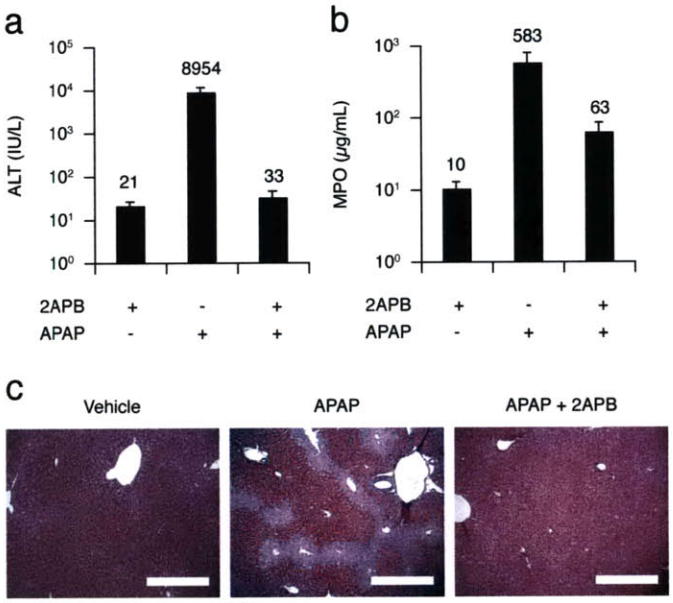

Figure 4. Acetaminophen (APAP) hepatotoxicity is limited by inhibition of hepatic gap junction communication. (a) Serum transaminase levels and (b) liver tissue myeloperoxidase activity (MPO) in wildtype mice 16 hours after treatment with 2APB (20 mg/kg), APAP (500 mg/kg) plus vehicle, or APAP (500 mg/kg) plus 2APB (20 mg/kg). (c) H&E staining of livers (original magnification 10X; scale bar = 400 μm) from wildtype mice 16 hours after treatment as described above.

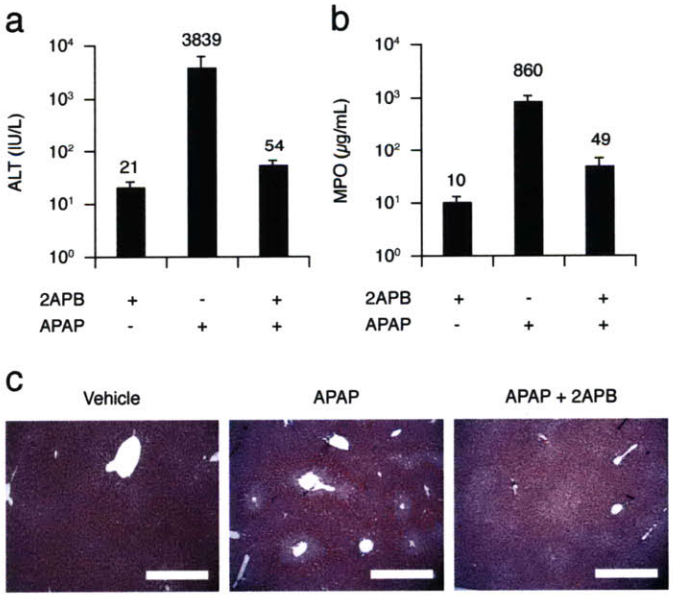

Supplementary Figure 4. Inhibition of hepatic gap junction communication limits APAP hepatotoxicity at

lethal doses. (a) Serum transaminase levels and (b) liver tissue myeloperoxidase activity (MPO) in mice 16 hours after treatment with 2APB (20 mg/kg), APAP (750 mg/kg) plus vehicle, or APAP (750 mg/kg) plus 2APB (20 mg/kg). (c) H&E staining of livers (original magnification 10X; scale bar = 400 μm) from mice 16 hours after treatment as described above.

4.4 Discussion

Our work reveals a key role for ROS in mediating gap junction dependent sterile inflammation, and raises the possibility that cell death and injury attributed to ROS generation can be limited by their inhibition. Blocking the amplification of sterile inflammation is a potentially attractive strategy not only to minimize the damage associated with drug-induced hepatotoxicity, but also to limit inflammation to tissue injury in general. These results could have significant medical implications. Drug-induced hepatotoxicity is the most common cause of acute liver failure, and with limited medical therapies for treatment, many cases result in liver transplantation or death due to a sterile inflammatory response that amplifies the initial insult [3-6]. Our findings demonstrate that drug-induced sterile liver injury is dependent on Cx32 gap junctions and selectively blocking them with small molecules can prevent liver failure and enhance survival. Similar therapies are currently in clinical trials for preventing life threatening sterile inflammation due to myocardial ischemia-reperfusion injury [20]. In summary, our work suggests that coformulation of gap junction inhibitors with hepatotoxic drugs may limit liver failure in humans, thereby increasing the number of clinically effective drugs, maximum allowable doses, and breadth of medical indications. These inhibitors may also have therapeutic potential in other types of liver injury and other organ systems.

4.5 Materials and Methods

Animals and cell lines

C57BL/6 mice were purchased from Jackson Laboratory. *Cx32*$^{-/-}$ mice were a generous gift (see Acknowledgements). All animal protocols were approved by Massachusetts General Hospital Subcommittee on Research Animal Care. For survival experiments, animals were euthanized when they became moribund according to the criteria of lack of response to stimuli or lack of righting reflex. H35 hepatocyte-derived cells were maintained as previously described [21]. Connexin 26, 32, and 43 expressing HeLa cells were gifts (see Acknowledgements).

TAA-induced hepatotoxicity

TAA (Sigma Aldrich) solution was made fresh for each experiment in 0.9% saline at 20 mg/ml. TAA was dosed at 200, 500 or 1000 mg/kg, depending on the experiment, and injected intraperitoneally. Control mice received the appropriate volume of 0.9% saline. Animals were

euthanized by ketamine/xylazine injection at 24 hours for collection of serum and liver tissue for qPCR, GSH/GST assay, MPO activity assay, and histology. For survival experiments, animals were observed every 24 hours for 30 days.

APAP-induced hepatotoxicity

APAP (Sigma Aldrich) solution was made fresh for each experiment in 0.9% saline at 20 mg/ml and heated until dissolved. APAP was dosed at 500 or 750 mg/kg, and injected intraperitoneally after 15 hours of starvation. Animals were euthanized by ketamine/xylazine injection at 12 hours for collection of serum, and liver tissue for MPO activity assay and histology.

2-Aminoethoxydiphenyl Borate treatment

2-APB (Sigma Aldrich) was made fresh for each experiment in DMSO as a vehicle at 200 mg/ml. 2-APB was dosed at 1 or 20 mg/kg, and coadministered concurrently with the appropriate dose of TAA or APAP. Vehicle control mice received the appropriate volume of DMSO with TAA or APAP.

DMSO treatment

Fresh anhydrous DMSO (Sigma Aldrich) was used for each experiment. DMSO was dosed at 0.1 or 1 ml/kg, and coadministered concurrently with 200 mg/kg TAA or saline.

Myeloperoxidase (MPO) activity assay

Mouse liver tissues were homogenized in MPO buffer (0.5% hexadecyl trimethyl ammonium bromide, 10 mM EDTA, 50 mM Na_2HPO_4, pH 5.4) using a Polytron homogenizer. Liver homogenates were then subject to three freeze-thaw cycles and cleared by centrifugation. MPO reaction was carried out using the Invitrogen EnzChek Myeloperoxidase Activity Assay Kit according to the manufacturer's protocol.

Quantitative RT-PCR

Mouse liver tissues were crushed to a powder in liquid nitrogen, and total RNA was extracted using the Invitrogen Trizol RNA extraction kit, and then purified using the RT^2 qPCR-Grade RNA Isolation Kit (SA Biosciences), according to the manufacturer's protocol. Total RNA (500 ng) was converted into cDNA using the RT^2 First Strand Kit (SA Biosciences). Quantitative RT-PCR was performed using the Stratagene Mx3000P QPCR System and the RT^2 qPCR Master Mix Kit (SA Biosciences). Quantitative RT-PCR was performed for mRNA expression of Gapdh, TNFα, pro-IL-1β, IL6, CCL5, Cyp1a1, Cyp1a2, Cyp2e1, Cyp2b10, and Cyp3a using primers designed by SA Biosciences. Expression of Gapdh was used to standardize the samples, and the results were expressed as a ratio relative to control.

Tissue scrape and load assay for GJIC

Mice were treated i.p. with saline, 2-APB (20 mg/kg), or 2-APB (20 mg/kg) plus TAA (200 mg/kg), and 3 hours later livers were excised and freshly sliced. A 27-gauge needle was dipped into a solution containing 0.5% Lucifer Yellow (Invitrogen) and 0.5% 10kDa dextran-Texas Red (Invitrogen), and the needle was used to both mechanically damage a small area of each slice and apply the dyes. The liver slices were incubated with the dye solution for 5 minutes, rinsed in saline, fixed in 4% paraformaldehyde for 30 minutes, frozen in OCT compound, cyro-sectioned into 7 μm sections, rinsed in saline, mounted, and imaged by fluorescence microscopy.

H2DCFH-DA and dihydroethidine hydrochloride (DEH) staining

Freshly cut frozen liver sections (7 μm) were stained with 10 μM H2DCFH-DA (Invitrogen) or 2 μM DEH (Invitrogen) for 30 minutes at 37°C, and imaged by fluorescence microscopy as previously described [22].

Fluorescence microscopy

Fluorescence images were captured on a Zeiss 200 Axiovert microscope at a fixed exposure and gain. Images for the tissue scrape load assay were quantified using custom image analysis routines written in MATLAB [10]. Briefly, images were median filtered, auto-thresholded, and segregated to identify discreet closed regions representing the spread of Lucifer Yellow dye and dextran-Texas Red. Regional outlines were plotted as contour maps by displaying iso-intensity lines at the determined threshold level.

Flow cytometry

Cultured H35 hepatocyte-derived cells were loaded with 10 μM H2DCFH-DA for 30 minutes at 37°C. This cell-permeable compound is converted into a non-fluorescent product (H2DCF), and oxidized by free radicals to the highly fluorescent dichlorofluoresceine (DCF). Cells were washed in PBS three times, and then treated with saline, TAA (25 μM), TASO (5 μM), or H_2O_2 (100 μM) for 2 hours, or subject to the transplant co-culture assay. After treatment, cells were trypsinized, washed in PBS, and analyzed by flow cytometry.

Transplant co-culture assay

Connexin 32 expressing HeLa (HeLa Cx32) and connexin 43 expressing HeLa (HeLa Cx43) cells were stimulated with saline, TASO (5 μM), or H_2O_2 (100 μM) in suspension for 2 hours, in the presence or absence of cell permeable anti-oxidant MnTMPyP (Calbiochem). Two hours after treatment, HeLa cells were washed 3 times in PBS, counted, and plated onto a sub-confluent layer of H35 cells, preloaded with H2DCFH-DA, at a cell ratio of 2:1. After 4 hours of co-culture, cells were trypsinized and H35 cells were analyzed for ROS activity, as indicated by H2DCFH-DA fluorescence, by flow cytometry.

HPLC-based quantification of TAA and TASO

To quantify TAA and TASO in plasma of mice, a reverse-phase HPLC assay was used, as previously described [23]. Briefly, 7% acetonitrile, 50 mM sodium sulfate, and 50 mM potassium phosphate buffer was used as the mobile phase. An SPS-ODS column (5 μm; Regis Technologies) was used to separate the components at 1 ml/min. TAA was detected by UV absorption at 212 nm, and TASO at 290 nm, using a photodiode array detector. Retention times for TAA and TASO were approximately 4.1 and 3 min, respectively. Standards were prepared by including known amounts of TAA and TASO in plasma from untreated mice.

Synthesis of TASO

Thioacetamide' S-Oxide (TASO) was synthesized as previously described [24]. Briefly, thioacetamide (TAA) was dissolved in acetone and chilled to -5°C. Then 30% H_2O_2 was added rapidly, the mixture was agitated thoroughly, and stored at 4°C for 24 hours until the product crystallized. The product, TASO, was recovered by filtration and washed with 5 portions of cold acetone. The purity was examined by HPLC, as previously described.

Analysis of GST activity and total GSH content

Mouse liver tissues were lysed in 100 mM potassium phosphate, containing 2 mM EDTA, and total protein content was determined. Enzymatic activity toward 1-chloro-2,4-dinitrobenzene (CNDB) (Sigma Aldrich) was assayed in a buffer containing 100 mM potassium phosphate, 0.1% Triton X-100, 1 mM glutathione and 1mM CNDB. Formation of glutathione/CNDB conjugate was measured in a spectrophotometer at 340 nm, as an indicator of GST activity. Total GSH content was measured using the Glutathione Assay Kit (Sigma Aldrich), as per the manufacturer's protocol. Briefly, mouse liver tissues were lysed and total protein content was determined. Samples were deproteinized with 5% 5-sulfosalicylic acid, and glutathione content of the samples was assayed using a kinetic assay in which catalytic amounts of glutathione cause a continuous reduction of 5,5′-dithiobis-(2-nitrobenzoic) acid (DTNB) to TNB. TNB was measured colorimetrically at 412 nm, as an indicator of total GSH content.

Acknowledgements

The authors thank K. Willecke (University of Bonn) and D. Paul (Harvard University) for the generous gift of $Cx32^{-/-}$ mice, K. Willecke (University of Bonn) for connexin expressing HeLa cells, H. Duffy (Harvard Medical School) for development of the tissue scrape and load assay for GJIC, and M. Izamis (Harvard Medical School) for HPLC assistance. S.J.P was supported in part by a Department of Defense CDMRP Prostate Cancer Predoctoral Training Award. The work was supported by grants from the US National Institutes of Health (DK059766, K01DK087770, and P41 EB-002503) and from the Shriners Hospital for Children.

4.6 References

1. Chen, C.J., *et al.* Identification of a key pathway required for the sterile inflammatory response triggered by dying cells. *Nat Med* **13**, 851-856 (2007).
2. Rock, K.L., Latz, E., Ontiveros, F. & Kono, H. The sterile inflammatory response. *Annu Rev Immunol* **28**, 321-342.
3. Navarro, V.J. & Senior, J.R. Drug-related hepatotoxicity. *N Engl J Med* **354**, 731-739 (2006).
4. Wysowski, D.K. & Swartz, L. Adverse drug event surveillance and drug withdrawals in the United States, 1969-2002: the importance of reporting suspected reactions. *Arch Intern Med* **165**, 1363-1369 (2005).
5. Gunawan, B.K. & Kaplowitz, N. Mechanisms of drug-induced liver disease. *Clin Liver Dis* **11**, 459-475, v (2007).
6. Kaplowitz, N. Idiosyncratic drug hepatotoxicity. *Nat Rev Drug Discov* **4**, 489-499 (2005).
7. Liu, Z.X. & Kaplowitz, N. Role of innate immunity in acetaminophen-induced hepatotoxicity. *Expert Opin Drug Metab Toxicol* **2**, 493-503 (2006).
8. Imaeda, A.B., *et al.* Acetaminophen-induced hepatotoxicity in mice is dependent on Tlr9 and the Nalp3 inflammasome. *J Clin Invest* **119**, 305-314 (2009).
9. Liu, Z.X., Govindarajan, S. & Kaplowitz, N. Innate immune system plays a critical role in determining the progression and severity of acetaminophen hepatotoxicity. *Gastroenterology* **127**, 1760-1774 (2004).
10. Patel, S.J., King, K.R., Casali, M. & Yarmush, M.L. DNA-triggered innate immune responses are propagated by gap junction communication. *Proc Natl Acad Sci U S A* **106**, 12867-12872 (2009).
11. Parthasarathi, K., *et al.* Connexin 43 mediates spread of Ca2+-dependent proinflammatory responses in lung capillaries. *J Clin Invest* **116**, 2193-2200 (2006).
12. Ey, B., Eyking, A., Gerken, G., Podolsky, D.K. & Cario, E. TLR2 mediates gap junctional intercellular communication through connexin-43 in intestinal epithelial barrier injury. *J Biol Chem* **284**, 22332-22343 (2009).
13. Segretain, D. & Falk, M.M. Regulation of connexin biosynthesis, assembly, gap junction formation, and removal. *Biochim Biophys Acta* **1662**, 3-21 (2004).
14. Jaeschke, H., *et al.* Mechanisms of hepatotoxicity. *Toxicol Sci* **65**, 166-176 (2002).

15. Ferret, P.J., *et al.* Detoxification of reactive oxygen species by a nonpeptidyl mimic of superoxide dismutase cures acetaminophen-induced acute liver failure in the mouse. *Hepatology* **33**, 1173-1180 (2001).

16. Bruck, R., *et al.* Prevention of hepatic cirrhosis in rats by hydroxyl radical scavengers. *J Hepatol* **35**, 457-464 (2001).

17. Behnia, K., *et al.* Xenobiotic metabolism by cultured primary porcine hepatocytes. *Tissue Eng* **6**, 467-479 (2000).

18. Tao, L. & Harris, A.L. 2-aminoethoxydiphenyl borate directly inhibits channels composed of connexin26 and/or connexin32. *Mol Pharmacol* **71**, 570-579 (2007).

19. Chun, L.J., Tong, M.J., Busuttil, R.W. & Hiatt, J.R. Acetaminophen hepatotoxicity and acute liver failure. *J Clin Gastroenterol* **43**, 342-349 (2009).

20. Kjolbye, A.L., Haugan, K., Hennan, J.K. & Petersen, J.S. Pharmacological modulation of gap junction function with the novel compound rotigaptide: a promising new principle for prevention of arrhythmias. *Basic Clin Pharmacol Toxicol* **101**, 215-230 (2007).

21. King, K.R., *et al.* A high-throughput microfluidic real-time gene expression living cell array. *Lab Chip* **7**, 77-85 (2007).

22. Owusu-Ansah, E., Yavari, A., Mandal, S. & Banerjee, U. Distinct mitochondrial retrograde signals control the G1-S cell cycle checkpoint. *Nat Genet* **40**, 356-361 (2008).

23. Chilakapati, J., *et al.* Toxicokinetics and toxicity of thioacetamide sulfoxide: a metabolite of thioacetamide. *Toxicology* **230**, 105-116 (2007).

24. Porter, W.R. & Neal, R.A. Metabolism of thioacetamide and thioacetamide S-oxide by rat liver microsomes. *Drug Metab Dispos* **6**, 379-388 (1978).

Chapter 5
Conclusions

5.1 Thesis Contributions

The major contribution of this thesis is the identification of a critical gap junction communication pathway for amplifying innate immune and inflammatory responses. Gap junction communication is typically used by cells to send signals rapidly over short length scales. As a result, gap junction research initially focused on electrically excitable cells such as neurons and cardiac myocytes. However, more recently, the roles for gap junctions have expanded to include communication in the context of immunity and inflammation [33, 34]. These new roles have generated many interesting questions: what is the significance of gap junction communication in the response to innate immune activation, and are secreted cytokines not already a mediator of intercellular communication for spreading immune signals during infection or injury? We believe the work completed in this thesis proposes the following possible explanation for why the innate immune system might have evolved such a signaling mechanism.

When a tissue is first faced with an infection, the total number of pathogens is limited, and the number of infected cells is small. Pathogens that infect host cells will activate intracellular innate immune signaling pathways (i.e. the TLR or NLR pathways) and cause release of key alarm cytokines such as IFNβ, TNFα, and IL-1β. **Without gap junctions**, the amount of secreted cytokine would be limited to that produced by the directly infected cells. However **with gap junctions**, a significantly larger population of host cells can be recruited to contribute to the initial secretion, thereby amplifying the cytokine response. This work shows that, depending on the nature of the cytokine, this amplification might be as much as 100-1000 fold. Such amplification is important since cytokines must accumulate in the extracellular space and diffuse to transmit warning signals to distal neighbors. In the case of sterile injury, the host inflammatory response to injury can contribute to the pathogenesis of disease, and serve as the initiator of organ dysfunction and ultimately failure. Our work shows that, in the absence of infection, gap junction communication pathways amplify pathologic, rather than protective, immune responses. Blocking this pathologic inflammatory response is a potentially attractive strategy to limit the damage of acute sterile inflammation and to stop the ongoing damage in chronic inflammation to tissue injury. This work shows that, in the case of drug-induced sterile liver injury, selectively blocking hepatic gap junctions with small molecules can prevent liver failure and enhance survival. This type of gap junction inhibition strategy may also have therapeutic potential in other

forms of liver injury and other organ systems. Similar therapies are currently in clinical trials for preventing life threatening sterile inflammation due to myocardial ischemia-reperfusion injury.

5.2 Thesis Conclusions

5.2.1 Overall

This thesis demonstrates the development of novel tools for investigating the spatiotemporal dynamics of cellular responses, describes how these tools were utilized to discover a basic gap junction communication pathway critical in innate immunity and inflammation

Through the use of stable GFP reporters, *in vitro* transplant coculture systems, and *in vivo* models of infection and sterile injury, we attempted to bridge the gap between basic discovery, at the cellular level, and application at the level of animal models. The first section describes the development of stable GFP reporters to study the spatiotemporal activation patterns of two key transcription factors in inflammation and innate immunity: NFκB and IRF3. Stimulation of NFkB-GFP reporters resulted in a spatially homogeneous pattern of activation, found to be largely mediated by the paracrine action of proinflammatory cytokine TNFα. In contrast, the activation of IRF3 was spatially heterogeneous, leading to the formation of multicellular colonies in an otherwise dark background of non-activated cells. The second section describes the discovery of a gap junction intercellular communication pathway necessary for the formation of these IRF3 active colonies of cells that collectively expressed more than 95% of critical secreted cytokines, including IFNβ and TNFα. Blocking gap junctions, with genetic specificity, limited the secretion of IFNβ and TNFα and the corresponding antiviral and inflammatory state. The third section demonstrates an application of the gap junction communication phenomenon in an animal model of sterile injury. Drug-induced liver injury was shown to be dependent on gap junction communication for amplifying sterile inflammatory signals. Mice deficient in hepatic gap junction protein Cx32 were protected against liver damage, inflammation, and death in response to hepatotoxic drug-induced injury. Coadministration of a selective pharmacologic Cx32 inhibitor with the hepatotoxic drugs significantly limited hepatocyte damage and sterile inflammation, and completely abrogated mortality, confirming the importance of hepatic gap junction communication in amplifying sterile injury and providing a potential novel therapeutic strategy for preventing drug hepatotoxicity.

The remainder of this section summaries the general conclusions drawn from each of the individual chapters.

5.2.2 Chapter 2

In this chapter we investigated the DNA-triggered molecular signaling pathways that lead to activation of the endothelium. We demonstrated that direct exposure to DNA induced activation of NFκB and MAPK pathways in endothelial cells. This lead to increased expression of endothelial adhesion molecules, and resulted in functional leukocyte adhesion to the endothelium. NFκB, JNK, and p38 MAPK were critical for leukocyte adhesion, as pharmacological inhibition resulted in decreased expression of adhesion molecules. We further showed that detection of DNA triggers robust secretion of TNFα for sustained secondary activation of the endothelium. Both IRF3 and NFκB were required for the production of the TNFα, and mice deficient in the TNF receptor were unable to mount an acute inflammatory response to dsDNA. Our findings identify NFκB and TNFα as an alternative innate immune mechanism to the inflammasome and IL1β, capable of initiating and amplifying a proinflammatory response to DNA. This work suggests the involvement of DNA-induced endothelial cell immune responses in host defense to infection or sterile injury.

5.2.3 Chapter 3

In this chapter we used a stable IRF3-GFP monoclonal reporter to explore the spatiotemporal patterns of IRF3 activation in response to DNA stimulation, and investigated the intercellular signaling pathways between infected and non-infected cells for establishing an antiviral state. We found that DNA stimulation induced spatially heterogeneous responses characterized by the formation of multicellular colonies of IRF3 activated cells that collectively expressed more than 95% of critical secreted cytokines, including IFNβ and TNFα. Functional gap junctions were necessary for the formation of these IRF3 active colonies and blocking gap junctions with genetic specificity limited the secretion of IFNβ and TNFα and the corresponding antiviral state. Our findings describe a previously unknown intercellular signaling pathway triggered by cytosolic dsDNA sensing and provide evidence that gap junction communication is critical for the amplification of antiviral and inflammatory responses, prior to paracrine-mediated propagation by cytokines. This work also suggests the key role of gap junction communication pathways in establishing immunity.

5.2.4 Chapter 4

In this chapter we showed that drug-induced liver injury is dependent on gap junction communication to amplify sterile inflammatory signals generated in response to the initial toxic injury. Mice deficient in hepatic gap junction protein Cx32 were protected against liver damage, inflammation, and death in response to hepatotoxic drug-induced injury. Administration of these

drugs resulted in the production of intracellular free radicals that propagated through gap junctions, damaging naïve surrounding cells and expanding the tissue injury front, thereby establishing the sterile inflammatory response. Coadministration of selective pharmacologic Cx32 inhibitors with the hepatotoxic drugs significantly limited hepatocyte damage and sterile inflammation, and completely abrogated mortality, confirming the importance of hepatic gap junction communication in sterile injury. These findings suggest inhibition of hepatic gap junctions as a viable novel therapeutic strategy for preventing drug hepatotoxicity and potentially other forms of sterile injury.